NASA Technical Memorandum

NASA TM- 86454

RADIAL SI LATCHES VIBRATION TEST DATA REVIEW

By Phillip M. Harrison and James Lee Smith

Systems Dynamics Laboratory

July 1984

National Aeronautics and Space Administration

George C. Marshall Space Flight Center

TECHNICAL REPORT STANDARD TITLE PAGE

1. REPORT NO.	2. GOVERNMENT ACCESSION NO.	3. RECIPIENT'S CATALOG NO.
NASA TM-86454		

4. TITLE AND SUBTITLE	5. REPORT DATE
Radial SI Latches Vibration Test Data Review	July 1984
	6. PERFORMING ORGANIZATION CODE

7. AUTHOR(S)	8. PERFORMING ORGANIZATION REPORT #
Phillip M. Harrison and James Lee Smith	

9. PERFORMING ORGANIZATION NAME AND ADDRESS	10. WORK UNIT NO.
George C. Marshall Space Flight Center Marshall Space Flight Center, Alabama 35812	11. CONTRACT OR GRANT NO.
	13. TYPE OF REPORT & PERIOD COVERED
12. SPONSORING AGENCY NAME AND ADDRESS	Technical Memorandum
National Aeronautics and Space Administration Washington, D.C. 20546	14. SPONSORING AGENCY CODE

15. SUPPLEMENTARY NOTES

Prepared by Systems Dynamics Laboratory, Science and Engineering

16. ABSTRACT

Dynamic testing of the Space Telescope Scientific Instrument Radial Latches was performed as specified by the designated test criteria. No structural failures were observed during the test. The alignment stability of the instrument simulator was within required tolerances after testing. Particulates were discovered around the latch bases, after testing, due to wearing at the "B" and "C" latch interface surfaces. This report covers criteria derivation, testing, and test results.

17. KEY WORDS	18. DISTRIBUTION STATEMENT
Space Telescope Scientific Instruments Radial Latches Vehicle Transients Random Vibration	Unclassified-Unlimited

19. SECURITY CLASSIF. (of this report)	20. SECURITY CLASSIF. (of this page)	21. NO. OF PAGES	22. PRICE
Unclassified	Unclassified	68	NTIS

MSFC - Form 3292 (May 1969)

For sale by National Technical Information Service, Springfield, Virginia 22151

Page intentionally left blank

Page intentionally left blank

TABLE OF CONTENTS

		Page
I.	INTRODUCTION	1
II.	DESCRIPTION OF TEST ITEMS	1
III.	TEST CRITERIA AND DEVELOPMENT	1
	A. Sinusoidal Diagnostic Survey	2
	1. 0.1 G Level	2
	2. 0.25 G Level	2
	B. Vehicle Transient	2
	1. Half Level	3
	2. Full Level	3
	C. Random Vibration	3
	1. Half Level	3
	2. Full Level	3
IV.	TEST APPARATUS	4
V.	TEST PROCEDURE	4
VI.	DATA AND EVALUATION	4
	A. Sinusoidal Diagnostic Survey	5
	B. Vehicle Transient	5
	C. Random Vibration	5
VII.	SUMMARY AND CONCLUSIONS	6
	A. Summary	6
	B. Conclusions	6
APPENDIX A - DATA AND ILLUSTRATIONS		7
APPENDIX B - DATA ANALYSIS PLOTS		33
APPENDIX C - ANALYSIS EQUATIONS		59

LIST OF ILLUSTRATIONS

Figure	Title	Page
1.	Test configuration	8
1.1.	Latch A, FPS half	9
1.2.	Latch A, SI half	10
1.3.	Latch B	11
1.4.	Latch C, SI half	12
1.5.	Latch C, FPS half	12
2.	Vehicle transients	13
3.	Vehicle transients	13
4.	V1 axis transient criteria	14
5.	V2 axis transient criteria	14
6.	V2 axis transient criteria	15
7.	V3 axis transient criteria	15
8.	V3 axis transient criteria	16
9.	Random vibration criteria - 145 dB basis	16
10.	Space shuttle cargo bay acoustic criteria	17
11.	Random vibration criteria - 139 dB basis	17
12.	Random vibration criteria	18
13.	Test configuration	18
14.	V1 axis sine sweep control average	19
15.	V1 axis c.g. pre- and post-test data	19
16.	V1 axis transient control average	20
17.	V1 axis c.g. transient response	20
18.	V1 axis random control average	21
19.	V1 axis c.g. random response	21
20.	V2 axis sine sweep control average	22

LIST OF ILLUSTRATIONS (Continued)

Figure	Title	Page
21.	V2 axis c.g. pre- and post-test data	22
22.	V2 axis transient control average - test 1	23
23.	V2 axis c.g. transient response	23
24.	V2 axis transient control average - test 2	24
25.	V2 axis c.g. transient response	24
26.	V2 axis random control average	25
27.	V2 axis c.g. random response	25
28.	V3 axis sine sweep control average	26
29.	V3 axis c.g. pre- and post-test data	26
30.	V3 axis transient control average - test 1	27
31.	V3 axis c.g. transient response	27
32.	V3 axis transient control average - test 2	28
33.	V3 axis c.g. transient response	28
34.	V3 axis random control average	29
35.	V3 axis random response	29
36.	"A" latch random input	30
37.	"B" latch random input	30
38.	"C" latch random input	31
39.	V1 "A" latch random auto spectral density	34
40.	V1 inside "A" latch random auto spectral density	34
41.	"A" latch transfer function	35
42.	"A" latch coherence	35
43.	V1 "B" latch random auto spectral density	36
44.	V1 inside "B" latch random auto spectral density	36
45.	"B" latch transfer function	37

LIST OF ILLUSTRATIONS (Continued)

Figure	Title	Page
46.	"B" latch coherence	37
47.	V1 "C" latch random auto spectral density	38
48.	V1 inside "C" latch random auto spectral density	38
49.	"C" latch transfer function	39
50.	"C" latch coherence	39
51.	V1 "A" latch random input auto spectral density	40
52.	V1 c.g. response auto spectral density	40
53.	V1 "A" latch input versus c.g. transfer function	41
54.	V1 input versus c.g. coherence	41
55.	V2 "A" latch random auto spectral density	42
56.	V2 "A" latch inside random auto spectral density	42
57.	V2 "A" latch transfer function	43
58.	V2 "A" latch coherence	43
59.	V2 "B" latch random auto spectral density	44
60.	V2 "B" latch inside random auto spectral density	44
61.	V2 "B" latch transfer function	45
62.	V2 "B" latch coherence	45
63.	V2 "C" latch random auto spectral density	46
64.	V2 "C" latch inside random auto spectral density	46
65.	V2 "C" latch transfer function	47
66.	V2 "C" latch coherence	47
67.	V2 "A" latch random input auto spectral density	48
68.	V2 c.g. response auto spectral density	48
69.	V2 input versus c.g. transfer function	49
70.	V2 input versus c.g. coherence	49

LIST OF ILLUSTRATIONS (Concluded)

Figure	Title	Page
71.	V3 "A" latch random auto spectral density	50
72.	V3 "A" latch inside random auto spectral density	50
73.	V3 "A" latch transfer function	51
74.	V3 "A" latch coherence	51
75.	V3 "B" latch random auto spectral density	52
76.	V3 "B" latch inside random auto spectral density	52
77.	V3 "B" latch transfer function	53
78.	V3 "B" latch coherence	53
79.	V3 "C" latch random auto spectral density	54
80.	V3 "C" latch inside random auto spectral density	54
81.	V3 "C" latch transfer function	55
82.	V3 "C" latch coherence	55
83.	V3 "A" latch random input auto spectral density	56
84.	V3 c.g. response auto spectral density	56
85.	V3 input versus c.g. transfer function	57
86.	V3 input versus c.g. coherence	57

TECHNICAL MEMORANDUM

RADIAL SI LATCHES VIBRATION TEST DATA REVIEW

I. INTRODUCTION

A dynamic test program of the Space Telescope Scientific Instruments Latches was requested by the Marshall Space Flight Center Latch Design Audit Team. The test program included random vibration, transient shock, and modal testing on the latches for the axial and radial scientific instruments. The test program was required for flight qualification of the SI latches.

This report describes the criteria development, types of testing, purposes for testing, test apparatus, test procedure, and results and analysis of test data for the radial SI latches.

II. DESCRIPTION OF TEST ITEMS

Latch "A" (Figs. 1, 1.1, and 1.2) consists of two parallel interfaced plates. A threaded ball is permanently bound within a socket between the two plates. In latching, a threaded rod is secured to the ball. Latch "A" will accept loads in all three directions.

Latches "B" and "C" are pin-and-socket configurations. Each latch consists of two halves that interface perpendicularly. Latch "B" (Figs. 1 and 1.3) accepts load in the V1 direction only. Latch "C" (Figs. 1, 1.4, and 1.5) accepts loads in the V1 and V2 directions.

To securely latch a radial scientific instrument to the Space Telescope, the pins of latches "B" and "C" are pulled into their receptors as the threaded rod is screwed into latch "A".

III. TEST CRITERIA AND DEVELOPMENT

The test criteria for the series of dynamic tests to be performed on the radial SI latches is designed to evaluate the dynamic response of the test article and to expose the test article to the simulated flight dynamic environments. The test criteria will be notched if necessary to avoid exceeding the following maximum design loads:

Axis	Peak G's
V1	6.23
V2	2.33
V3	3.11

A. Sinusoidal Diagnostic Survey Test Criteria

Sinusoidal test criteria levels were chosen at levels and sweep rates to preclude exceedance of the above designated maximum design loads. Natural frequencies and damping of the test article were predicted and the test level was determined such that the loading of the test article would not be significant during the sine sweep tests.

1. 0.1 G Level

A 0.1 g sine sweep from 5 to 2000 Hz at 3 octaves/min was used to identify fundamental frequencies, to determine the damping factor, and to determine if notching was required in the 0.25 g sine sweep. This test also allowed checking of control and center-of-gravity (c.g.) accelerometers before beginning the 0.25 g sine sweep. This was the initial vibration test in each axis. A 0.1 g sine sweep was selected at random for convenience because of its low level. A 0.05 g or 0.15 g test could have been used.

2. 0.25 G Level

A 0.25 g level test was chosen because it produced the desired response level. The 0.25 g sine sweep was conducted at 3 octaves/min from 5 to 2000 Hz before and after the random and the transient vibration tests. The vibration "signatures" from the pre- and post-test sine sweeps were analyzed to determine if any changes occurred in the latches due to random or transient testing. Changes in the "signatures" usually indicate some structural change in the test specimen (broken or overstressed members, loose bolts and nuts, binding, or work interfaces).

B. Vehicle Transient Criteria

Shock spectra and time histories were calculated by space shuttle coupled loads computer simulation analysis. Five liftoff and five landing cases were selected as "worst" cases. Forcing functions used in the computer model included space shuttle main engine (SSME) thrust, solid rocket booster (SRB) thrust, SRB internal pressure, SRB ignition overpressure, SSME side loads, steady state wind and gusts, ground reactions at the base of the SRB's, and in landing: angle of attack, cross winds, horizontal velocity, and sink speeds. Figures 2 and 3 are examples of the shock spectra and time histories. See NASA memorandum ED22-84-25 for all of the data.

Neither the response time histories nor the shock response spectra could be reproduced in the test laboratory due to test equipment limitations. Consequently, a fast sinusoidal sweep in the appropriate frequency range was chosen to simulate the transient environment. Amplitudes for the test were obtained from the peak values of the calculated response time histories. Frequency ranges were determined from the shock response spectra of the transient time histories. Sinusoidal sweep rates were adjusted to produce a factor of 3 on the number of peaks (between the maximum amplitude and six decibels below maximum amplitude) from the transient time histories. The resulting test criteria are presented in Figures 4 through 8.

1. Half Level

A half-level transient test was conducted as a calibration run. Data from this test were evaluated to determine if the desired response amplitude and number of cycles would be achieved during the full-level transients. Adjustments were made, if necessary, to the amplitude and sweep rate of the full-level transient test criteria, to achieve the desired response.

2. Full Level

A full-level transient test was then conducted at levels and sweep rates formulated from the half-level transient test data. The purpose of this test is to simulate the liftoff vehicle transients of actual flight.

C. Random Vibration Criteria

The original predicted cargo bay acoustic criteria for the space shuttle was 145 dB. Space Telescope (ST) random criteria were based on measured vibration data from the ST-Structural Dynamic Test Vehicle (SDTV) vibroacoustic test. The resulting random criteria for the scientific instruments were 9.5 grms, as shown in Figure 9.

Based upon the data from the first four shuttle missions, the cargo bay acoustic criteria were revised downward to 139 dB. Figure 10 compares 145 dB and 139 dB acoustic levels. Likewise, the random criteria were scaled downward to 4.6 grms, as shown in Figure 11.

Evaluating STS flight payload data from missions 1 through 9 indicated that structure-borne excitation exceeds acoustically induced vibration in the 20 to 200 Hz frequency range. A third criteria modification was made to include this low frequency exceedance. Figure 12 illustrates the modified criteria used in the latch test.

1. Half Level

A half-level random test was conducted to verify control system capability, to determine magnification factor (Q) at the fundamental frequency, to check cross axis response, and to determine if notching is required to stay within the maximum design loads.

2. Full Level

A 60-second full-level random test was conducted to qualify the latches for the maximum expected flight random vibration environment. Single mission random vibration test time is based upon the actual time the environment is present times a factor of three (a factor of safety on the quality of the test article); however, a minimum test time of 1 min is recommended for adequate equalization of the control system and to provide sufficient time for data acquisition. Test time for the SI latches is set by the 1 min minimum.

IV. TEST APPARATUS

Figure 1 illustrates the scientific instrument simulator. Attached to the simulator are the latches. Also the latches are attached to the test fixture. Figure 1 also illustrates the locations of the control and response accelerometers.

Figure 13 illustrates the test fixture and shaker table configurations for the three axes. In the V1 axis only one shaker is used. The latches, simulator and an aluminum plate attach directly to the shaker. In the V2 and V3 axes, the following configuration is used: two large granite "team" tables mount onto a concrete floor. A 2-in. thick magnesium plate is mounted upon the team tables. This plate is oil lubricated. A 6-in. thick aluminum plate is bolted to the mangesium plate. This aluminum plate is machined out and foam filled. Another 2-in. thick aluminum plate bolts above. The latches then bolt to this plate. Four shakers attach to the 6-in. aluminum plate at the four corners as indicated in the figure. A computer system controls and monitors the shakers and processes data.

V. TEST PROCEDURE

The various tests were performed in the following order in each axis.

1) 0.1 g sine sweep

2) 0.25 g sine sweep

3) Low level random vibration

4) Full level random vibration

5) -6 dB transient

6) Full level transient

7) 0.25 g sine sweep

For a detailed list of test procedures see ST-SIL-TCP-001, December 15, 1982.

VI. TEST DATA AND EVALUATION

Figures 14 through 35 present the control average and c.g. response in each axis for the 0.25 g sine tests (pre- and post-), the full-level transient tests, and the full-level random tests.

Figures 14 through 19, 20 through 27, and 28 through 35 are data from the V1, V2, and V3 axes, respectively.

A. Sinusoidal Diagnostic Survey

Figure 21 illustrates the center-of-gravity (c.g.) response for the V2 axis for input in the V2 axis. The fundamental response frequency is 34 Hz. The magnification factor (Q) can be calculated as follows:

$$Q = \frac{\text{Peak Response Level}}{\text{Input Level}}$$

$$Q = \frac{0.6\ g}{0.25\ g} = 2.4 \quad .$$

Examining c.g. response data of V1 axis, V1 input and V3 axis, V3 input reveals a system response frequency of approximately 35 Hz and a magnification factor, Q = 3.

Comparison of the V2 axis pre- and post-test 0.25 g sine sweep data indicates a positive frequency shift in the post-test data, as in Figure 21. Examination of the "B" and "C" latches after V2 axis testing revealed degradation of the internal interface surfaces of the latch halves and particulates in the area around these interfaces. Contact marks were observed on the point "C" bases — SI and FPS (focal plane structure) halves.

B. Vehicle Transient

Figure 16 is an example of the V1 axis input for the 5 to 14 Hz vehicle transient test. Figure 17 is the c.g. response for the above input in the V1 axis. The V1 c.g. response, 4.17 g's, is well within the fifth cycle load limit of 6.23 g's. The number of cycles is a factor of 3 to 4 due to test control system limitations (sweep rate, rise rate, and control feedback loop).

C. Random Vibration

In each axis the -6 dB random test indicated that notching of the full level random vibration input criteria was not required to maintain c.g. response loads within the maximum design limits. Figures 36, 37, and 38 illustrate the inputs into each latch for the full level random V1 axis test. Fixture resonances resulted in over testing at some frequencies, this may be seen in Figures 26 and 34 — the V2 and V3 control averages. In addition, there was over testing resulting from cross-axis fixture resonances at some frequencies above 400 Hz. However, these exceedances are narrow band and well above the first fundamental frequency of the test article and are not considered significant.

The figures in Appendix B illustrate auto spectral density, transfer function, and coherence plots for selected random vibration time histories. Appendix C describes how the plots in Appendix B were calculated. The following description describes the results of frequency domain analysis for the "A" latch in the V1 axis:

Figure 39 is an auto spectral density plot for the R2 accelerometer, located outside of the "A" latch. Figure 40 is an auto spectral density plot for the R5

accelerometer, located inside of the "A" latch. Figure 41 is a transfer function plot for the energy transfer between the R5 and R2 data. This describes the energy transfer through the latch. Notice that negligible energy transfer occurs above 200 Hz. However, below 200 Hz considerable energy transfer occurs. Figure 42 illustrates the coherence of the transfer of energy through the latch. Notice that considerable energy transfer occurs only at particular frequencies.

In examining the other H(f) plots and coherence plots, one can see that at some locations energy transfer was minimal, while at other locations energy transfer was as much as 95 percent.

VII. SUMMARY AND CONCLUSIONS

A. Summary

Dynamic testing of the space telescope scientific instruments radial latches was performed as specified by the designated criteria. The specified test procedure was carefully followed. No failures were discovered in testing. The alignment stability after exposure to the dynamic environments was within the required tolerances. Particulates were discovered in the latch interfaces after testing.

B. Conclusions

Pending positive dye penetrant test results, the latches are considered structurally qualified for the flight dynamic environment.

Increased friction due to the worn latch surfaces may account for the frequency increase in the V2 axis post-test 0.25 g sine sweep. Another possibility is increased friction due to binding produced by misalignment in the V2 axis. The random vibration time history data recorded during the V2 axis test indicated that impacting occurred at the point "B" and "C" latches. This is attributed to setup error which caused the clearance between the bases to be below the minimum allowable. The setup error was corrected before proceeding with the V3 and V1 axes. No further impacting of latch half bases was observed.

A lubricant must be added to trap particulate matter that was produced by wearing of the latch registration interfaces. This lubricant is necessary since particulate contamination of the Space Telescope optical surfaces could render it useless.

APPENDIX A

DATA AND ILLUSTRATIONS

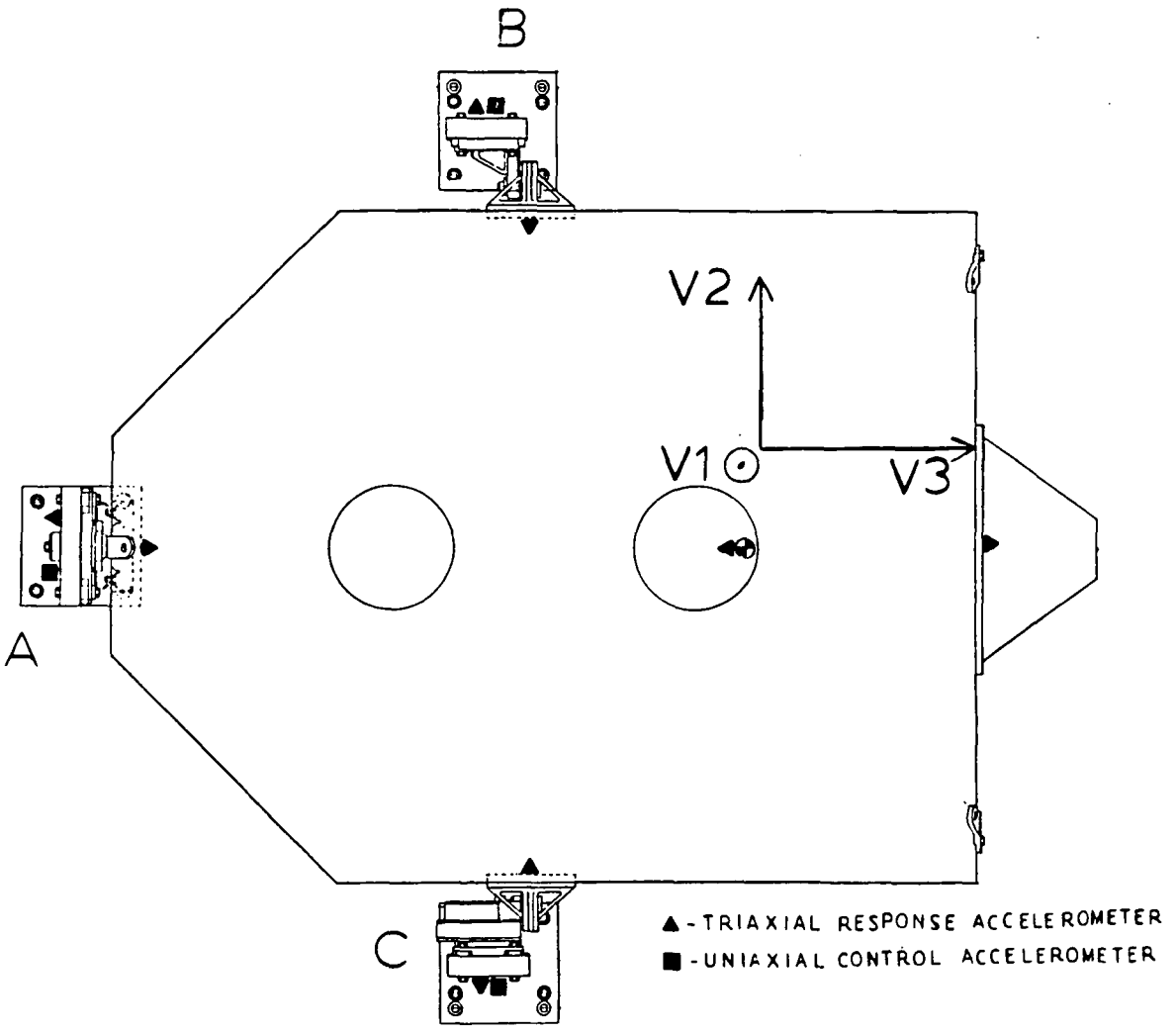

Figure 1. Test configuration.

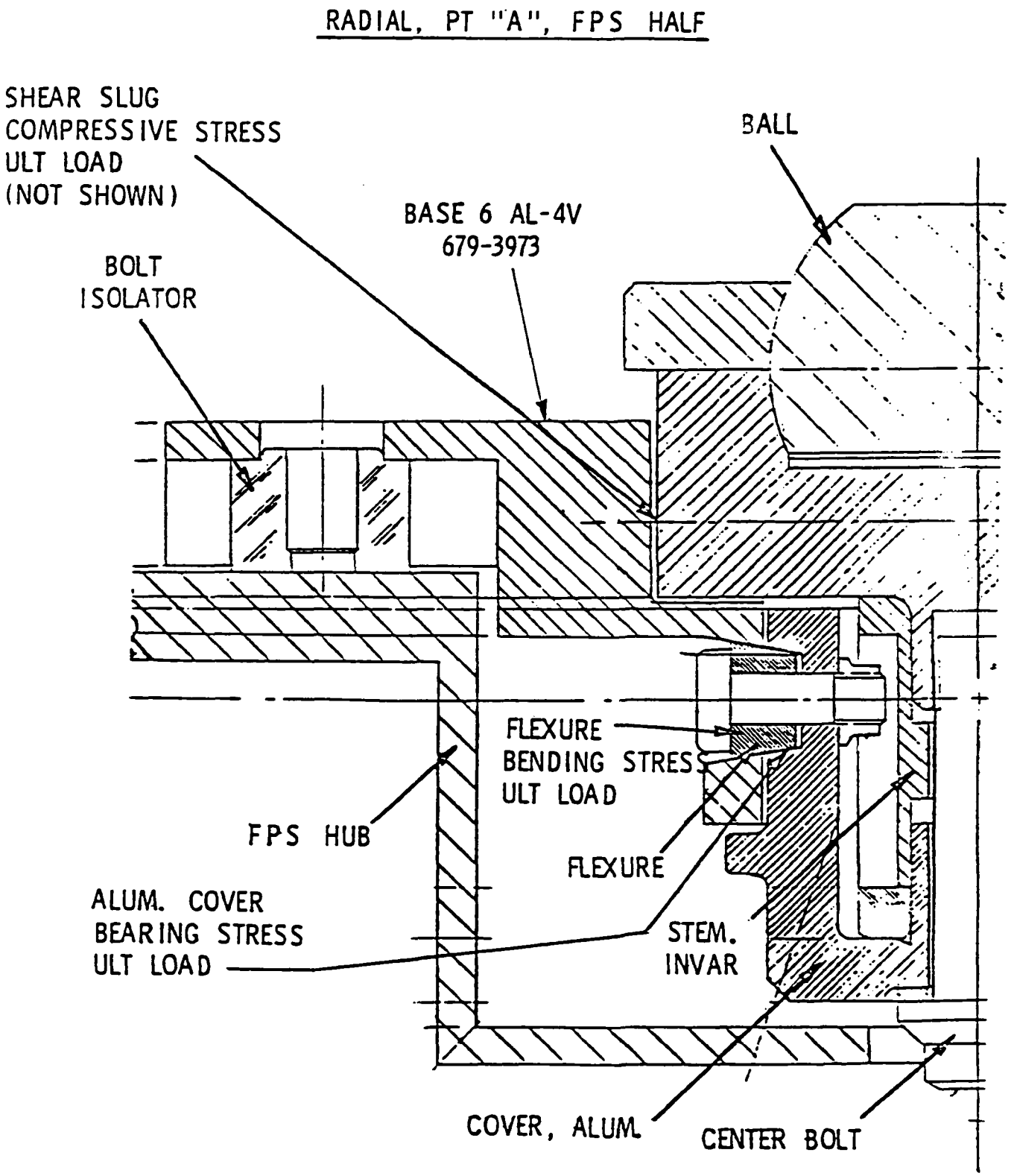

Figure 1.1. Latch A, FPS half.

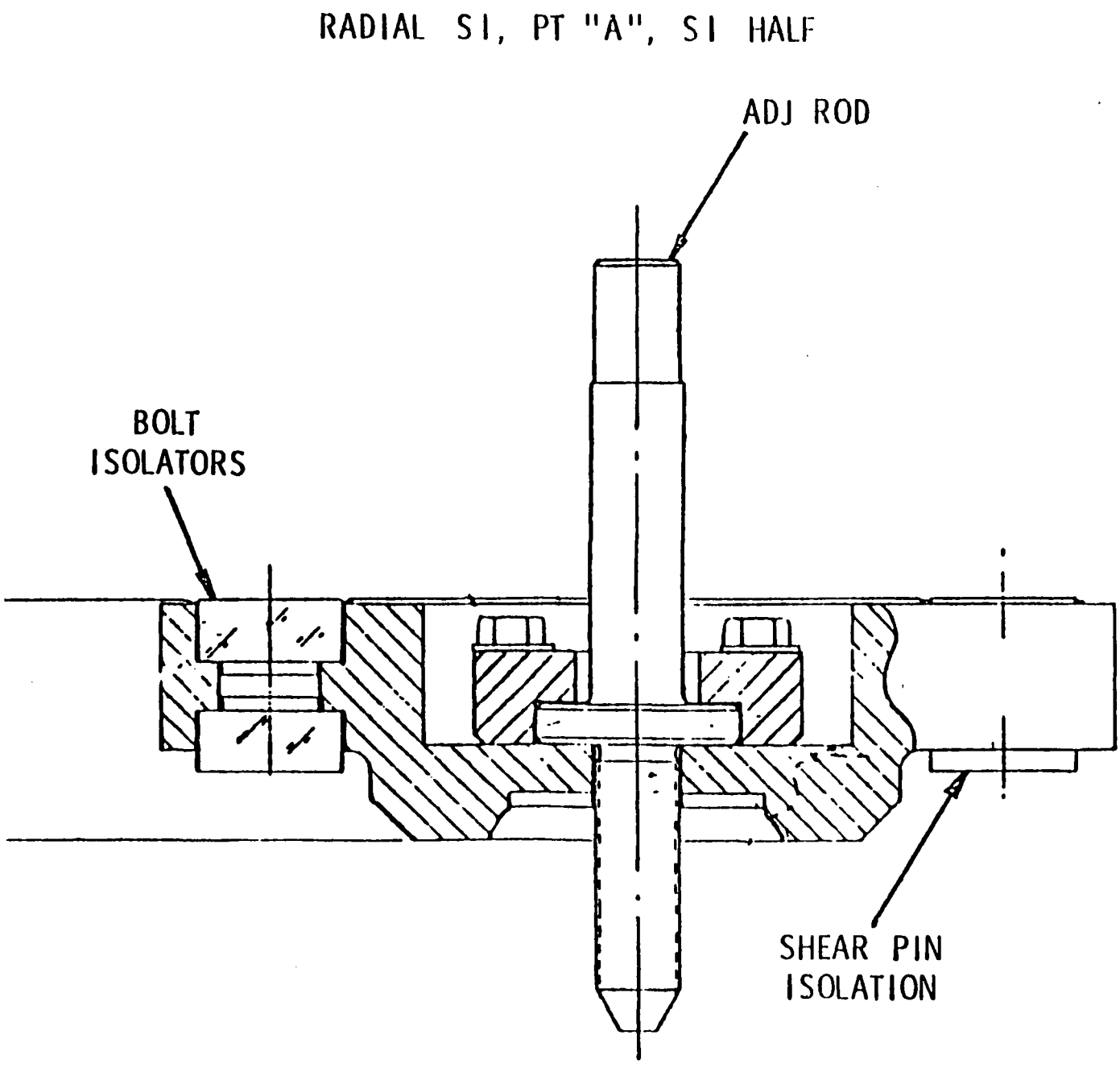

Figure 1.2. Latch A, SI half.

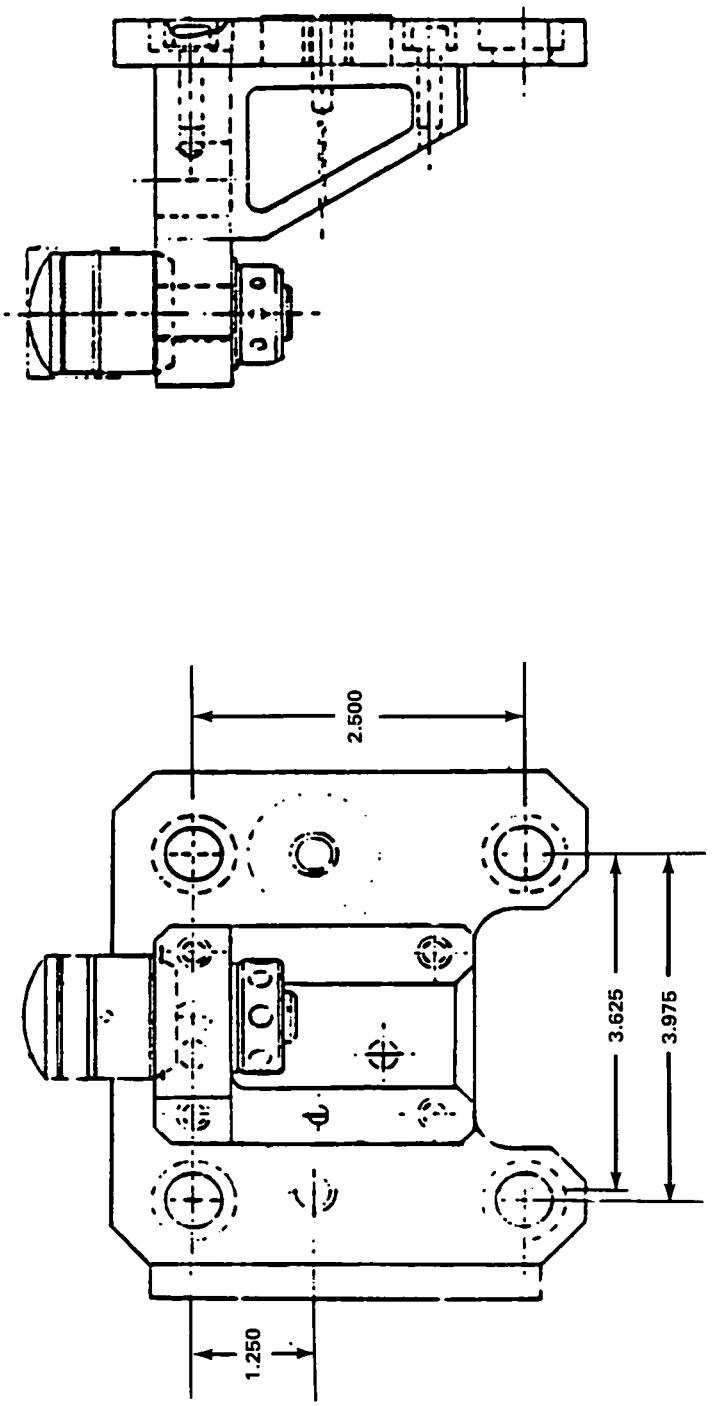

Figure 1.3. Latch B.

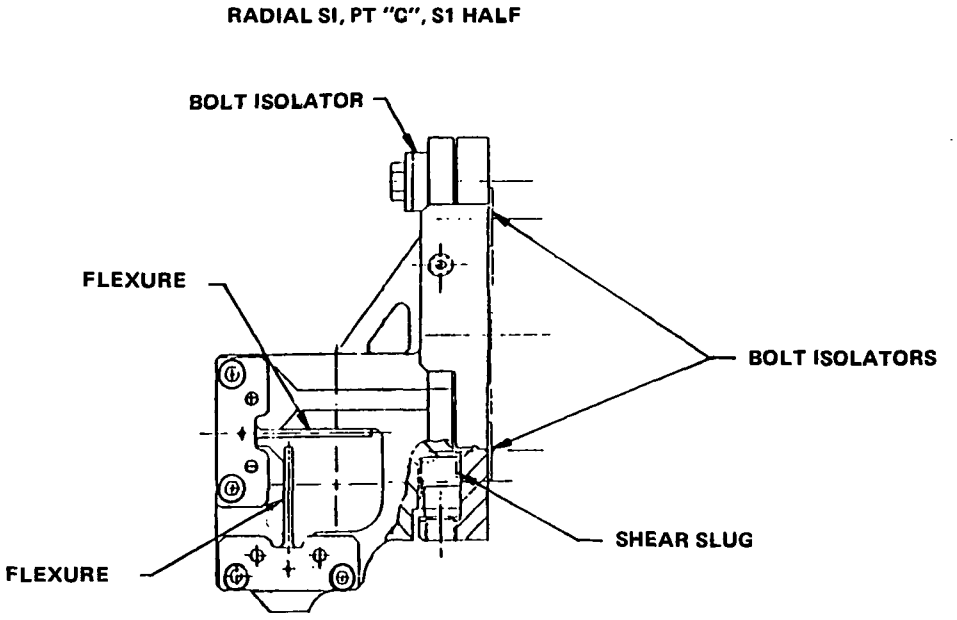

Figure 1.4. Latch C, SI half.

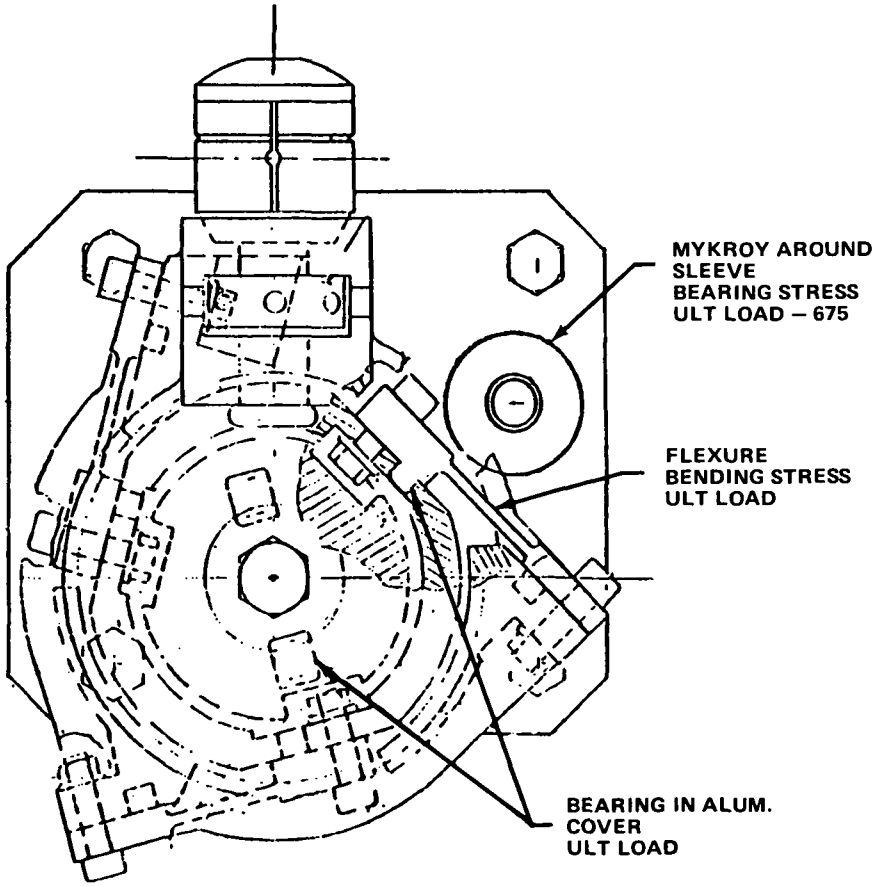

Figure 1.5. Latch C, FPS half.

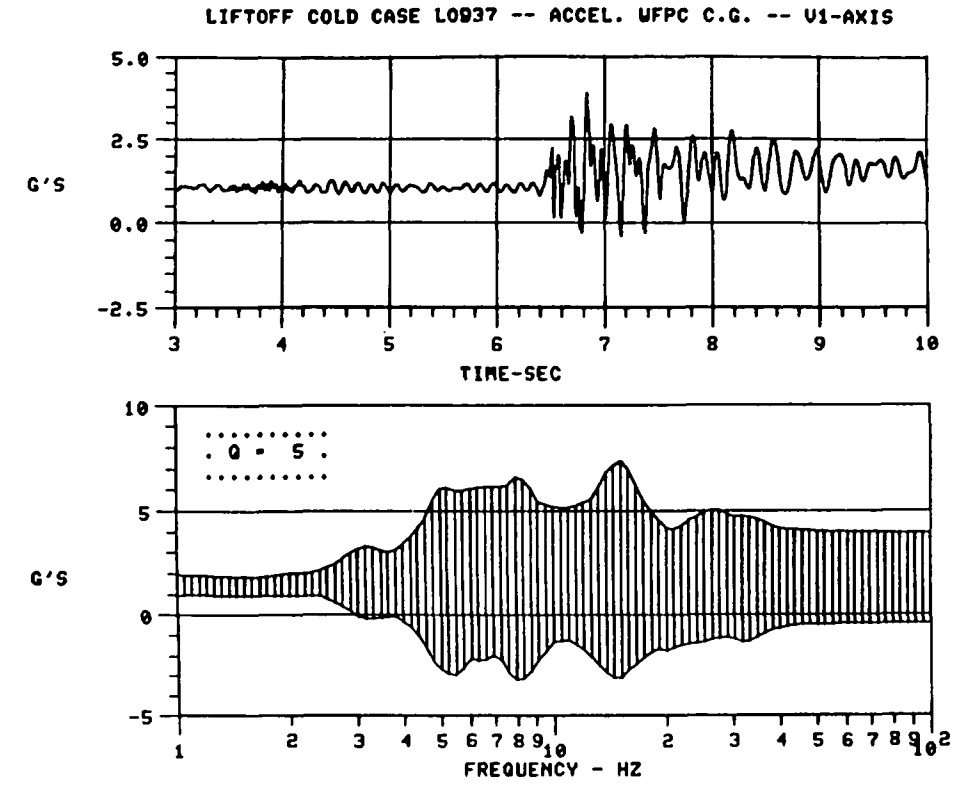

Figure 2. Vehicle transients.

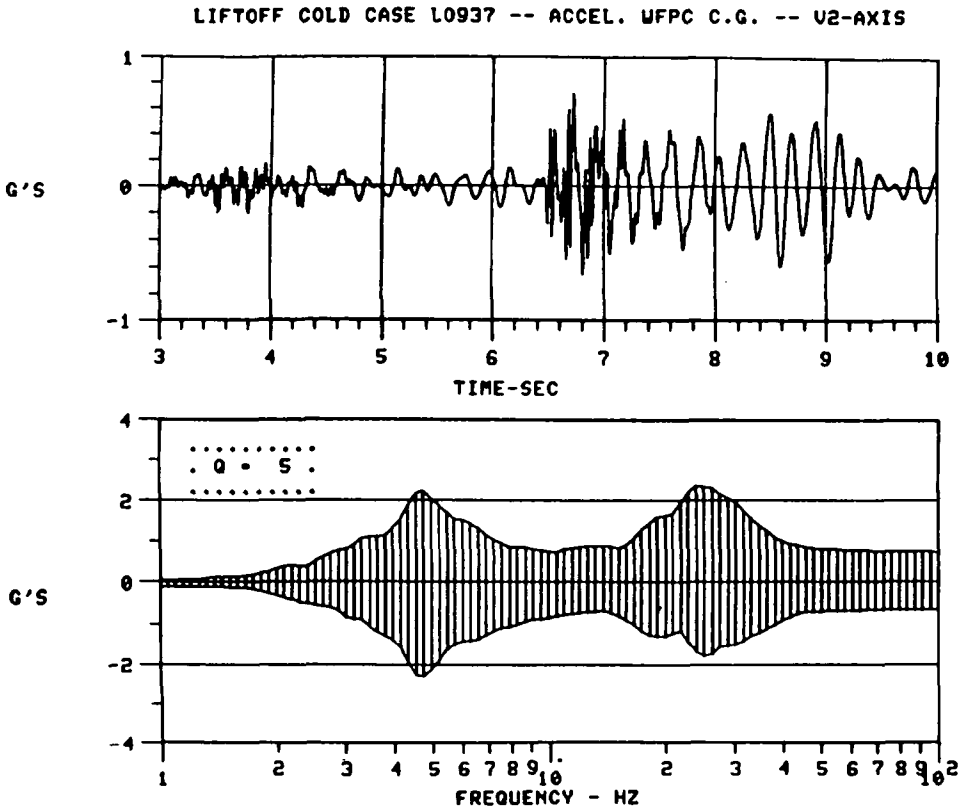

Figure 3. Vehicle transients.

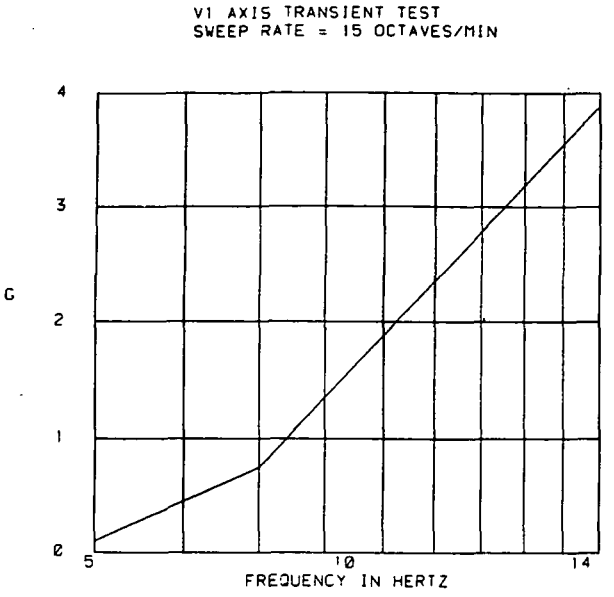

	5.00 Hz @	0.10 Gpk	
5.00-	7.00 Hz @	0.078 INCHES D.A.	DISPLACEMENT
	7.00 Hz @	0.75 Gpk	
7.00-	14.00 Hz @	0.300 INCHES D.A.	DISPLACEMENT
	14.00 Hz @	3.88 Gpk	

Figure 4. V1 axis transient criteria.

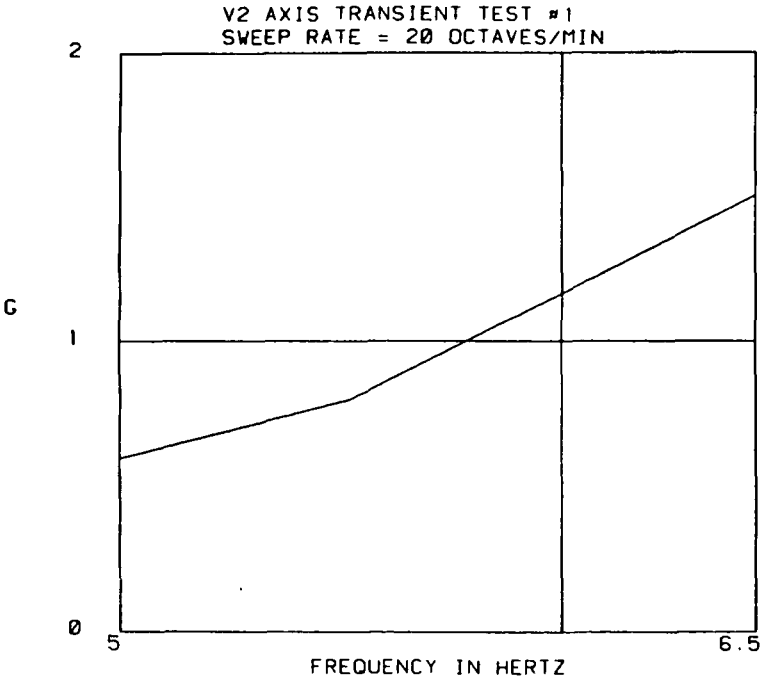

	5.00 Hz @	0.60 Gpk	
5.00-	5.50 Hz @	0.470 INCHES D.A.	DISPLACEMENT
	5.50 Hz @	0.80 Gpk	
5.50-	6.50 Hz @	0.518 INCHES D.A.	DISPLACEMENT
	6.50 Hz @	1.50 Gpk	

Figure 5. V2 axis transient criteria.

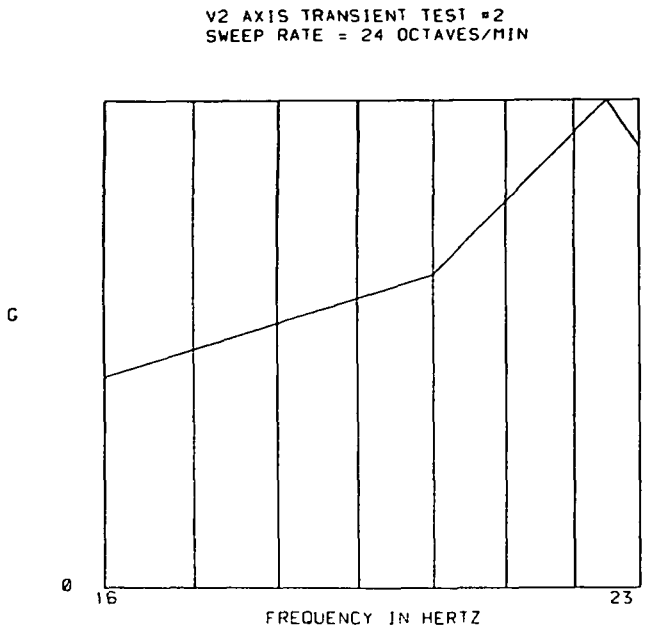

16.00 Hz @ 0.08 Gpk
16.00- 20.00 Hz @ 0.006 INCHES D.A. DISPLACEMENT
20.00 Hz @ 0.64 Gpk
20.00- 22.50 Hz @ 0.031 INCHES D.A. DISPLACEMENT
22.50 Hz @ 1.00 Gpk
22.50- 23.00 Hz @ 0.039 INCHES D.A. DISPLACEMENT
23.00 Hz @ 0.90 Gpk

Figure 6. V2 axis transient criteria.

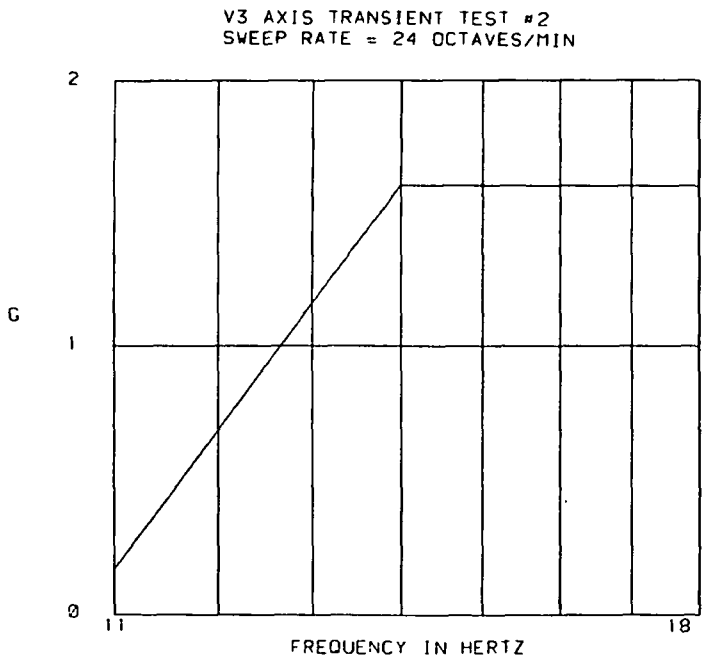

5.00 Hz @ 0.60 Gpk
5.00- 7.00 Hz @ 0.470 INCHES D.A. DISPLACEMENT
7.00 Hz @ 1.75 Gpk
7.00- 8.00 Hz @ 1.75 Gpk

Figure 7. V3 axis transient criteria.

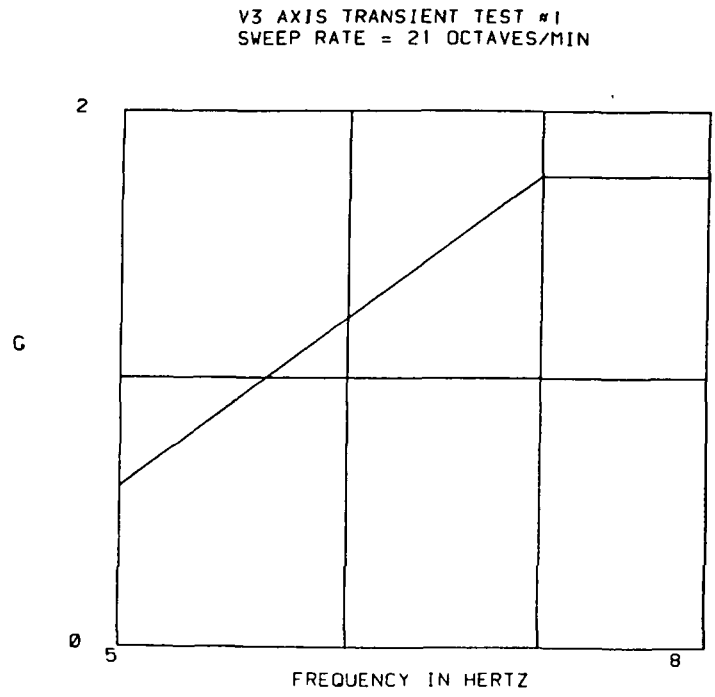

Figure 8. V3 axis transient criteria.

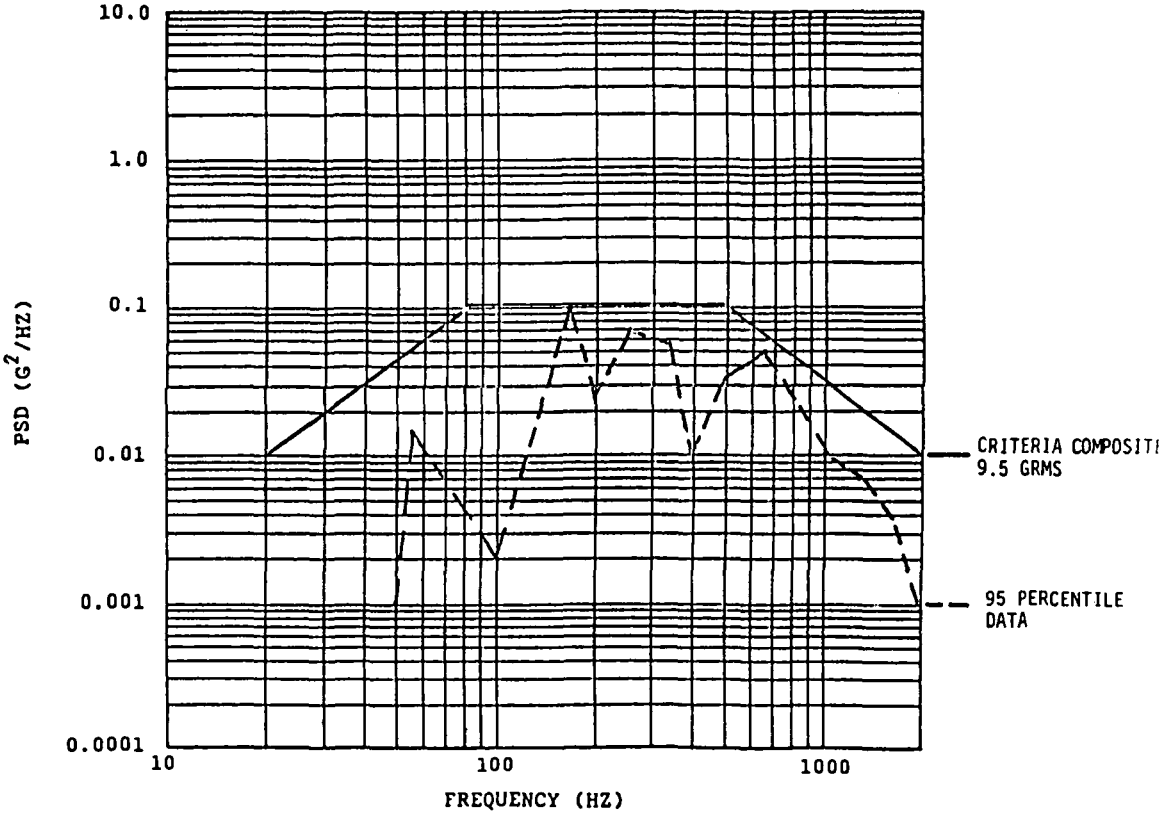

Figure 9. Random vibration criteria - 145 dB basis.

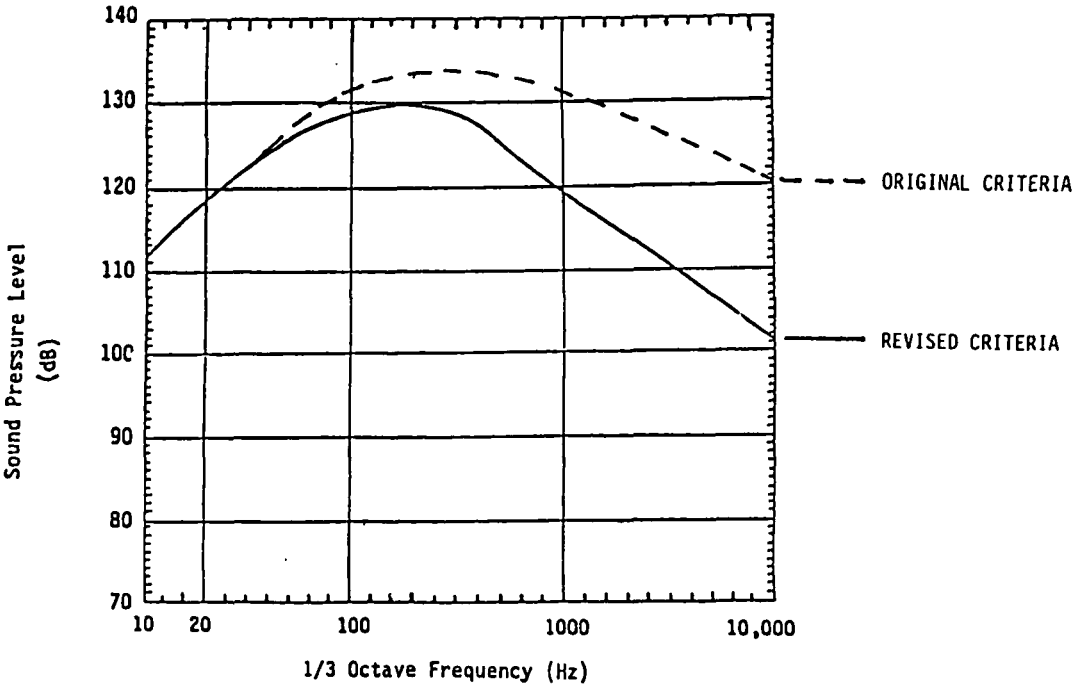

Figure 10. Space shuttle cargo bay acoustic criteria.

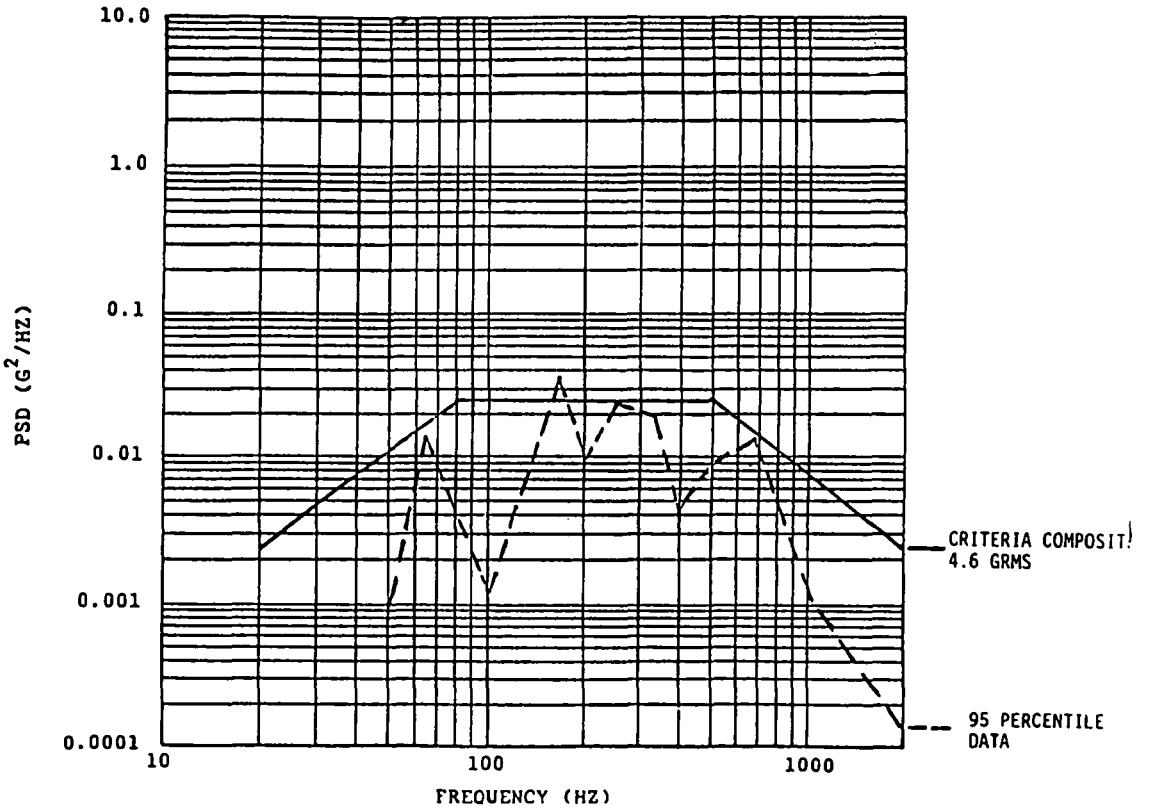

Figure 11. Random vibration criteria - 139 dB basis.

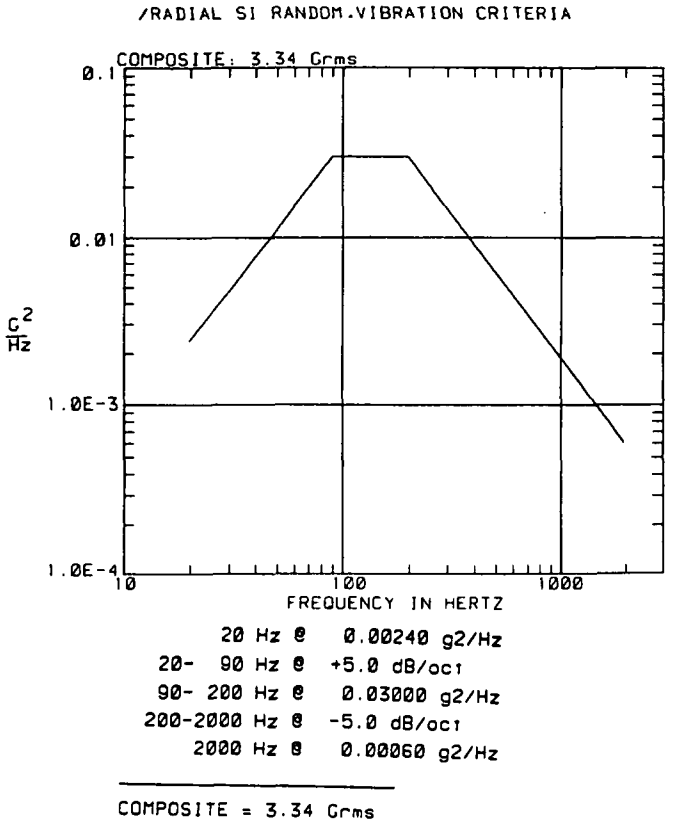

Figure 12. Random vibration criteria.

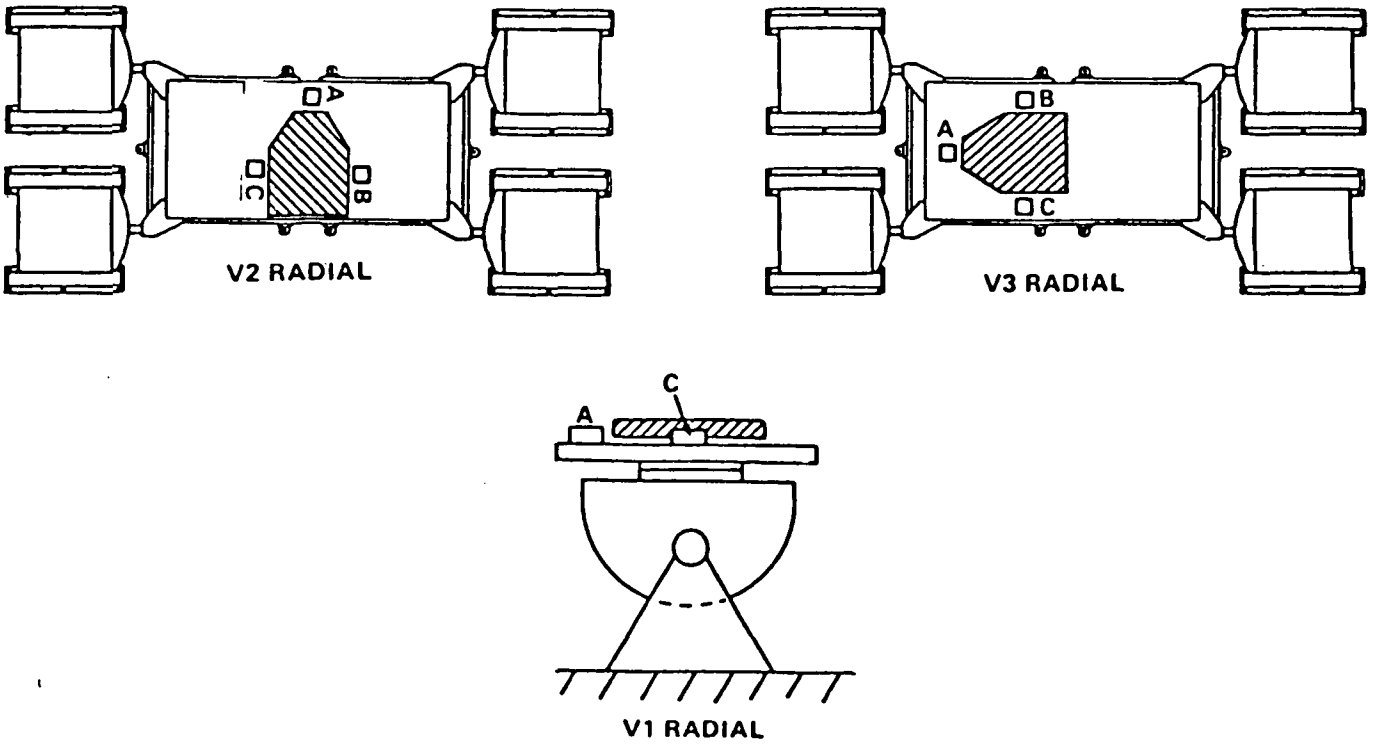

Figure 13. Test configuration.

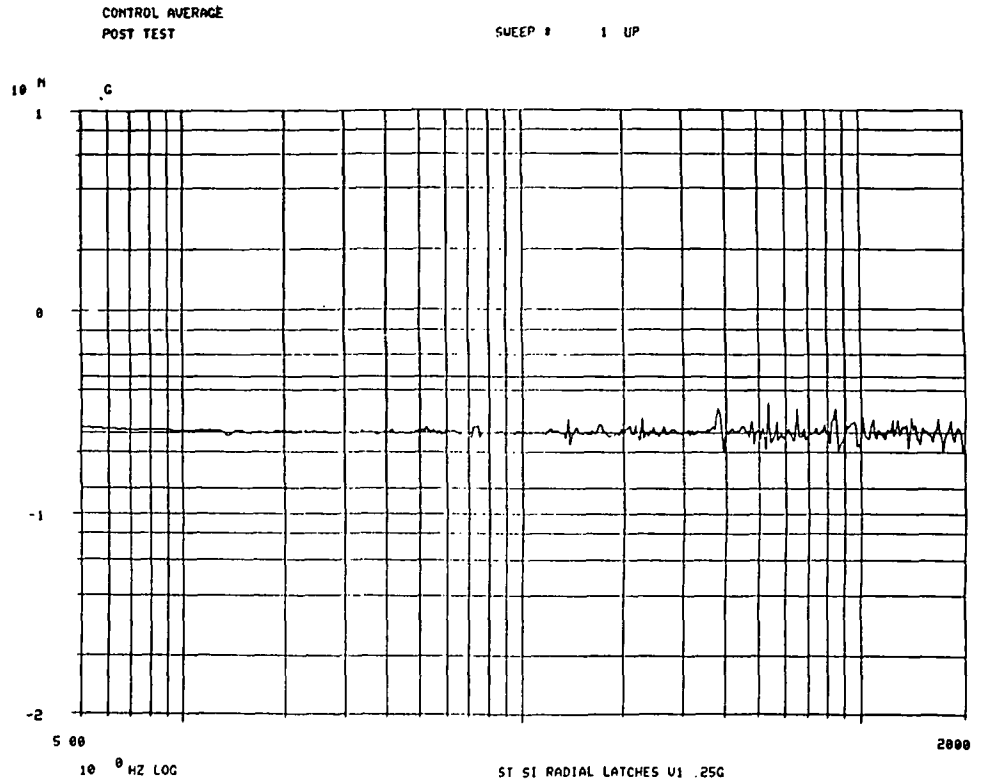

Figure 14. V1 axis sine sweep control average.

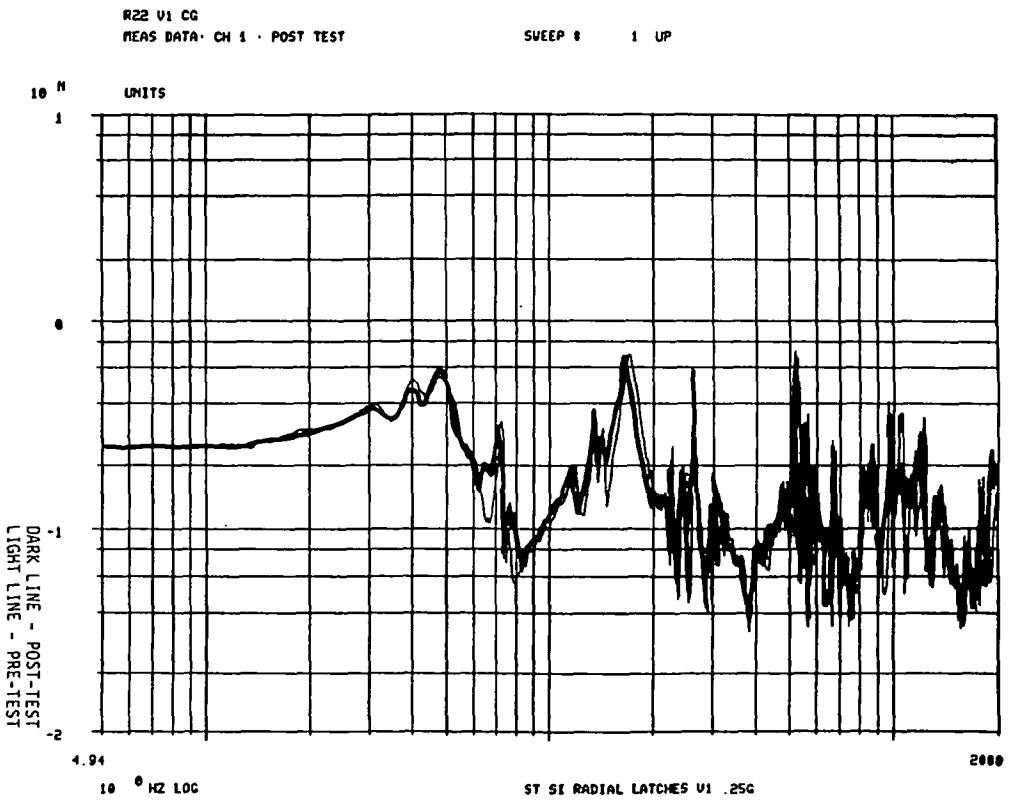

Figure 15. V1 axis c.g. pre- and post-test data.

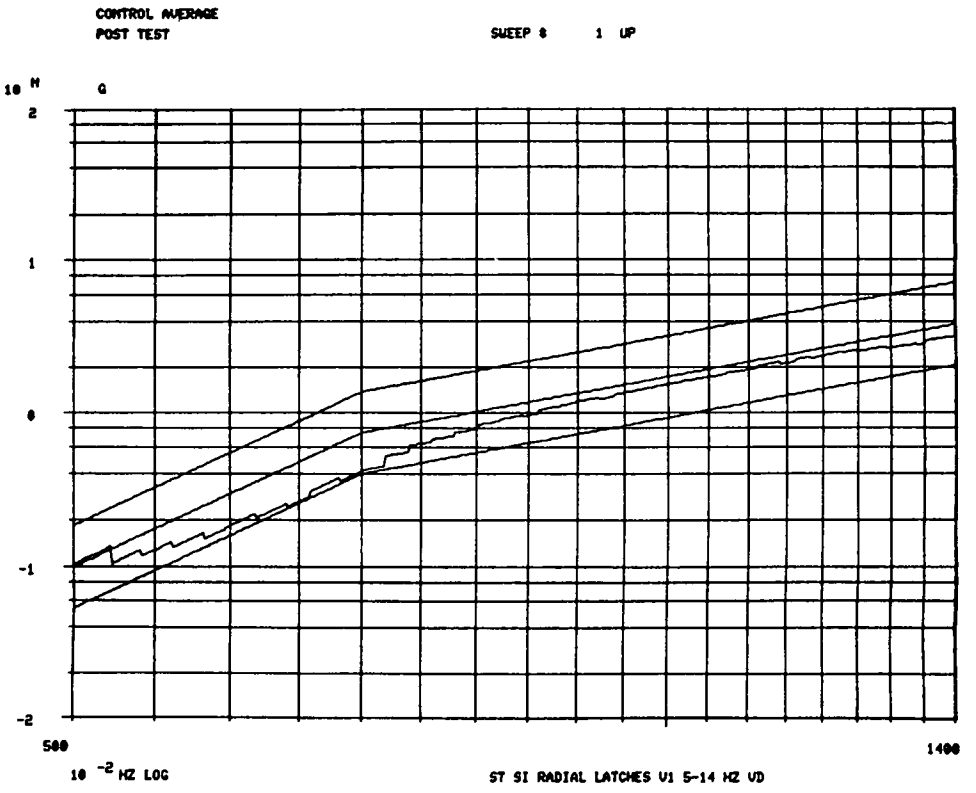

Figure 16. V1 axis transient control average.

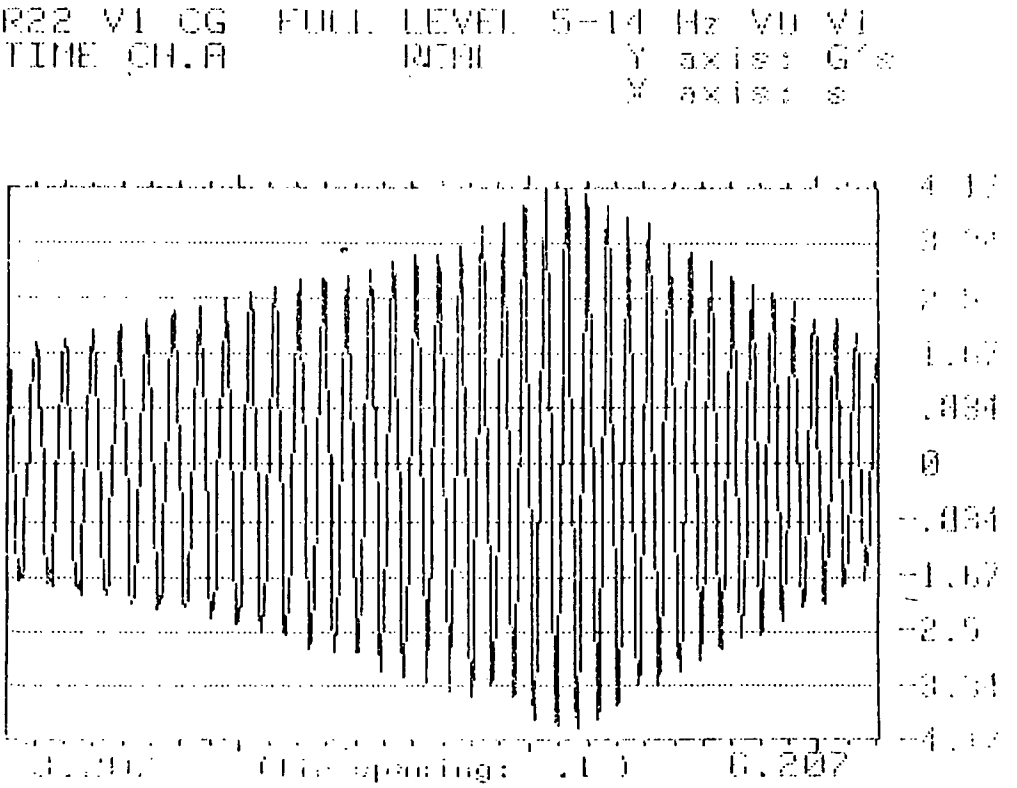

Figure 17. V1 axis c.g. transient response.

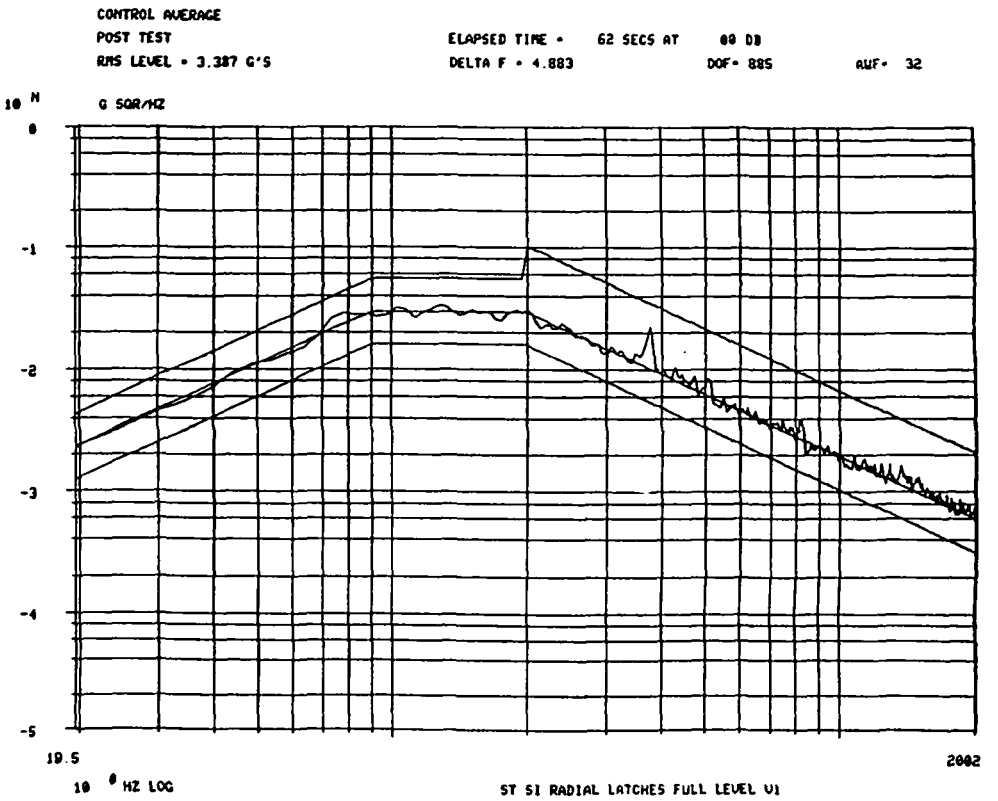

Figure 18. V1 axis random control average.

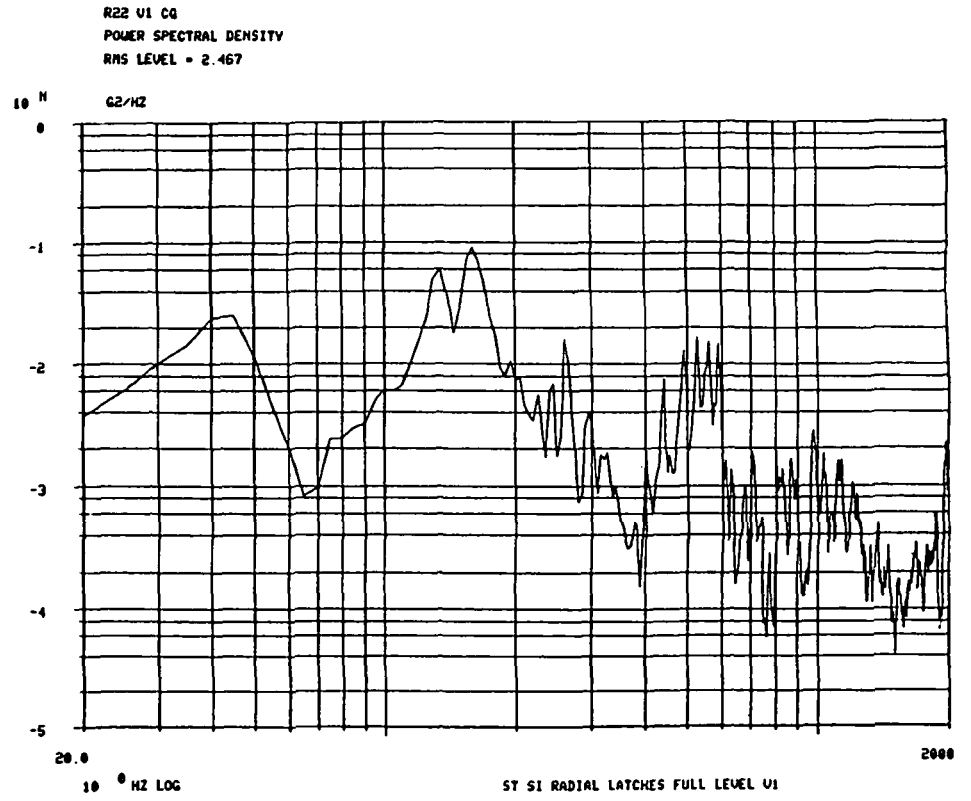

Figure 19. V1 axis c.g. random response.

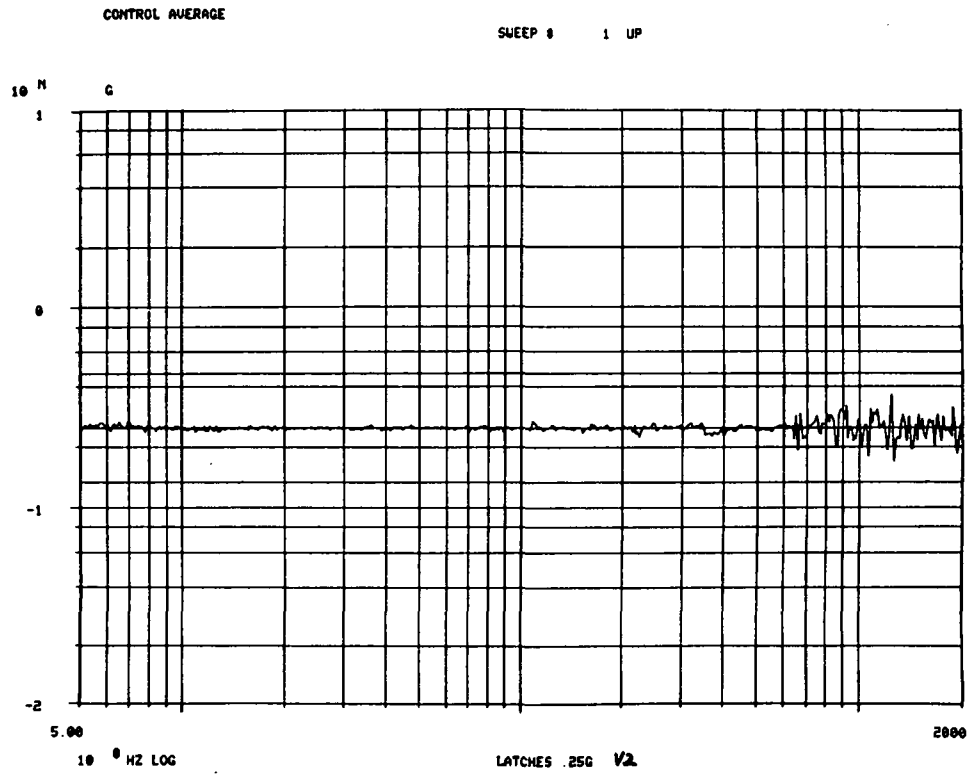

Figure 20. V2 axis sine sweep control average.

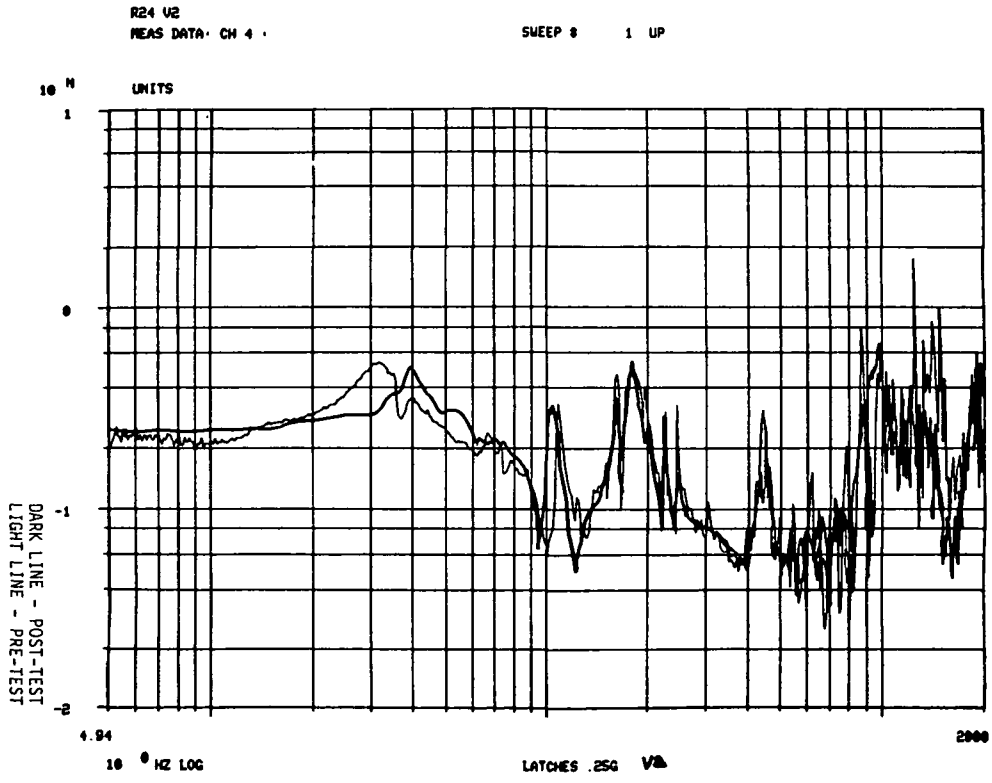

Figure 21. V2 axis c.g. pre- and post-test data.

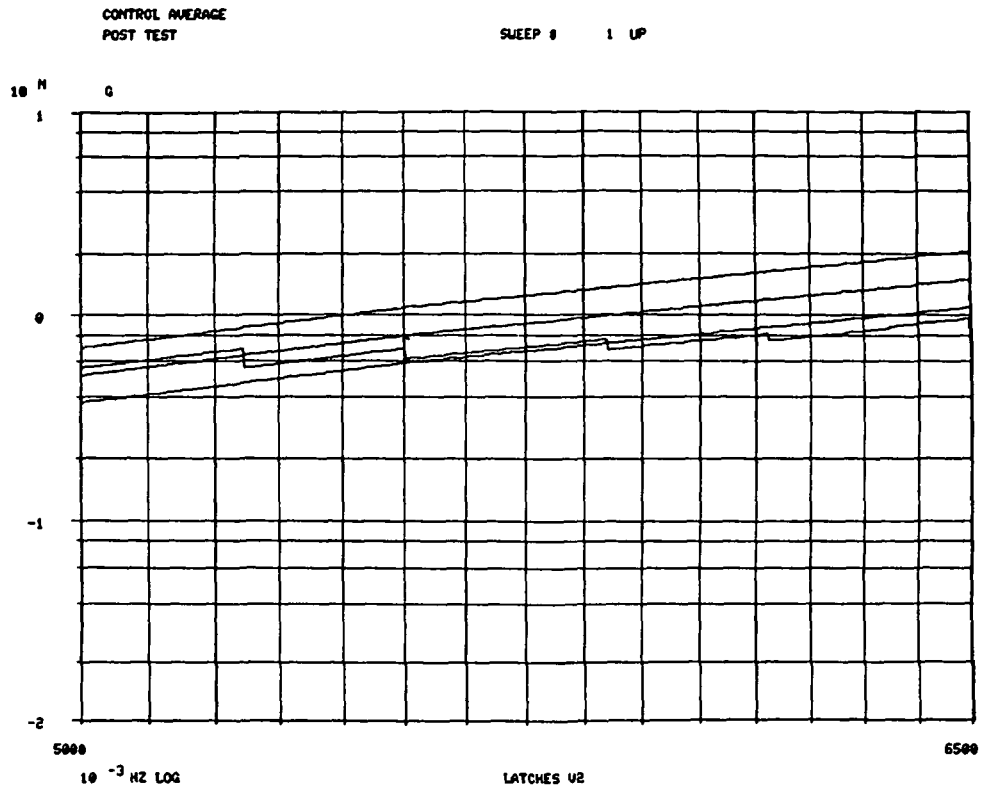

Figure 22. V2 axis transient control average - test 1.

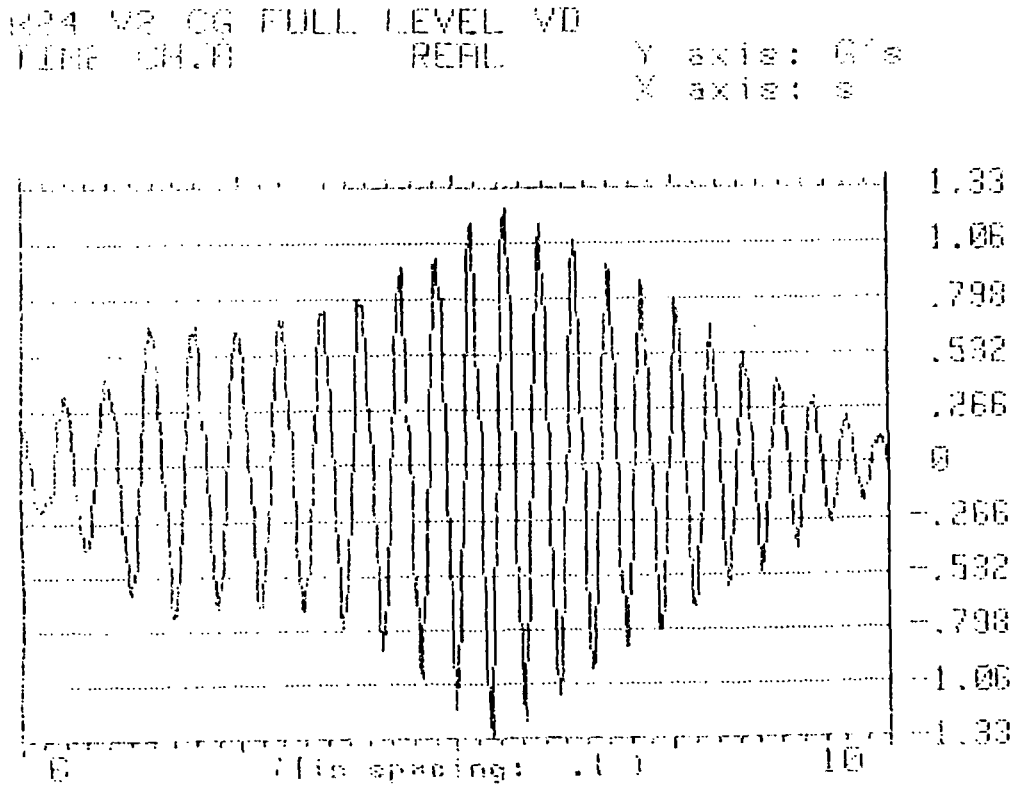

Figure 23. V2 axis c.g. transient response.

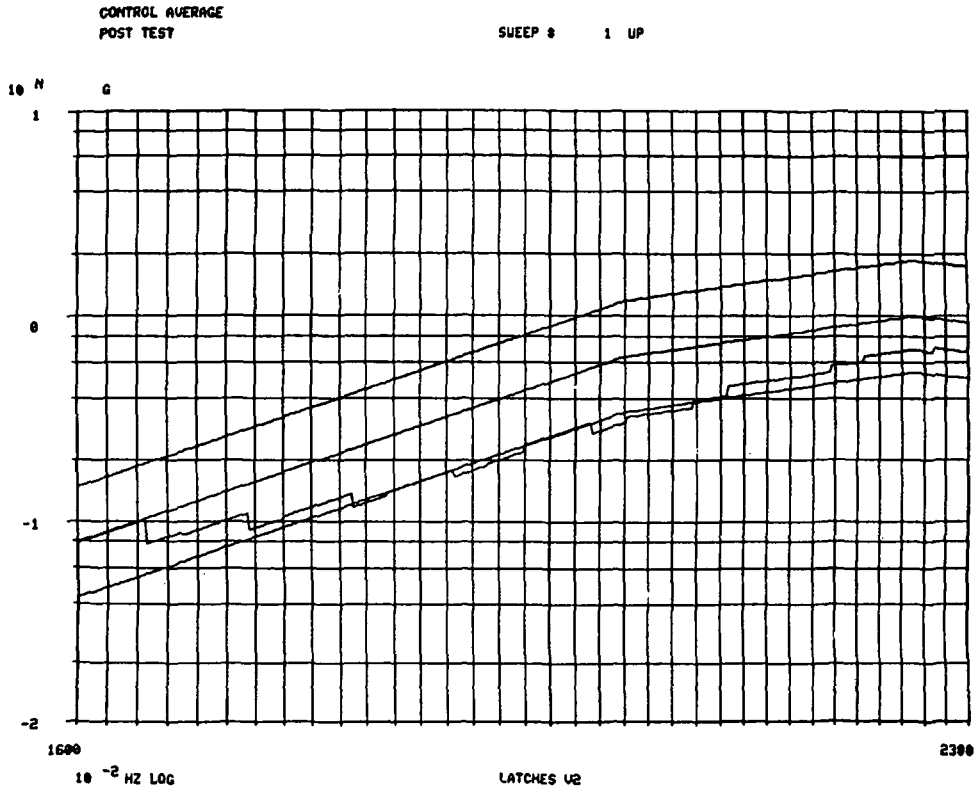

Figure 24. V2 axis transient control average - test 2.

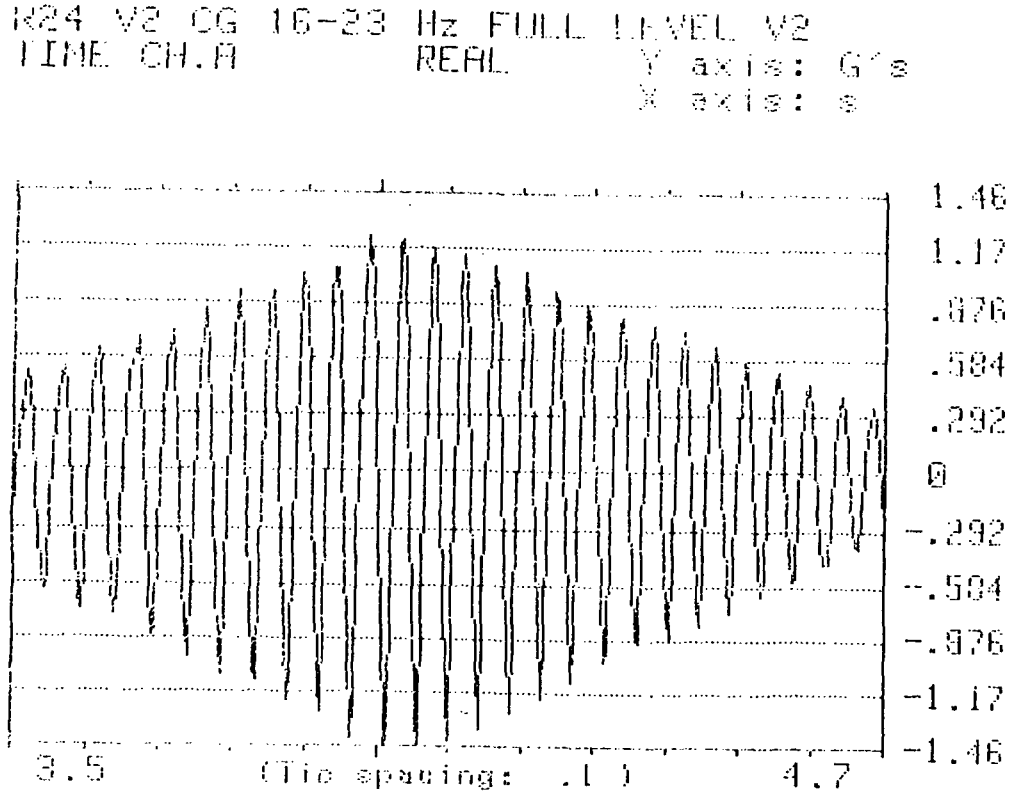

Figure 25. V2 axis c.g. transient response.

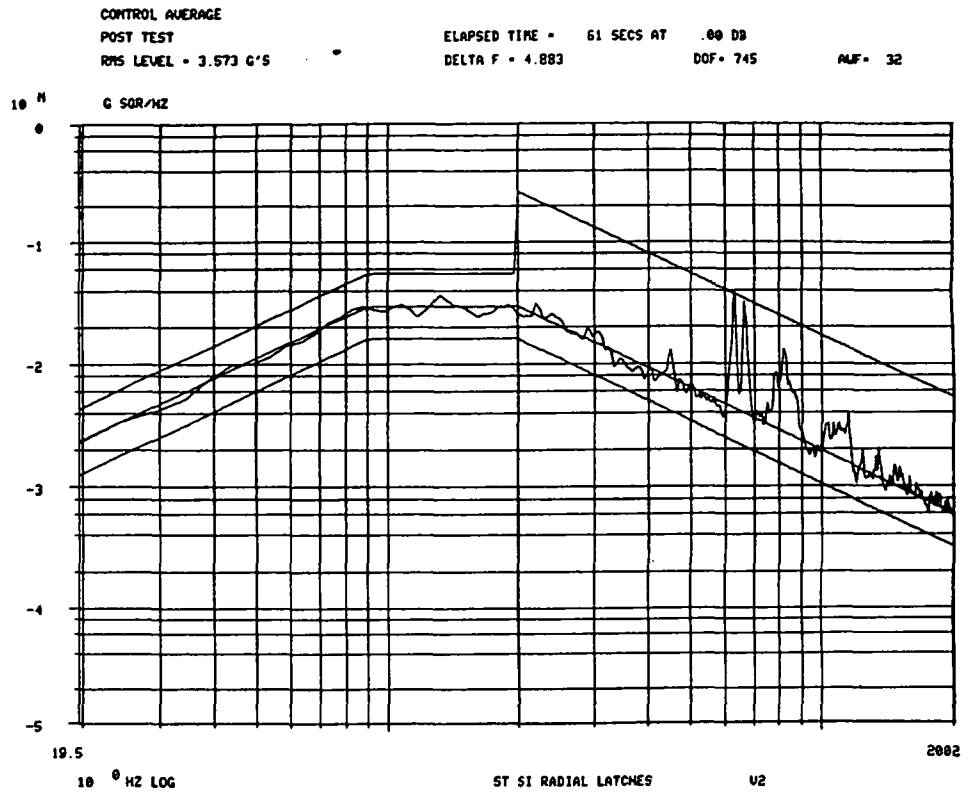

Figure 26. V2 axis random control average.

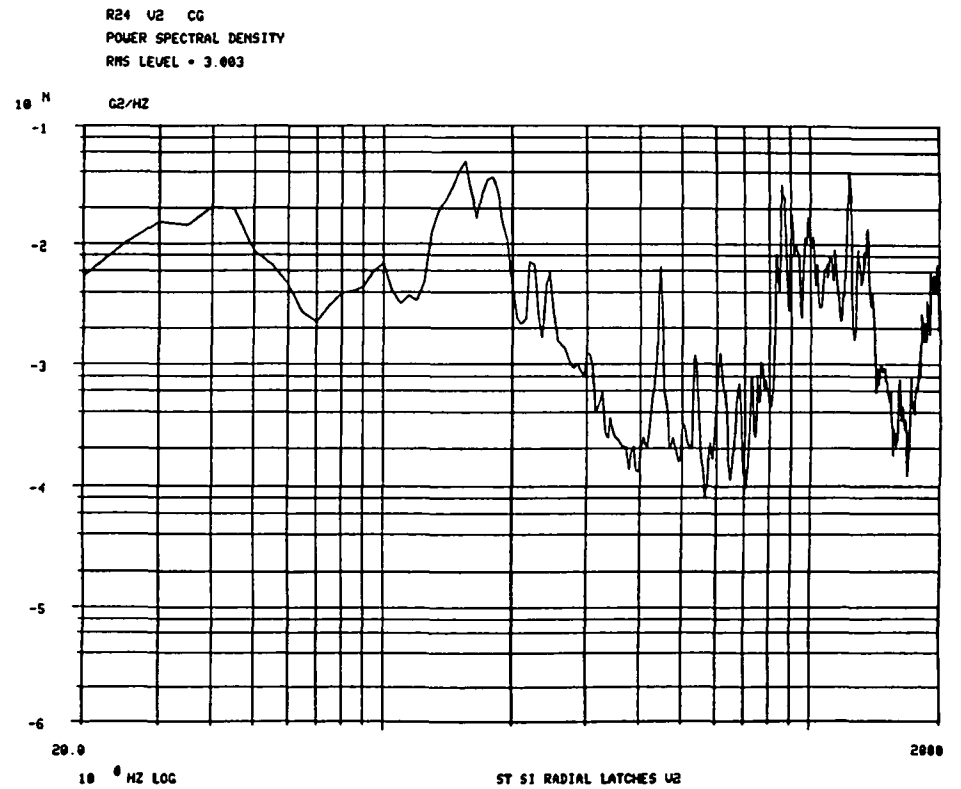

Figure 27. V2 axis c.g. random response.

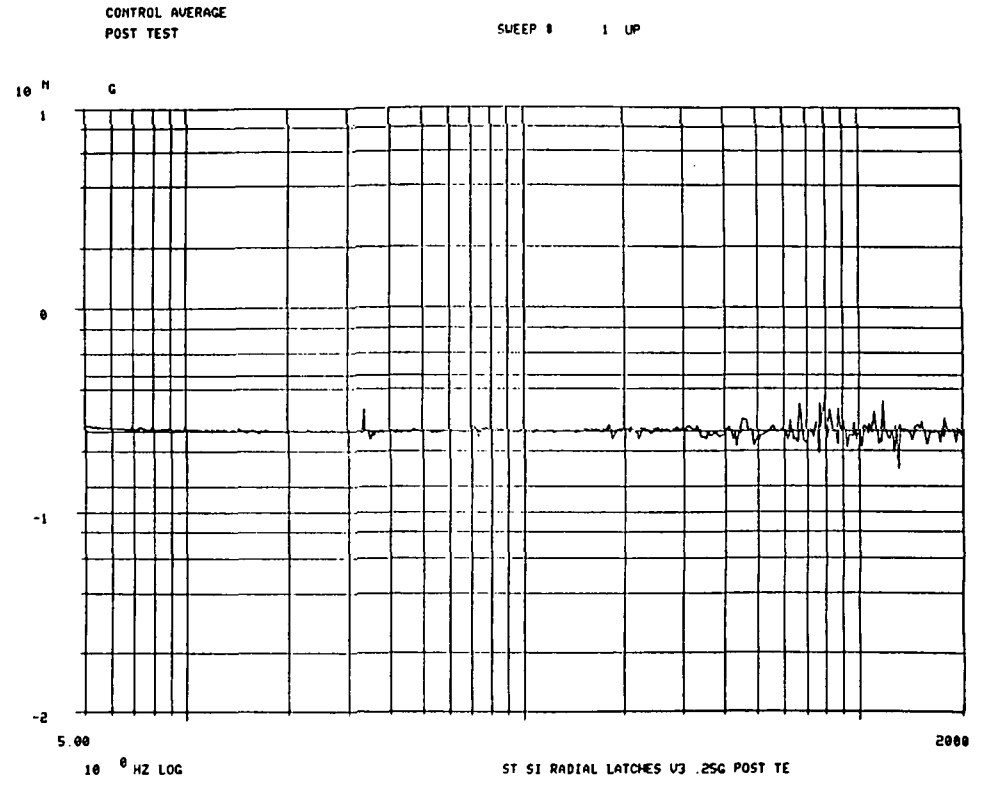

Figure 28. V3 axis sine sweep control average.

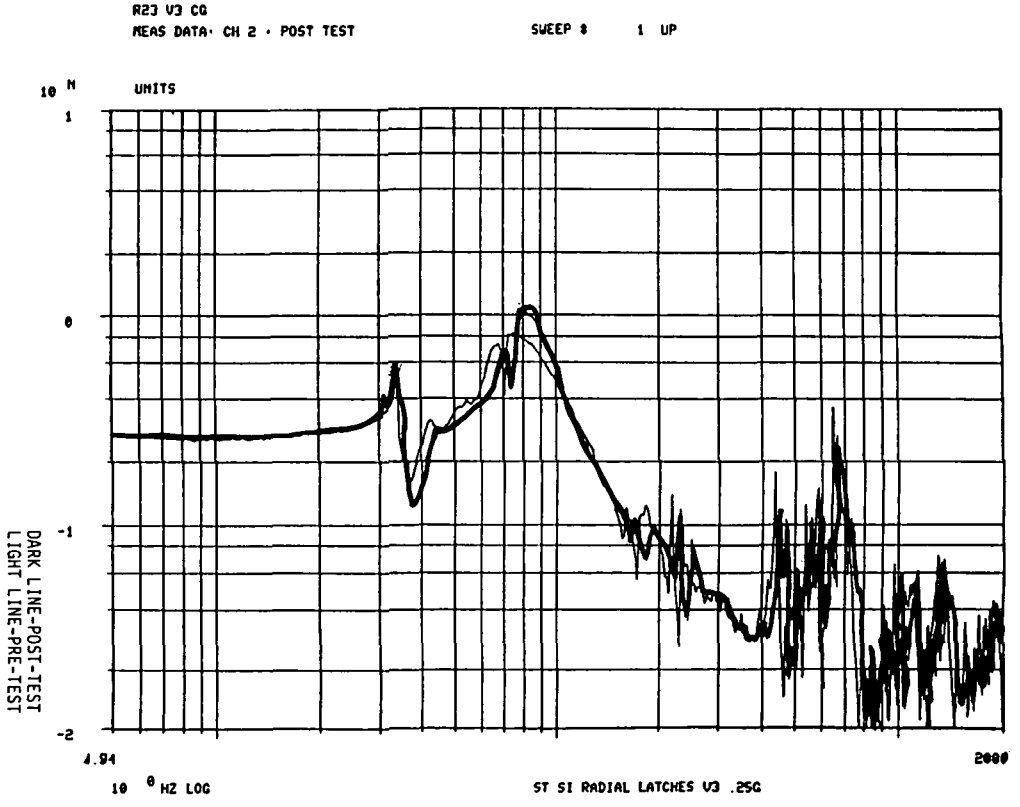

Figure 29. V3 axis c.g. pre- and post- test data.

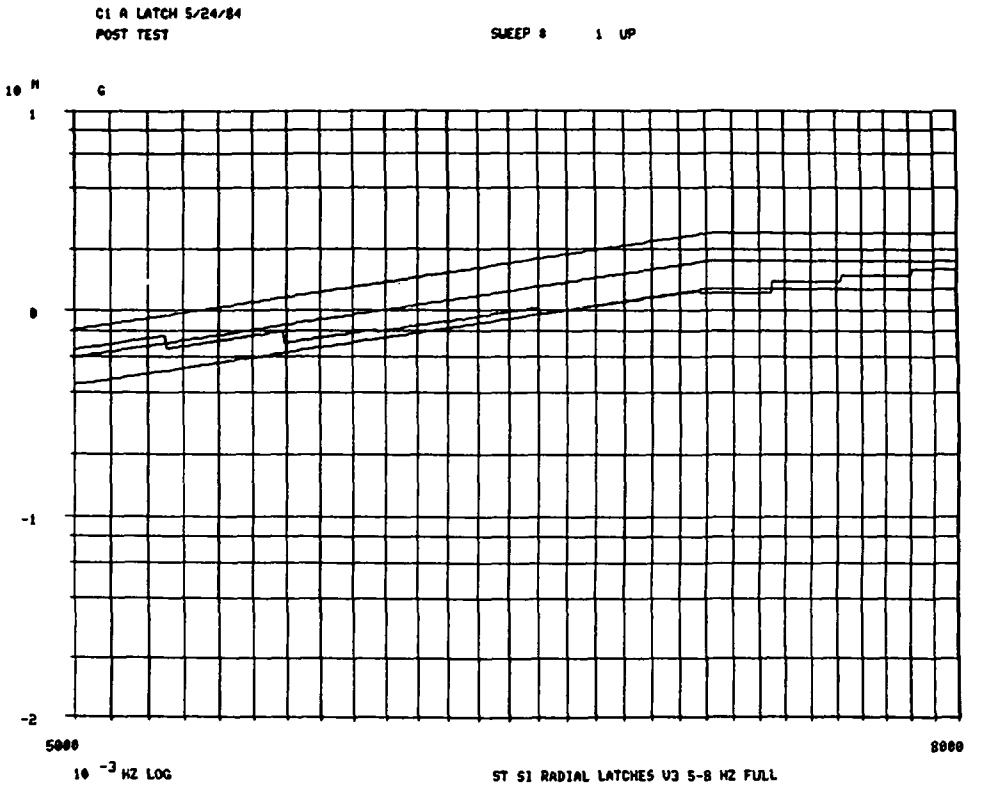

Figure 30. V3 axis transient control average - test 1.

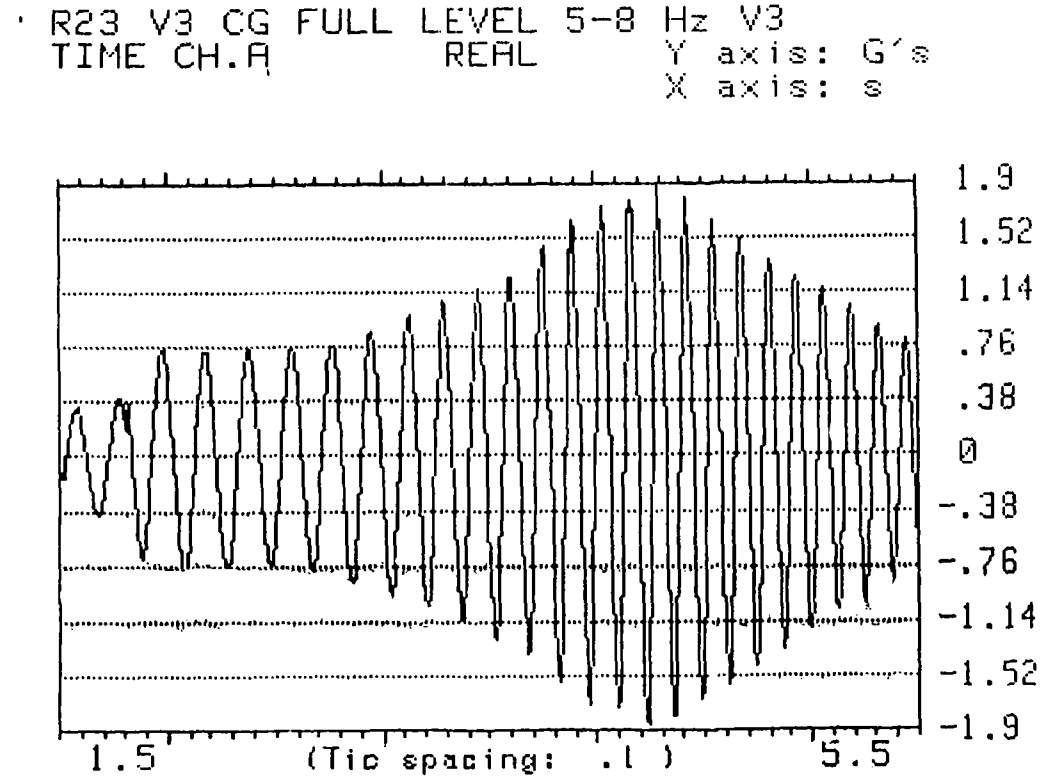

Figure 31. V3 axis c.g. transient response.

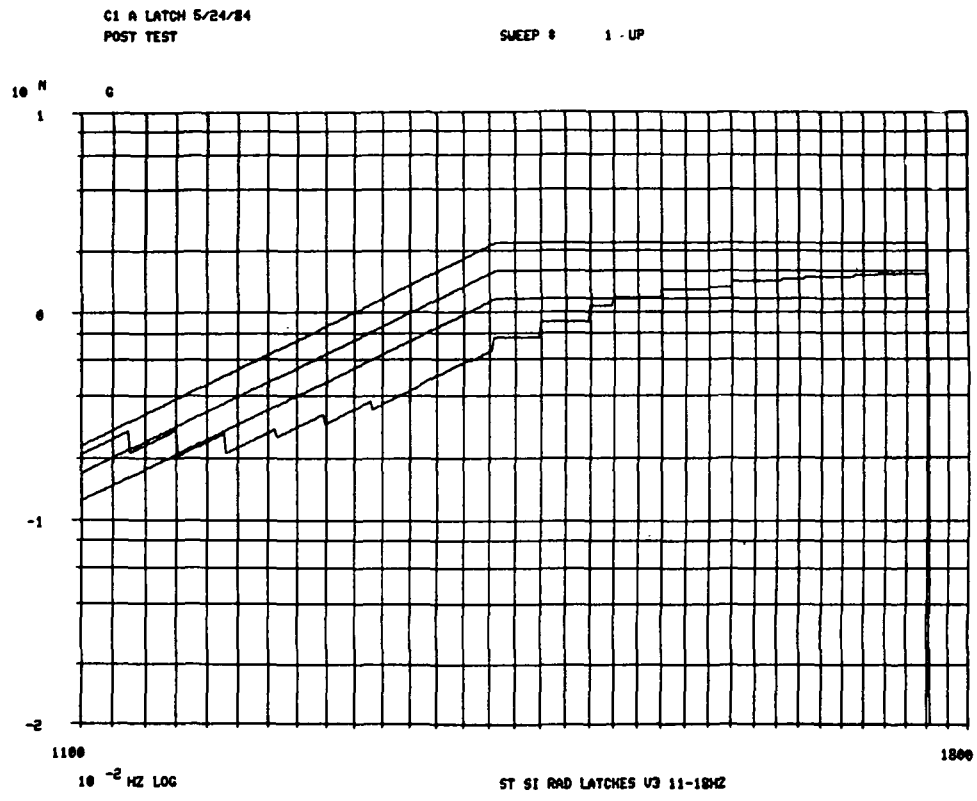

Figure 32. V3 axis transient control average - test 2.

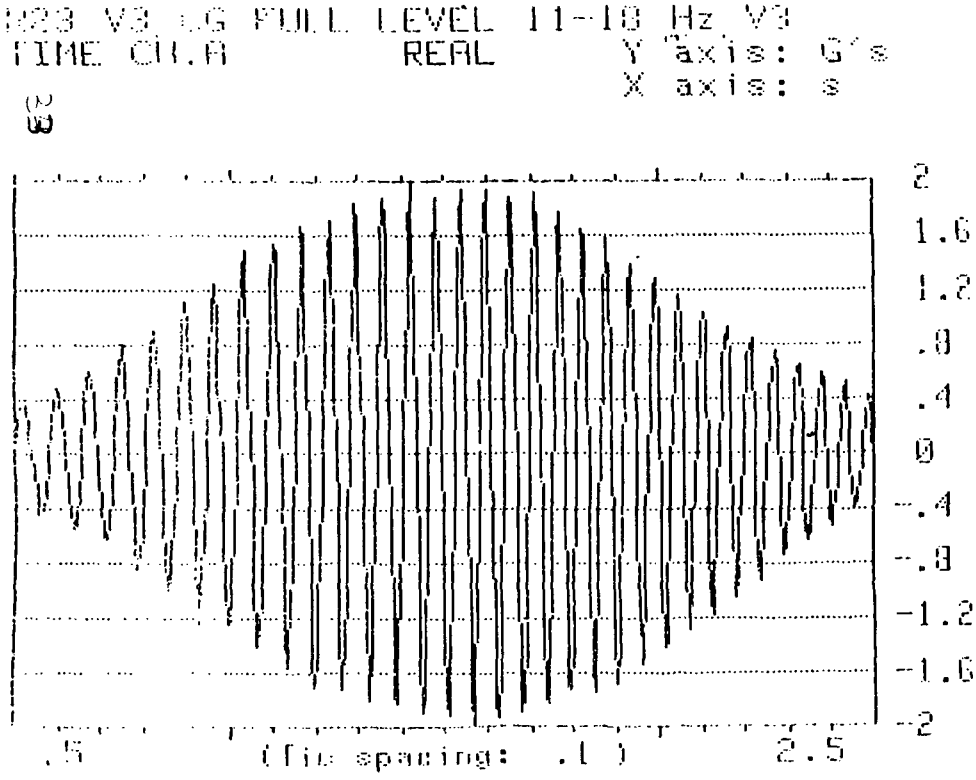

Figure 33. V3 axis c.g. transient response.

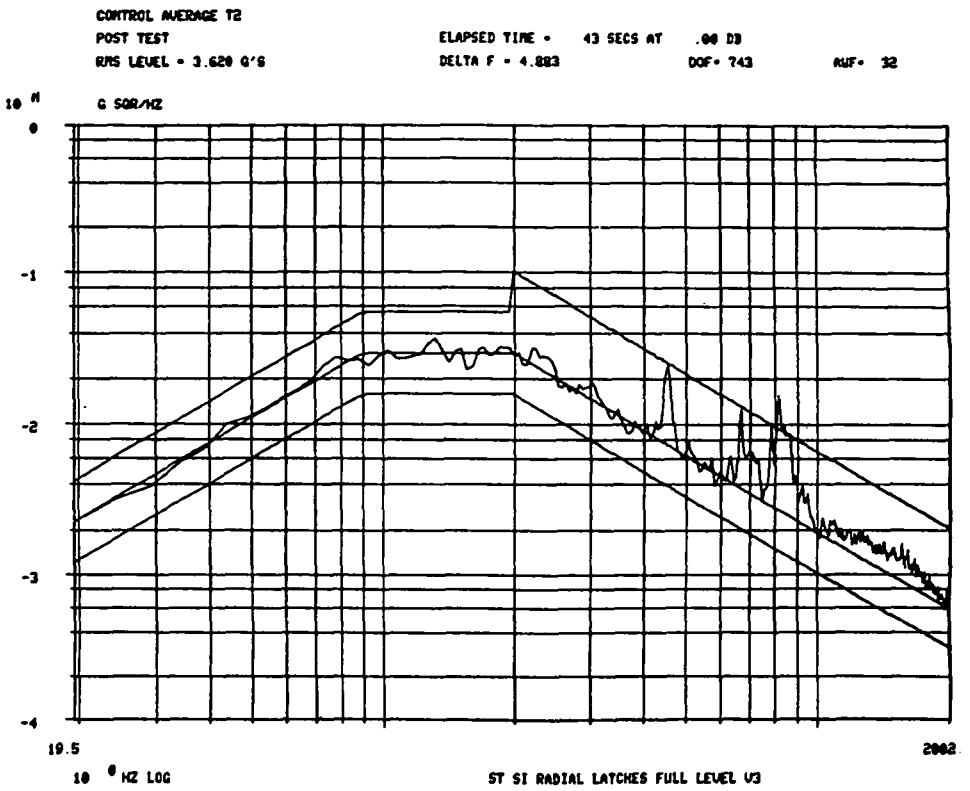

Figure 34. V3 axis random control average.

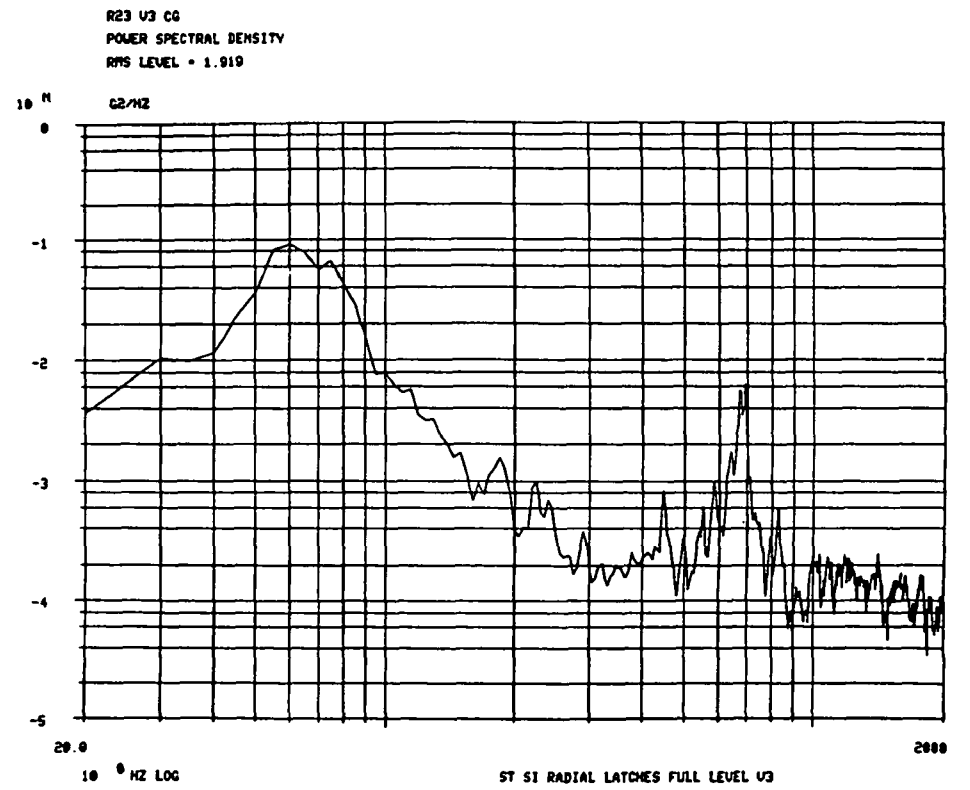

Figure 35. V3 axis random response.

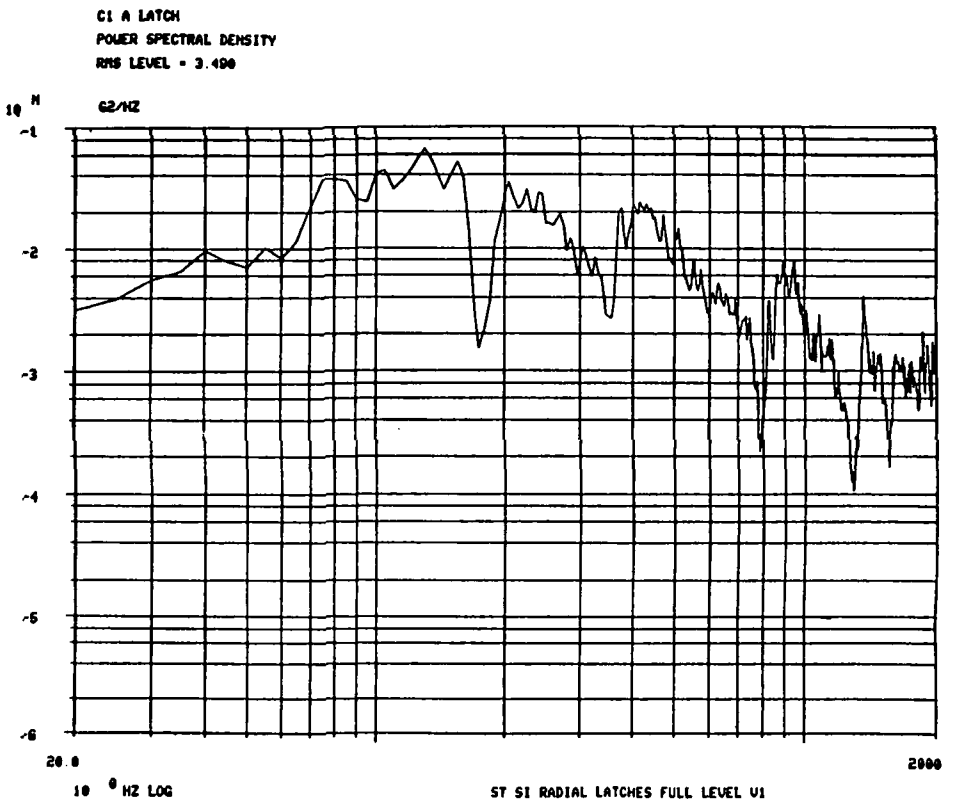

Figure 36. "A" latch random input.

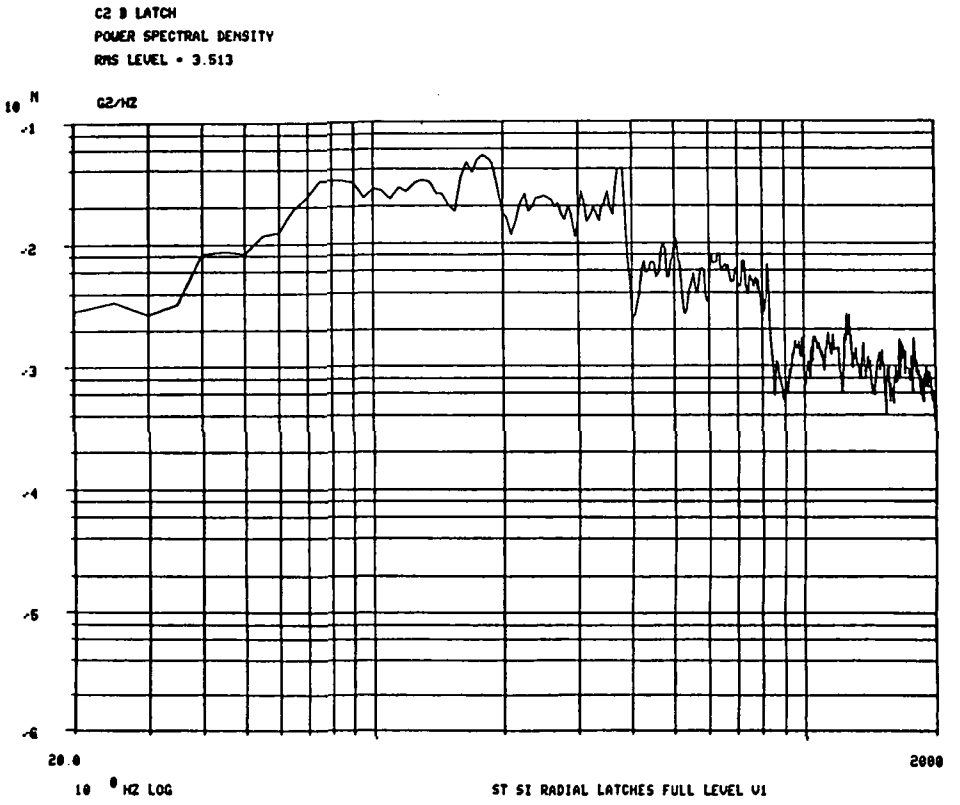

Figure 37. "B" latch random input.

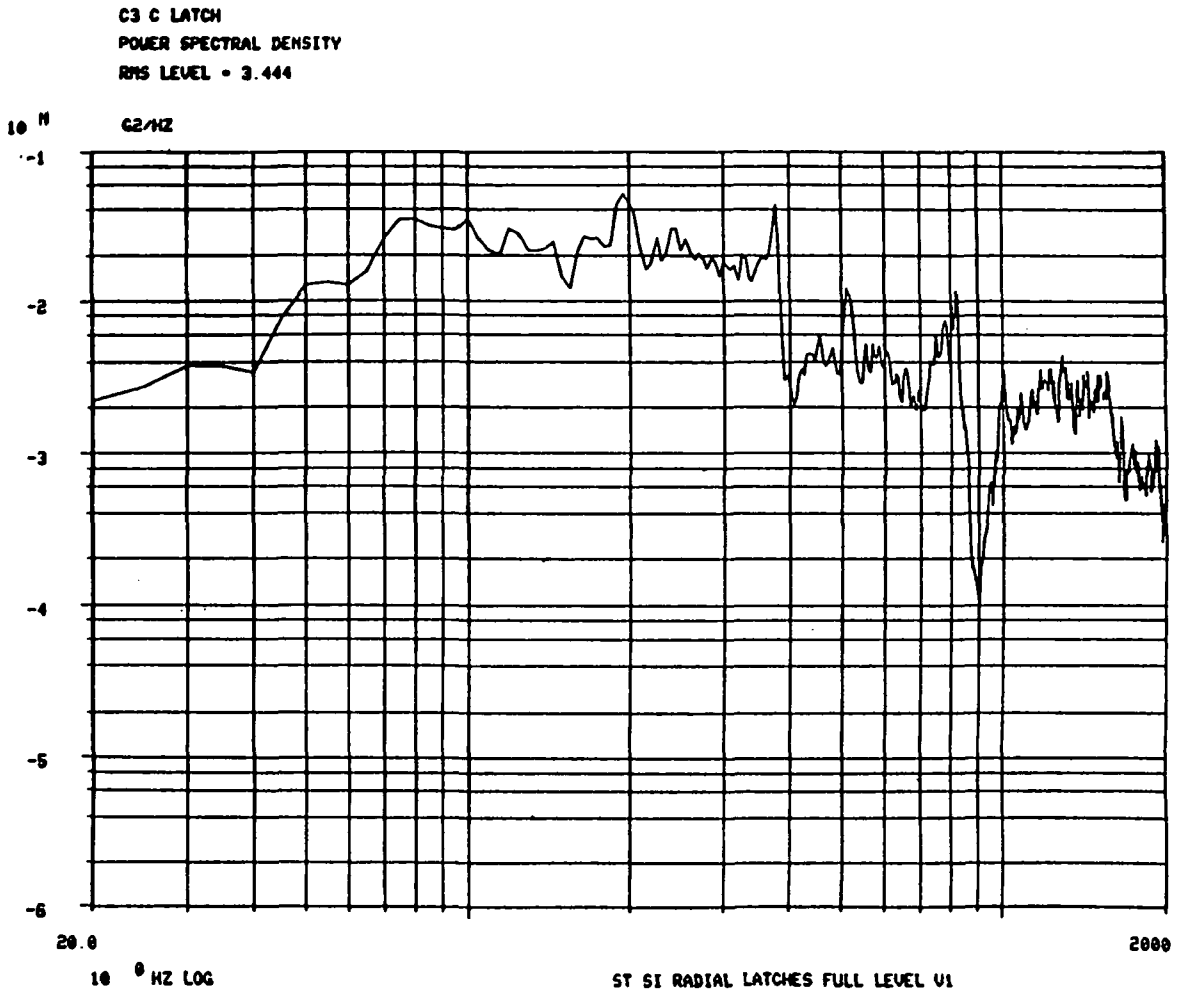

Figure 38. "C" latch random input.

Page intentionally left blank

Page intentionally left blank

APPENDIX B

DATA ANALYSIS PLOTS

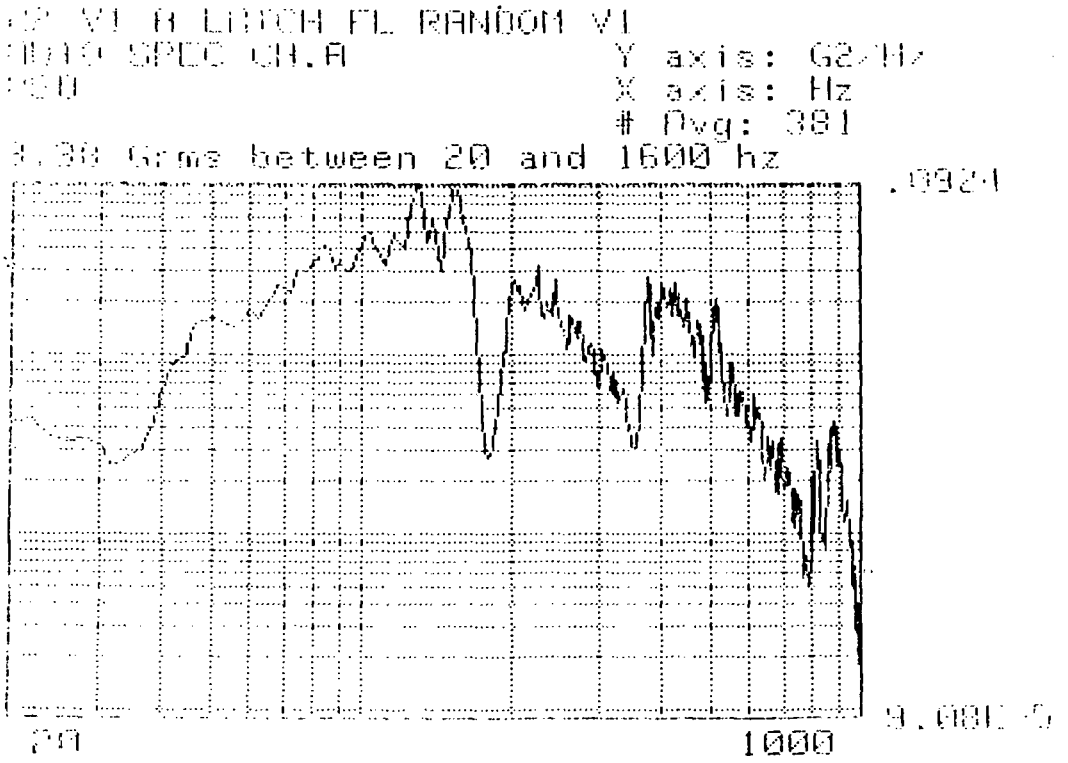

Figure 39. V1 "A" latch random auto spectral density.

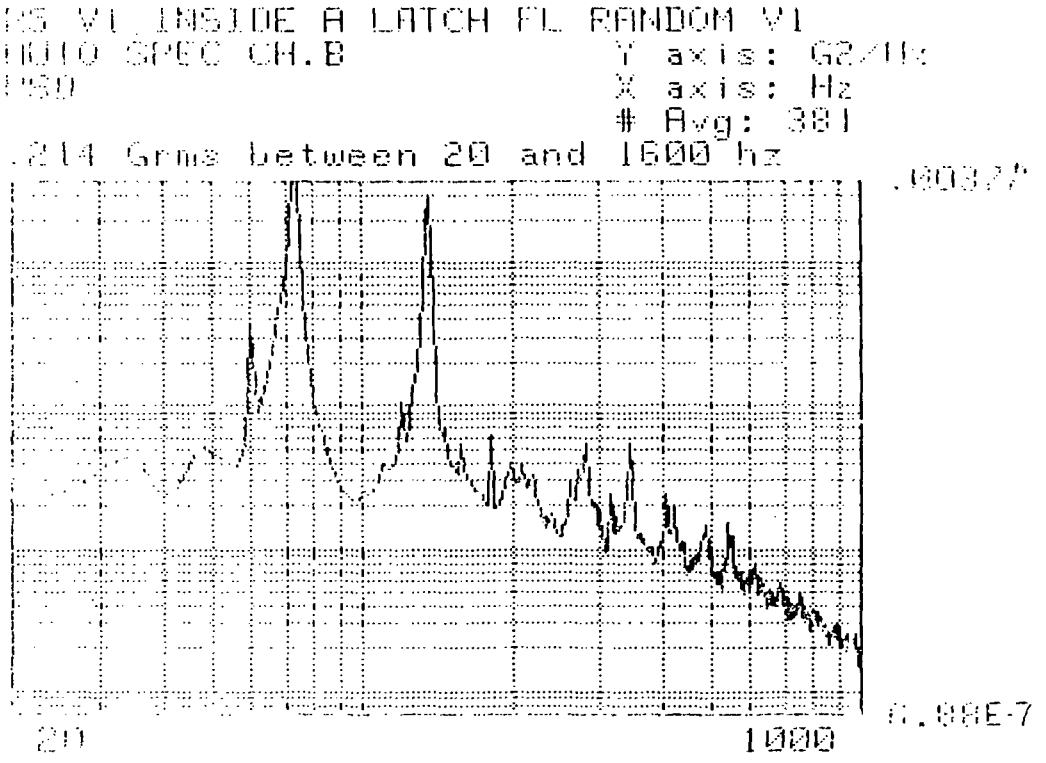

Figure 40. V1 inside "A" latch random auto spectral density.

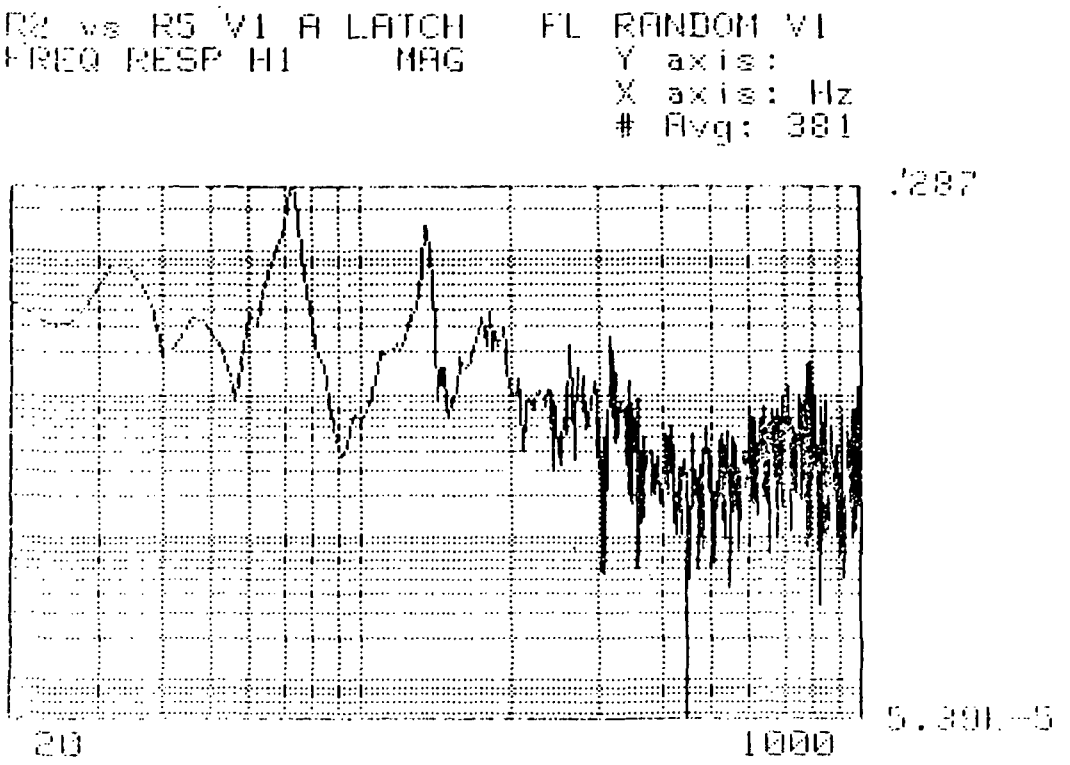

Figure 41. "A" latch transfer function.

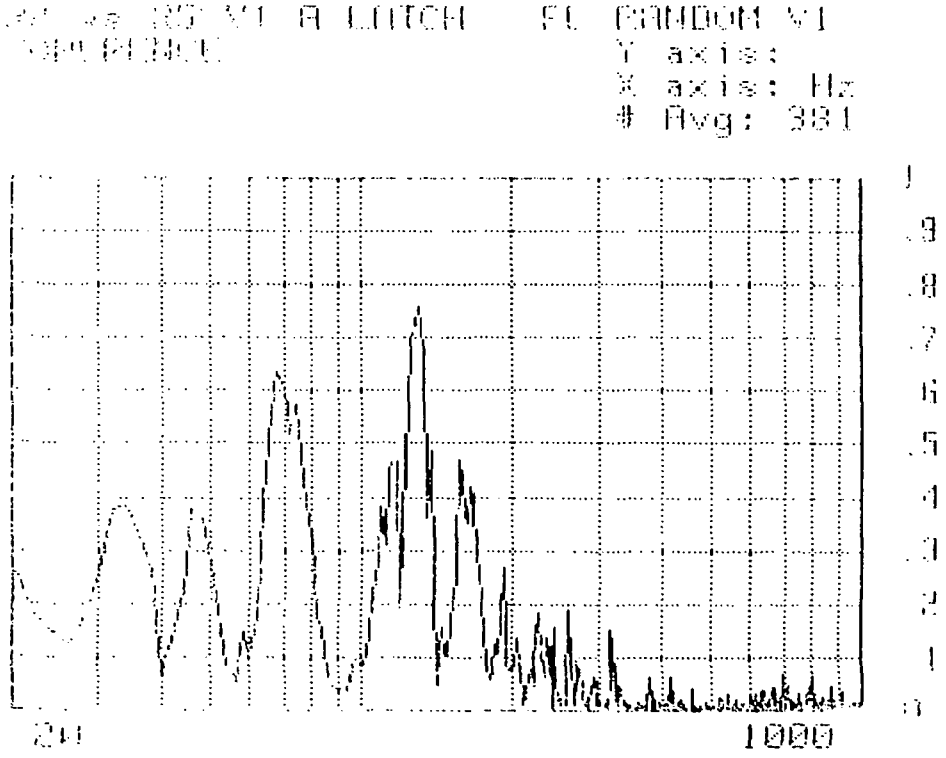

Figure 42. "A" latch coherence.

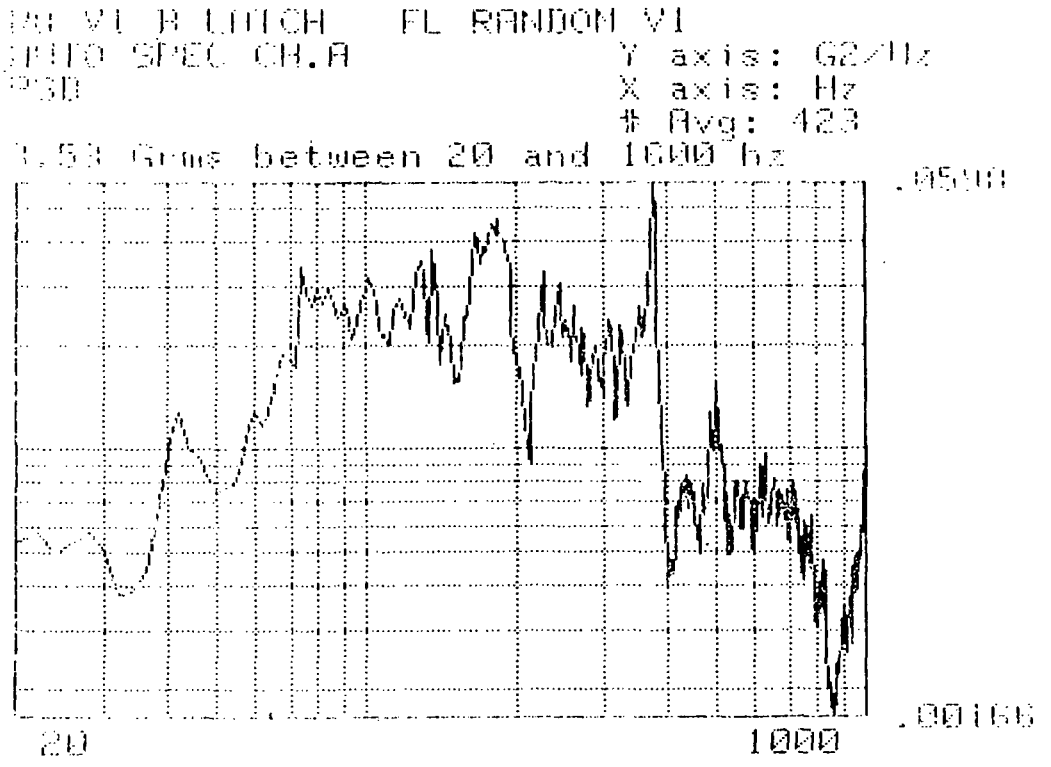

Figure 43. V1 "B" latch random auto spectral density.

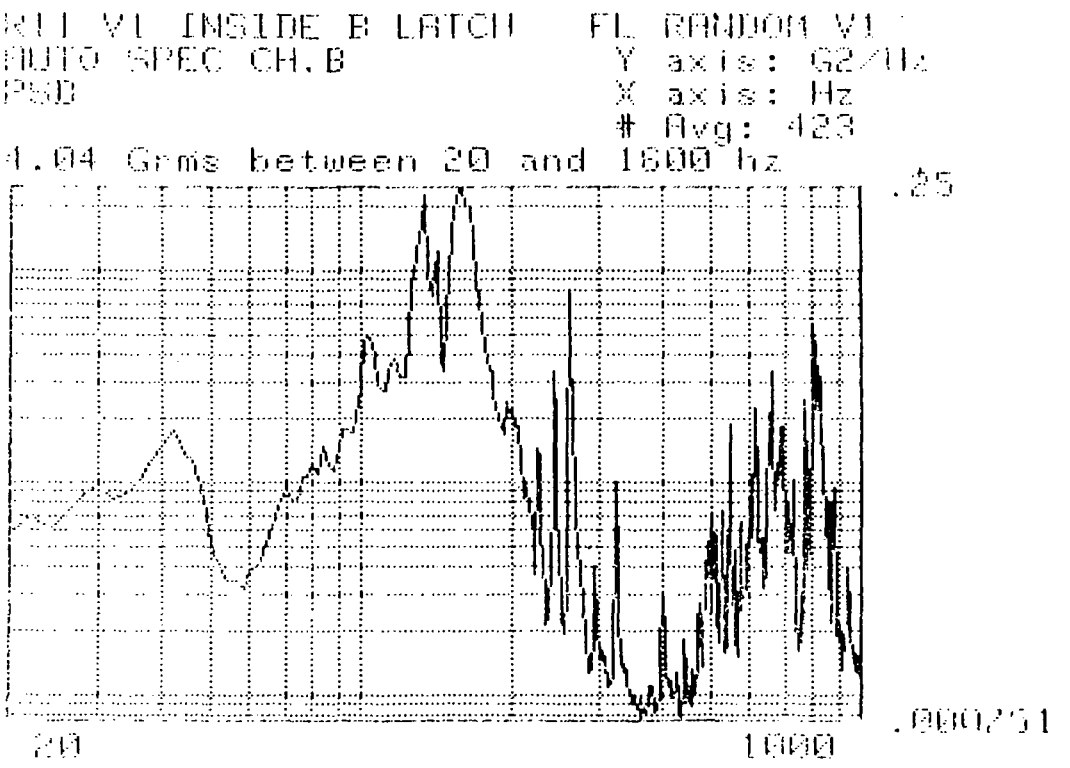

Figure 44. V1 inside "B" latch random auto spectral density.

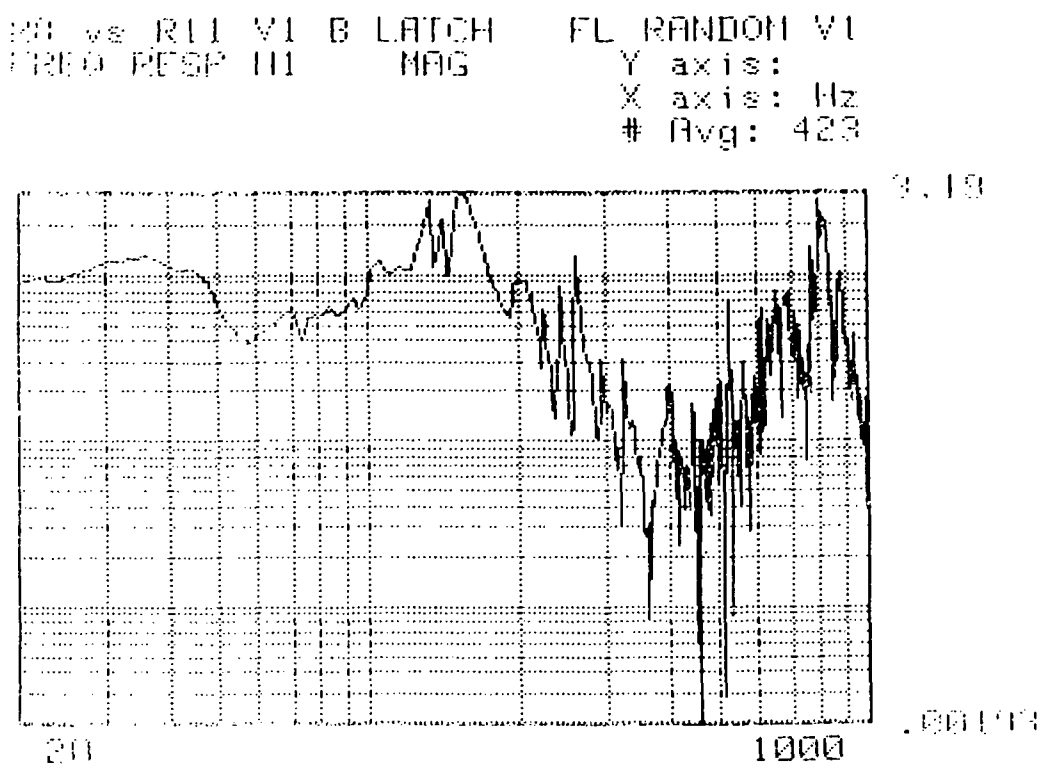

Figure 45. "B" latch transfer function.

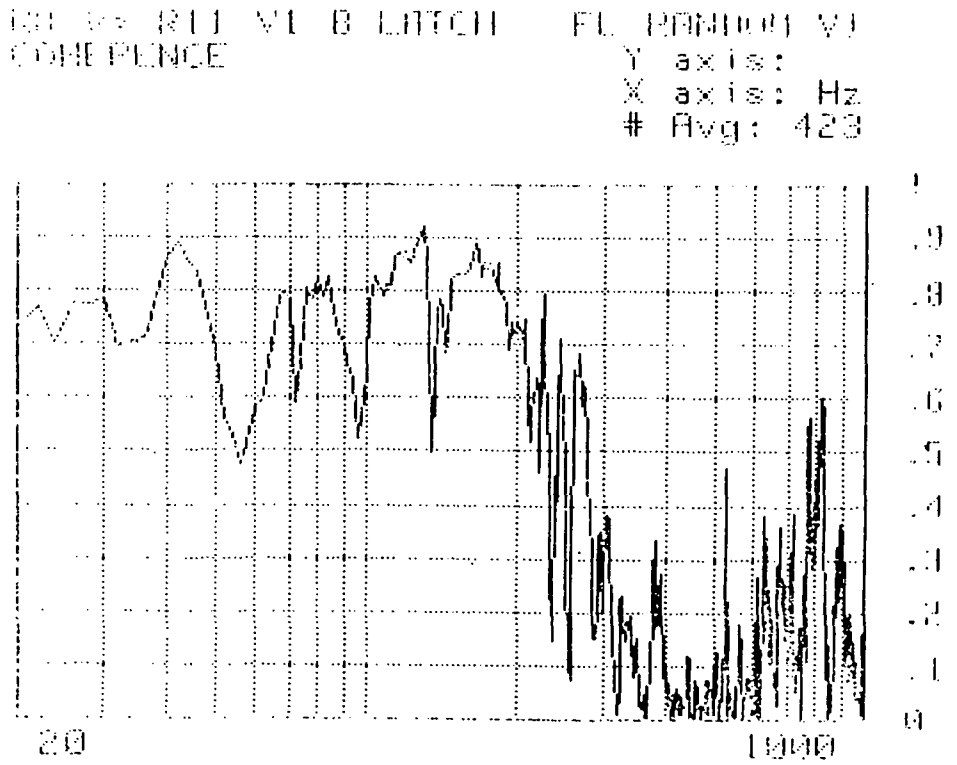

Figure 46. "B" latch coherence.

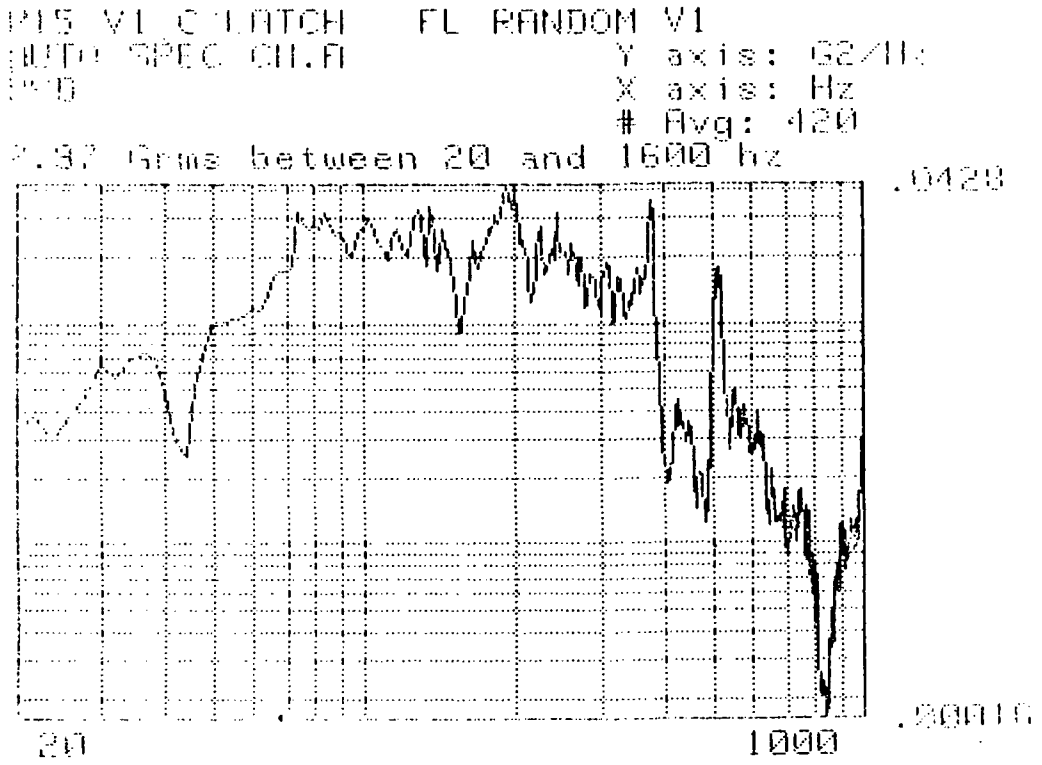

Figure 47. V1 "C" latch random auto spectral density.

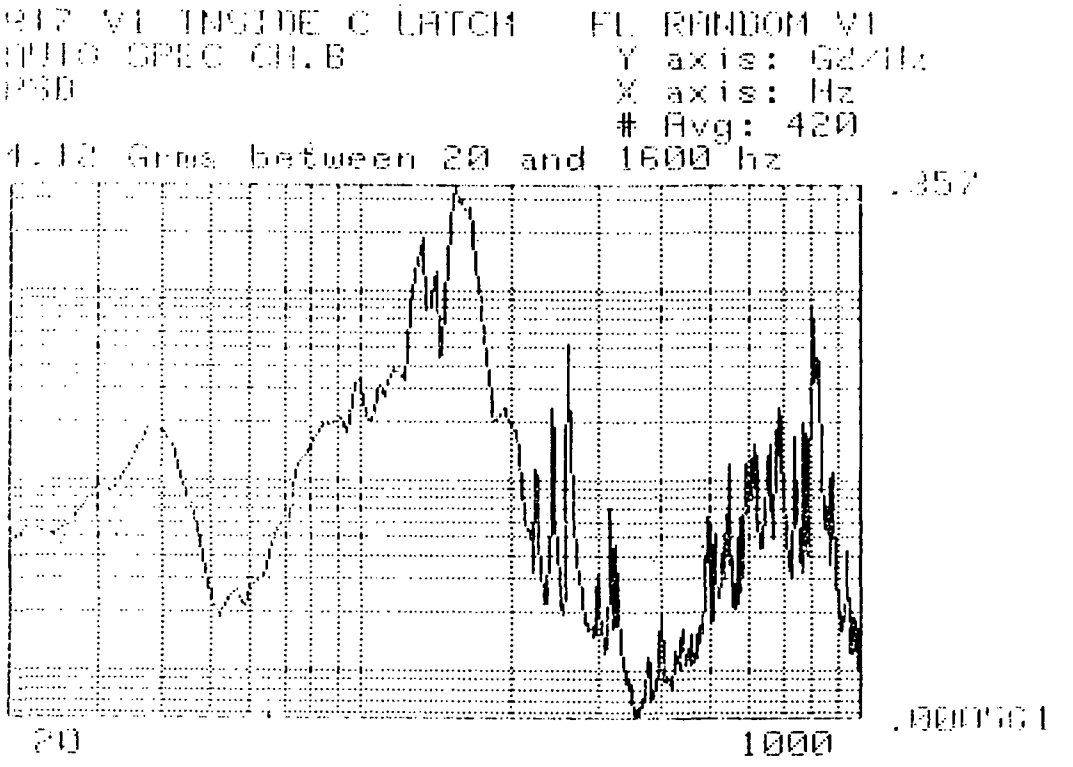

Figure 48. V1 inside "C" latch random auto spectral density.

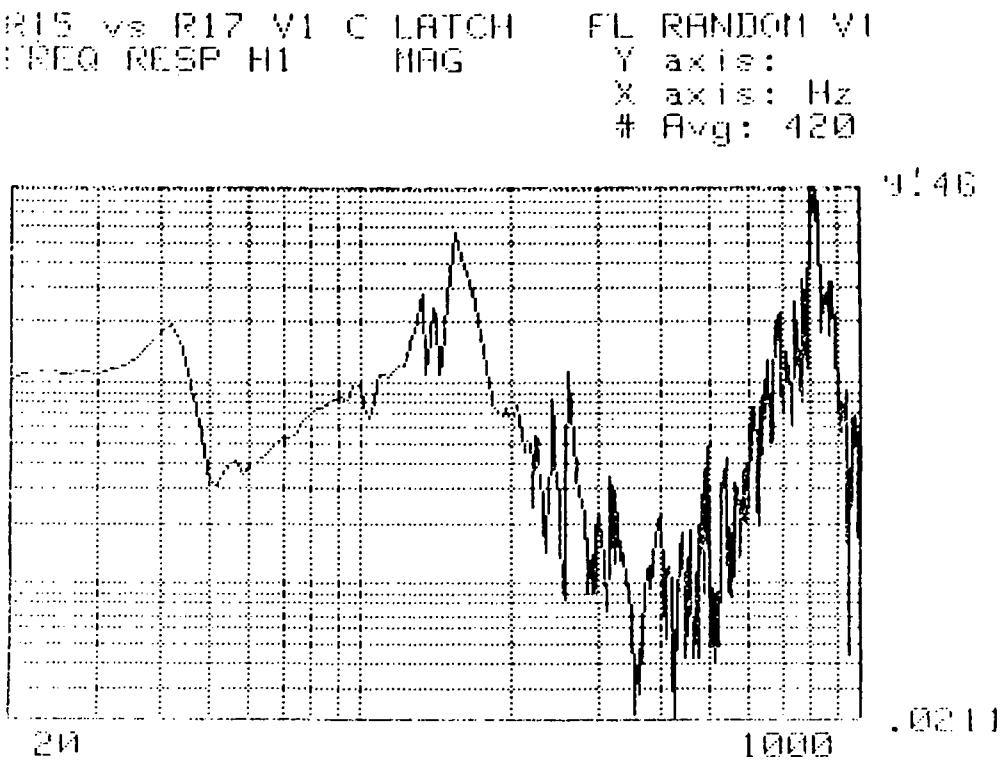

Figure 49. "C" latch transfer function.

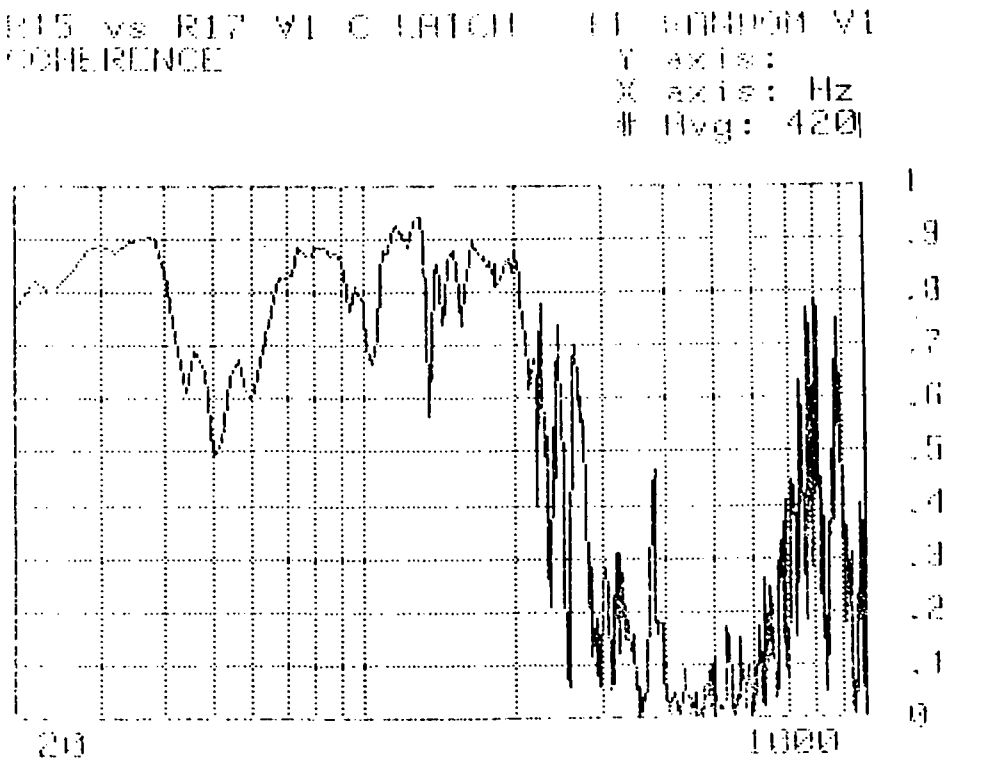

Figure 50. "C" latch coherence.

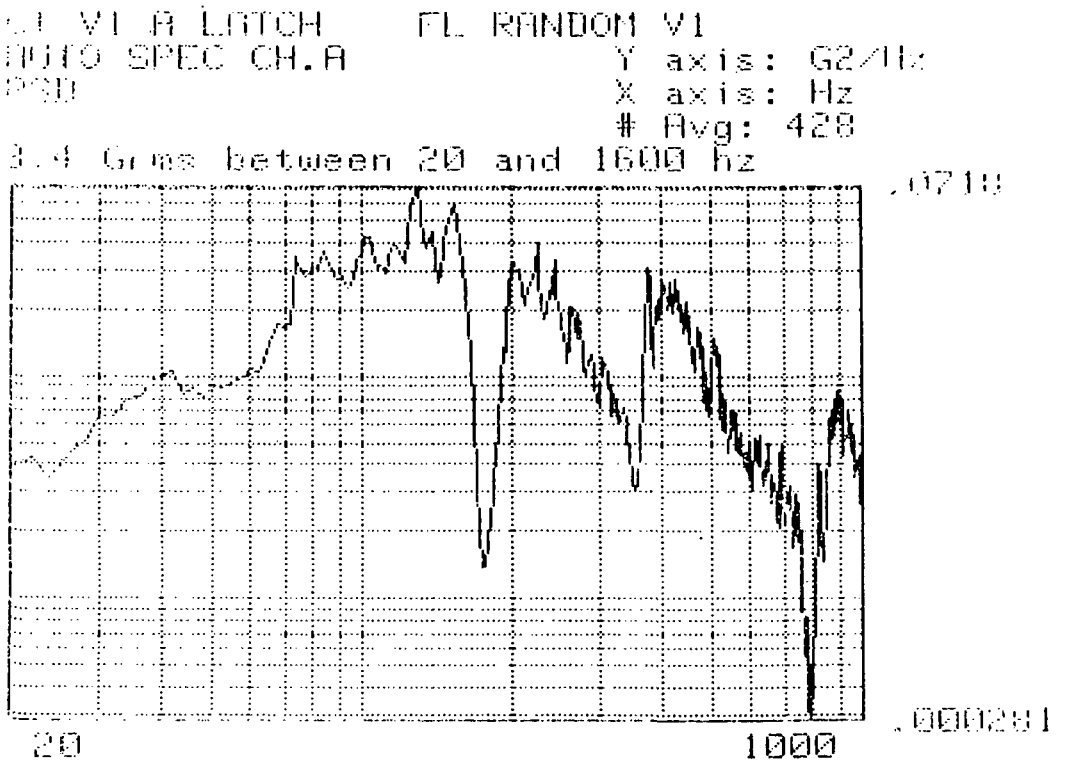

Figure 51. V1 "A" latch random input auto spectral density.

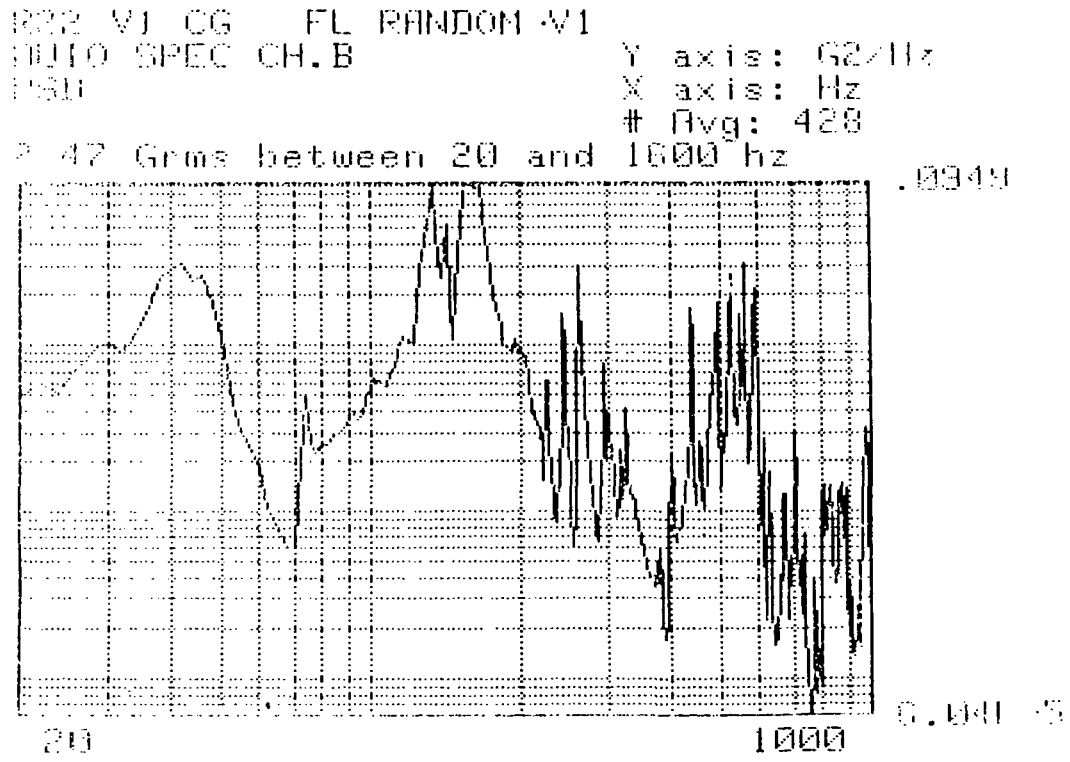

Figure 52. V1 c.g. response auto spectral density.

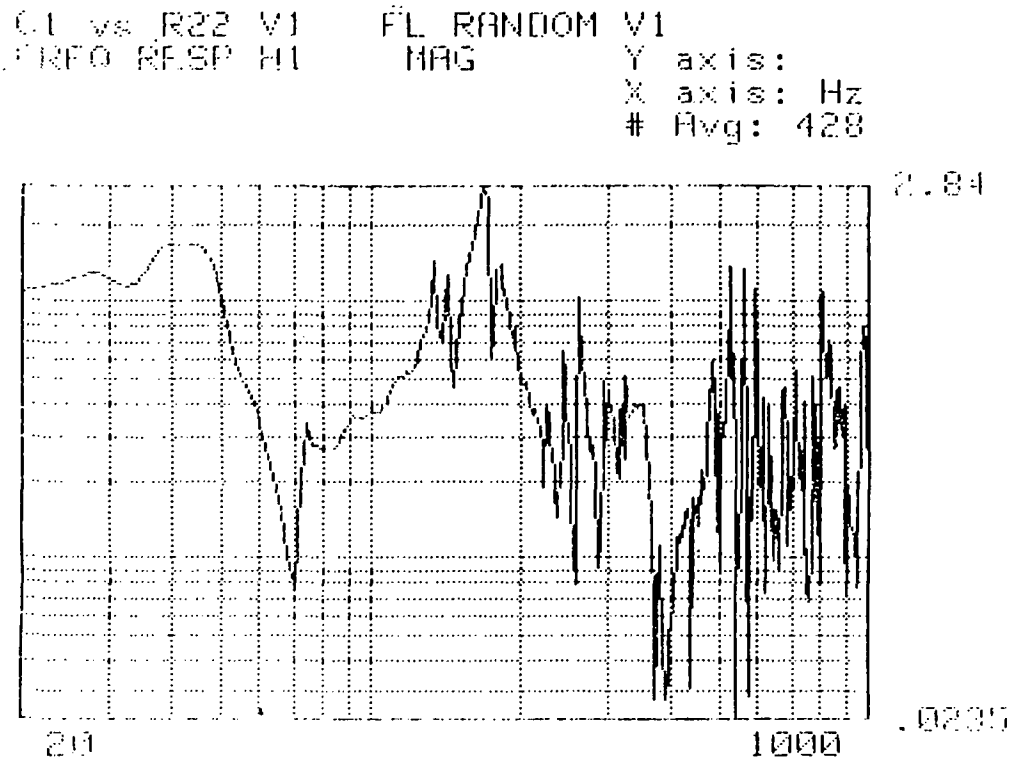

Figure 53. V1 "A" latch input versus c.g. transfer function.

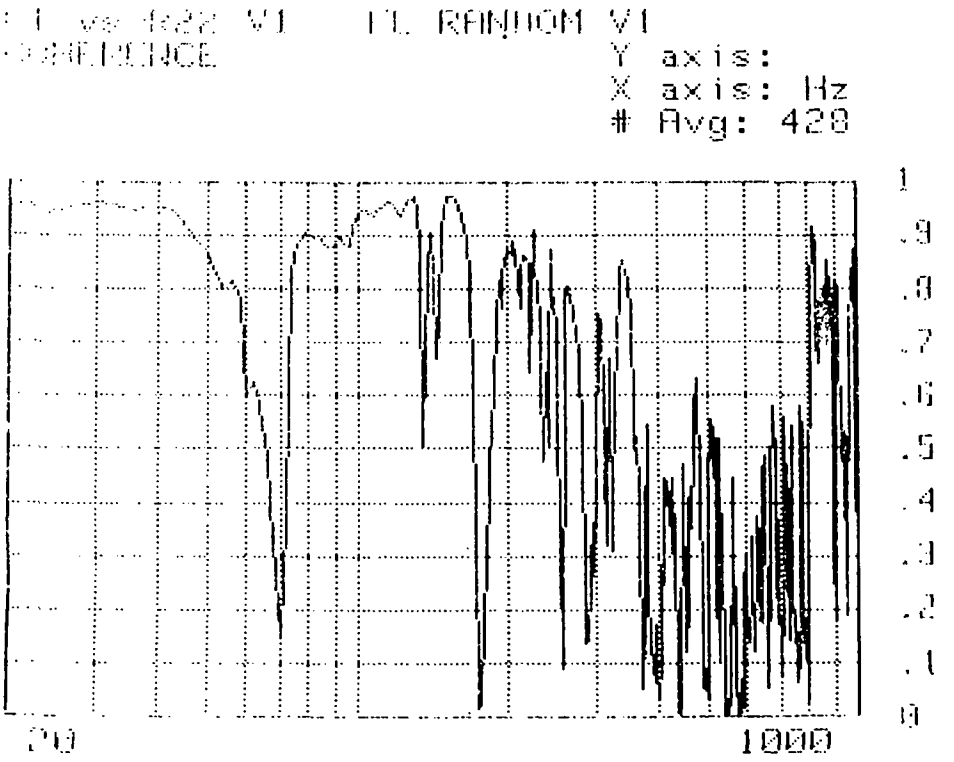

Figure 54. V1 input versus c.g. coherence.

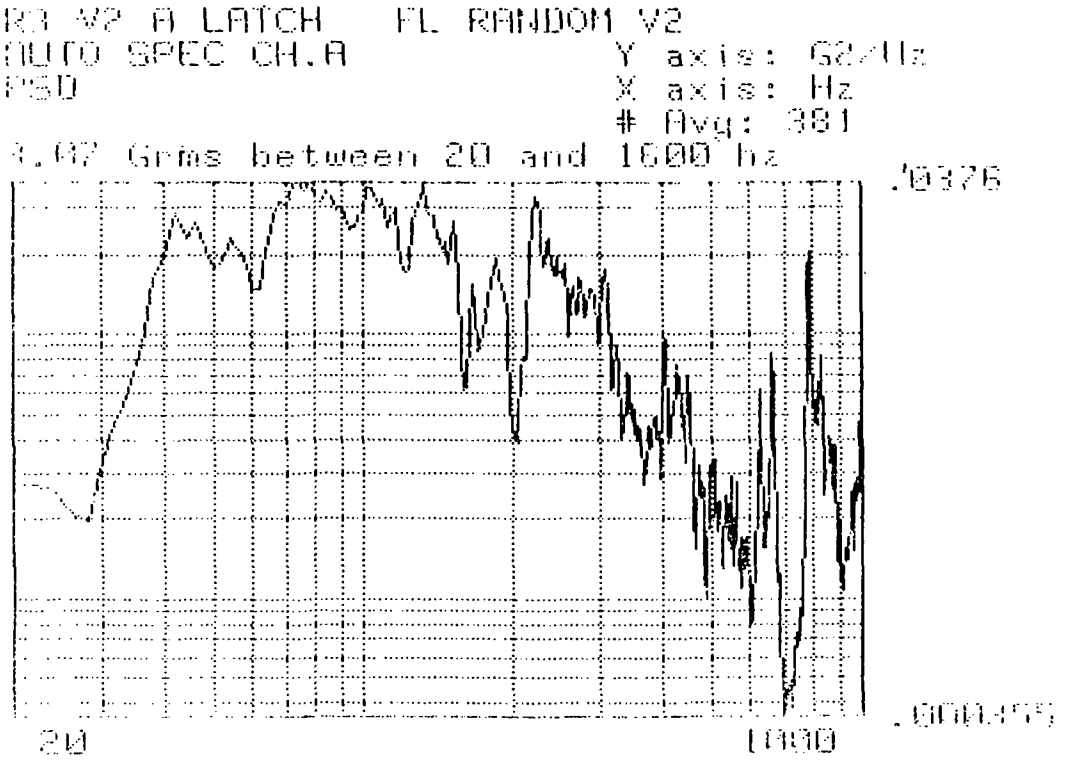

Figure 55. V2 "A" latch random auto spectral density.

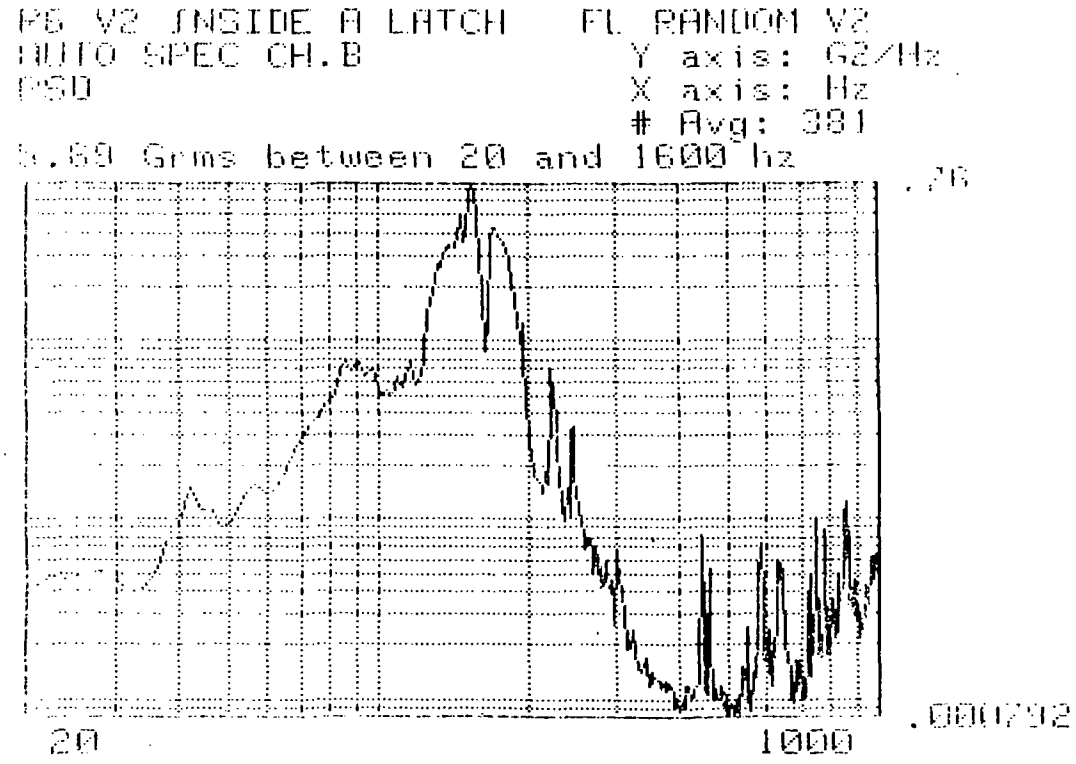

Figure 56. V2 "A" latch inside random auto spectral density.

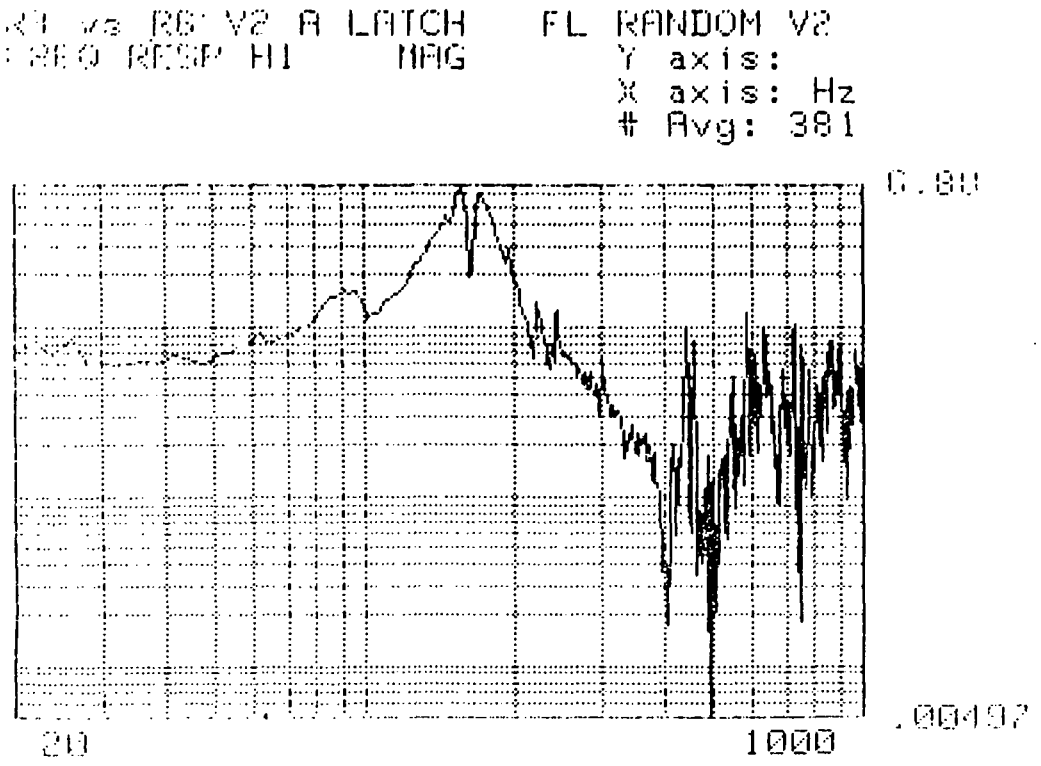

Figure 57. V2 "A" latch transfer function.

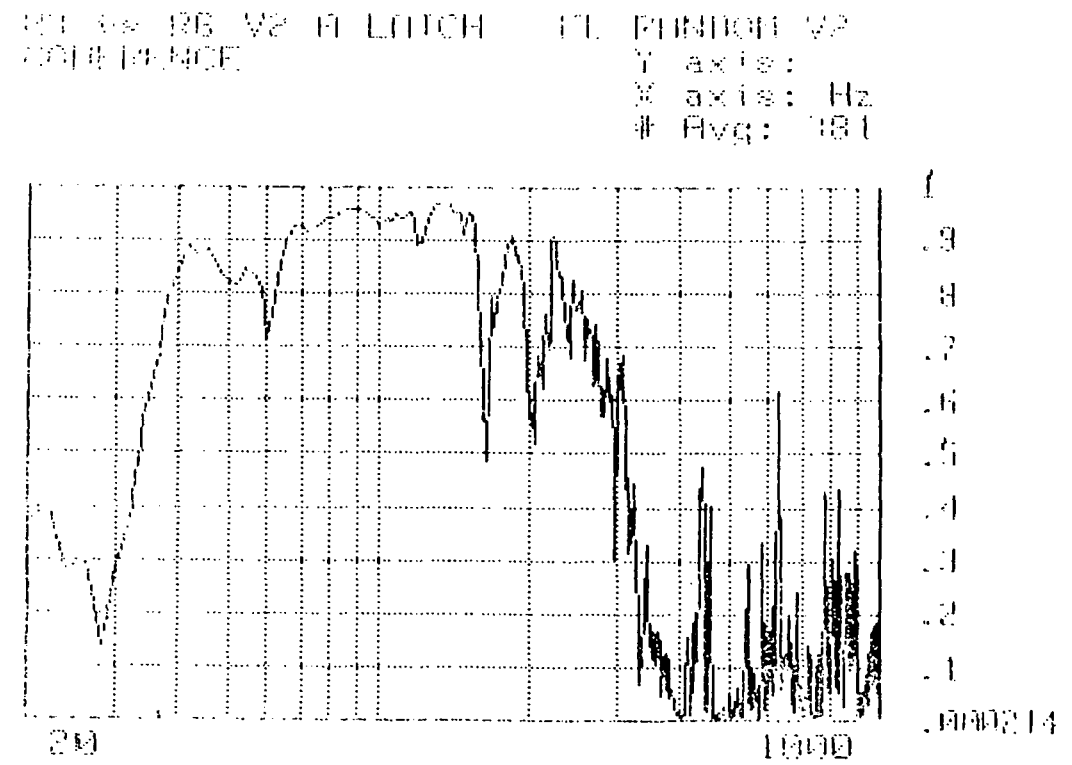

Figure 58. V2 "A" latch coherence.

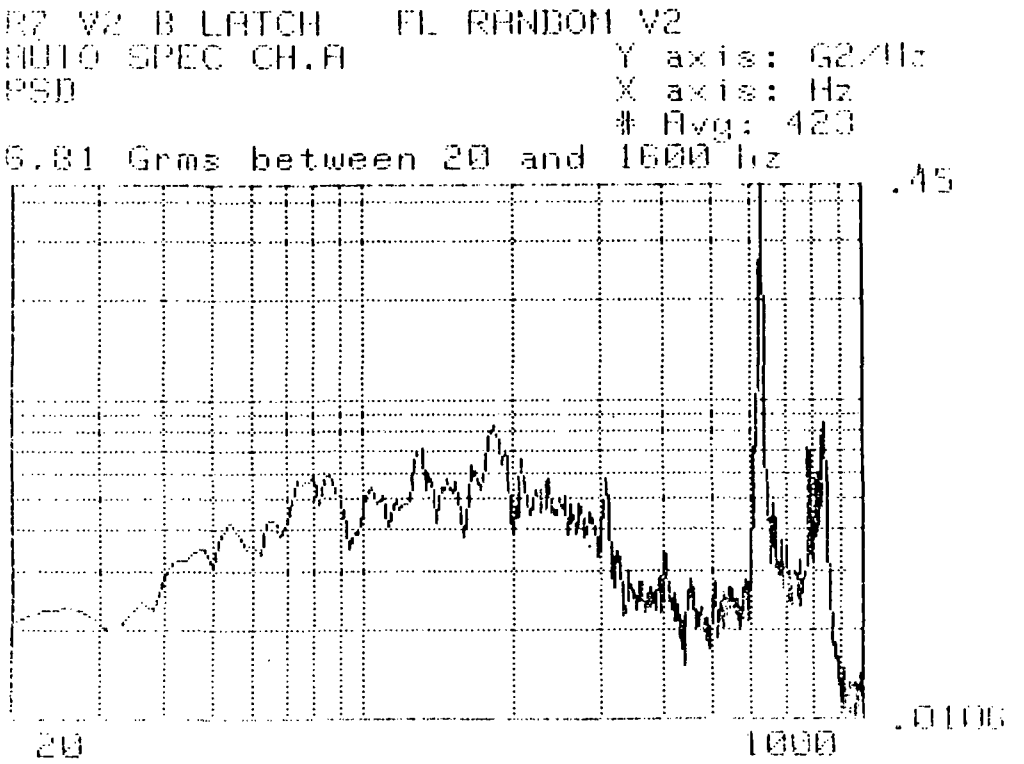

Figure 59. V2 "B" latch random auto spectral density.

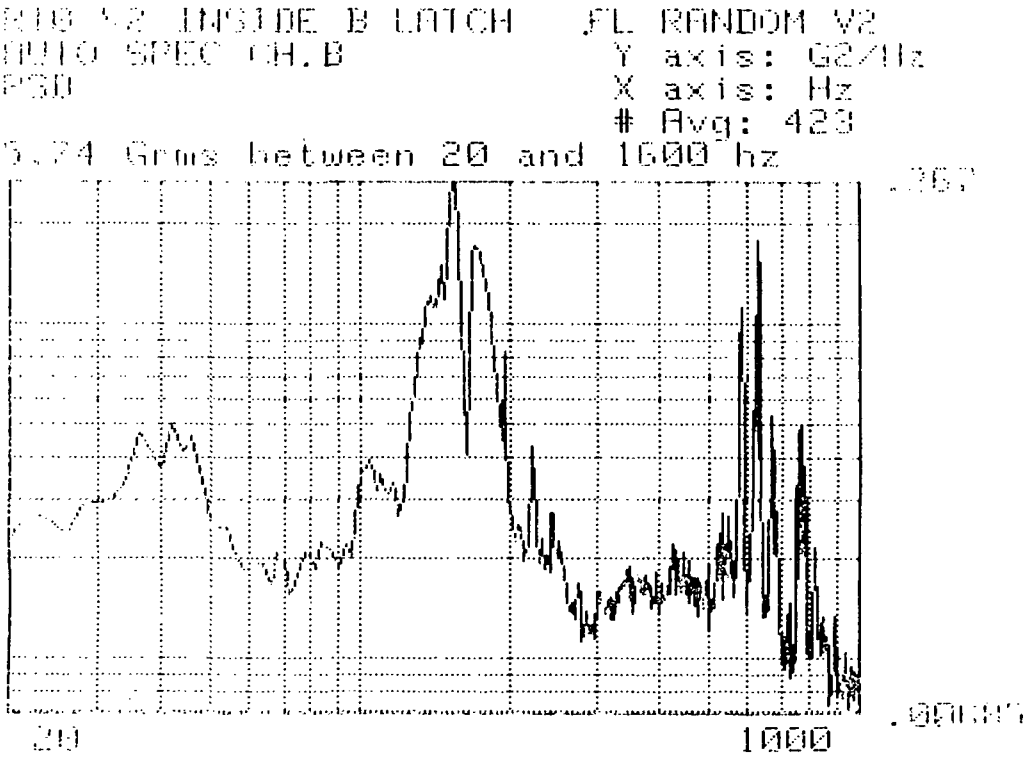

Figure 60. V2 "B" latch random auto spectral density.

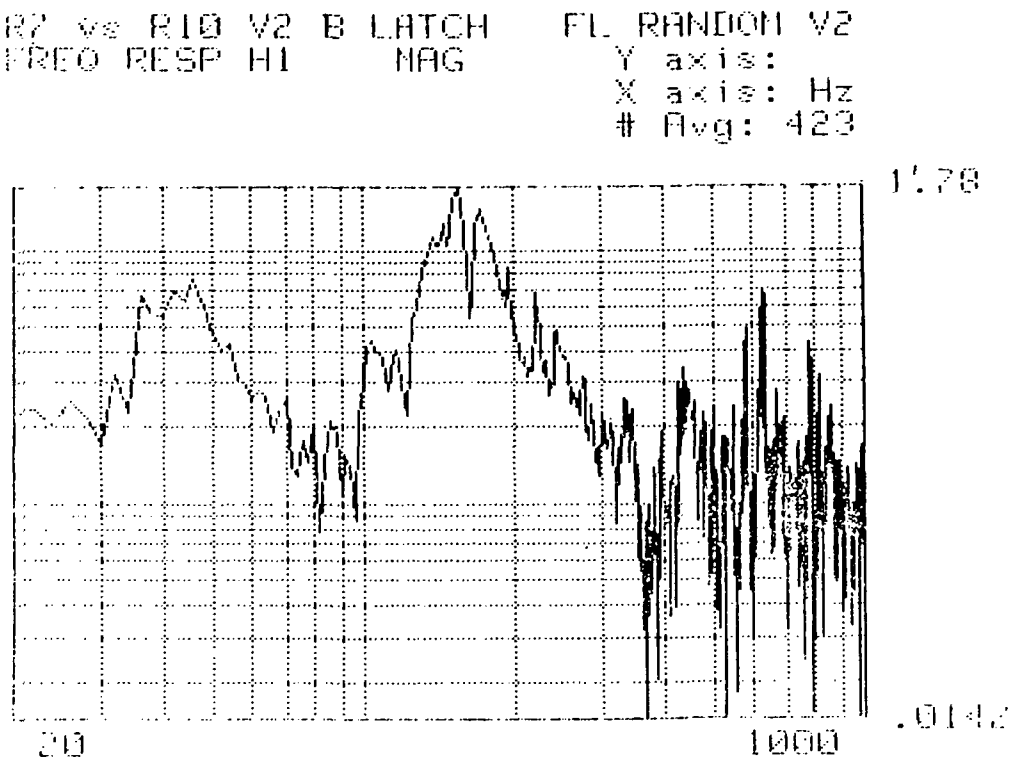

Figure 61. V2 "B" latch transfer function.

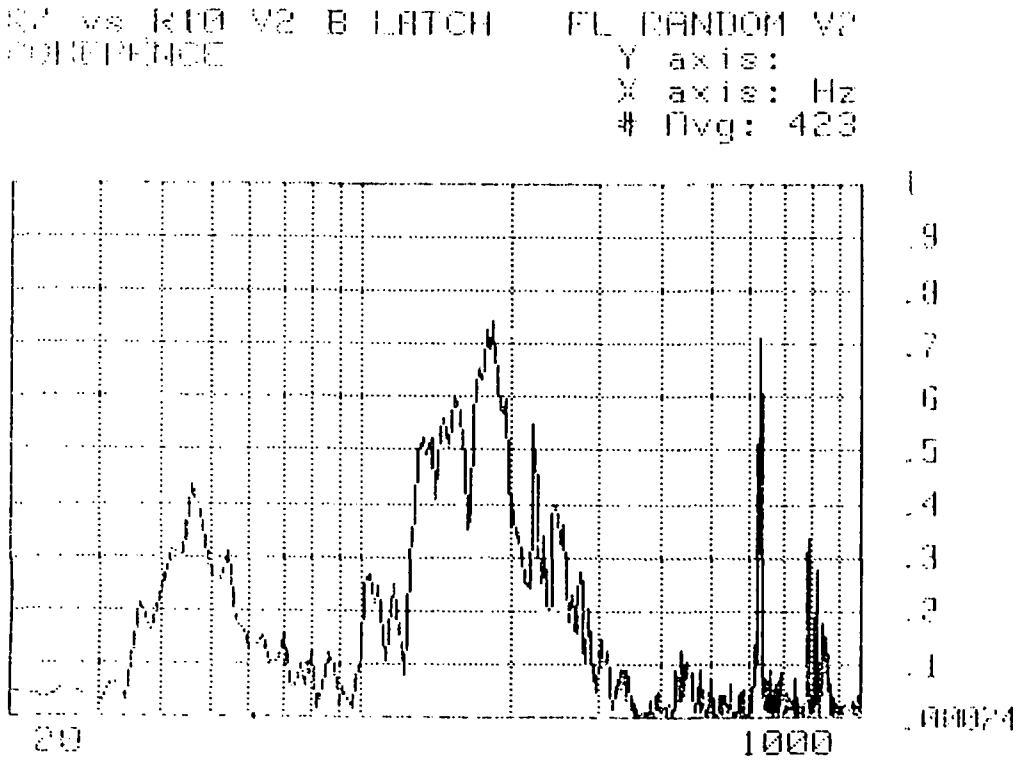

Figure 62. V2 "B" latch coherence.

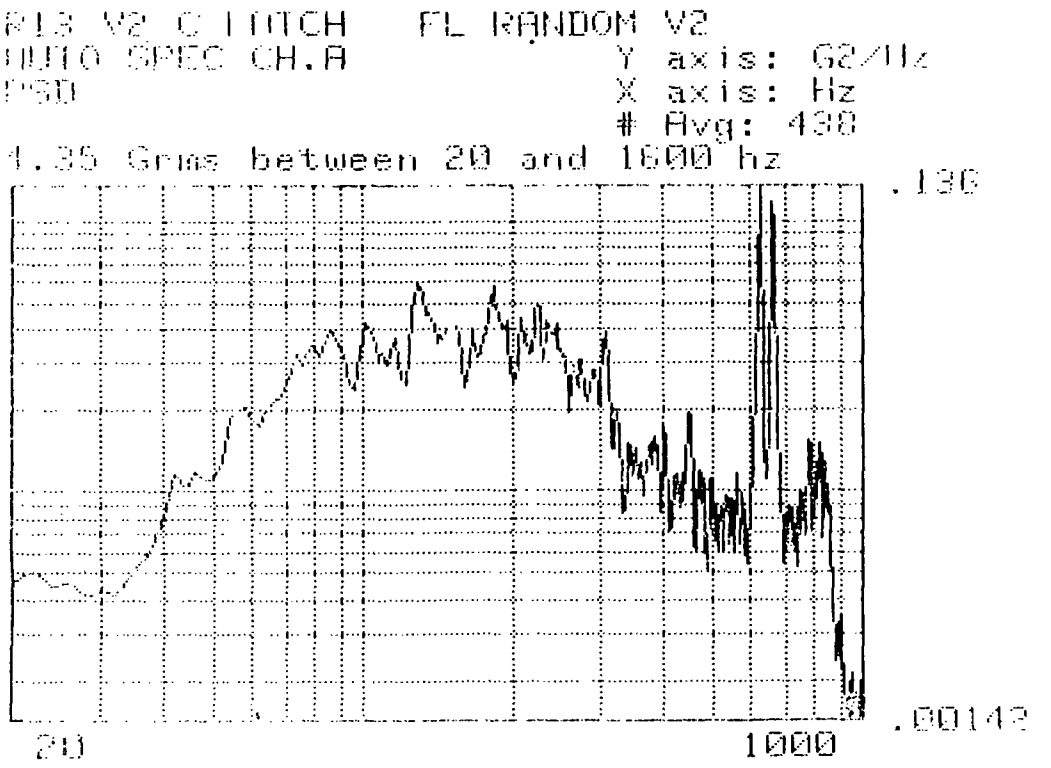

Figure 63. V2 "C" latch random auto spectral density.

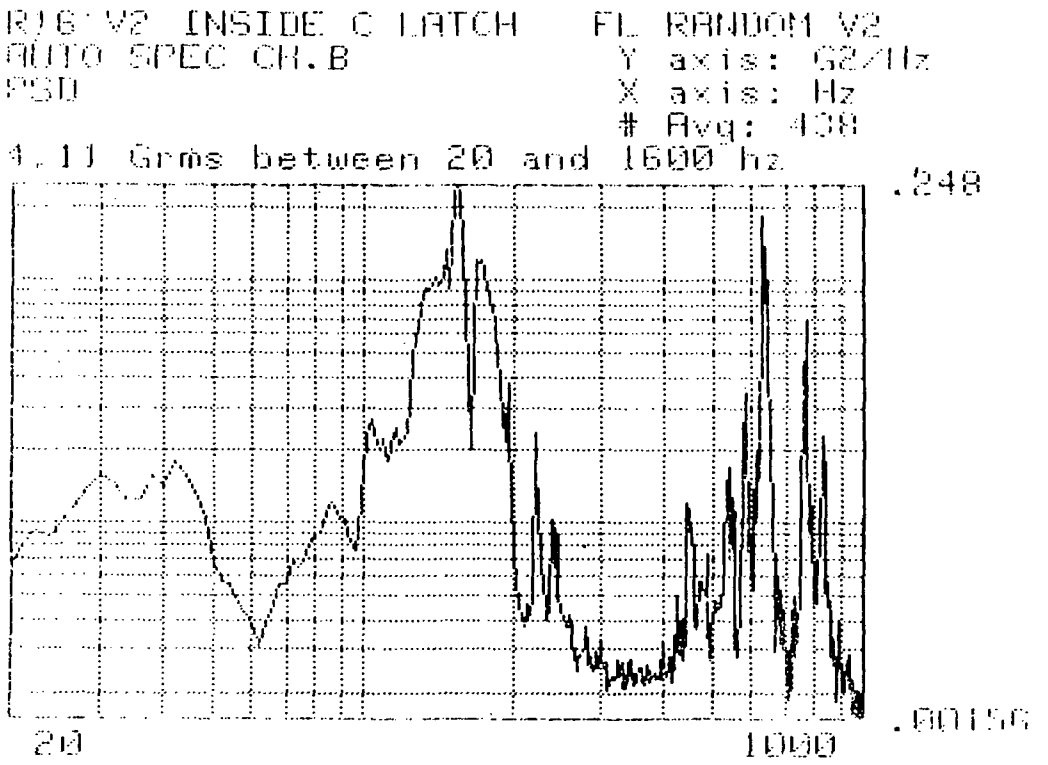

Figure 64. V2 "C" latch inside random auto spectral density.

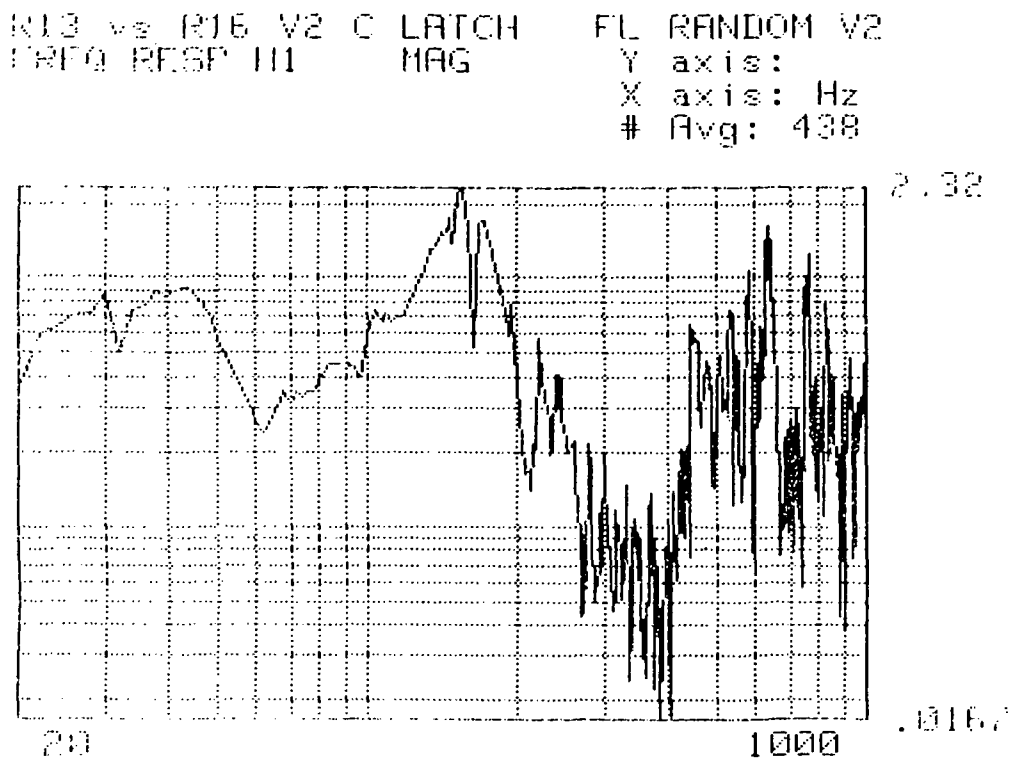

Figure 65. V2 "C" latch transfer function.

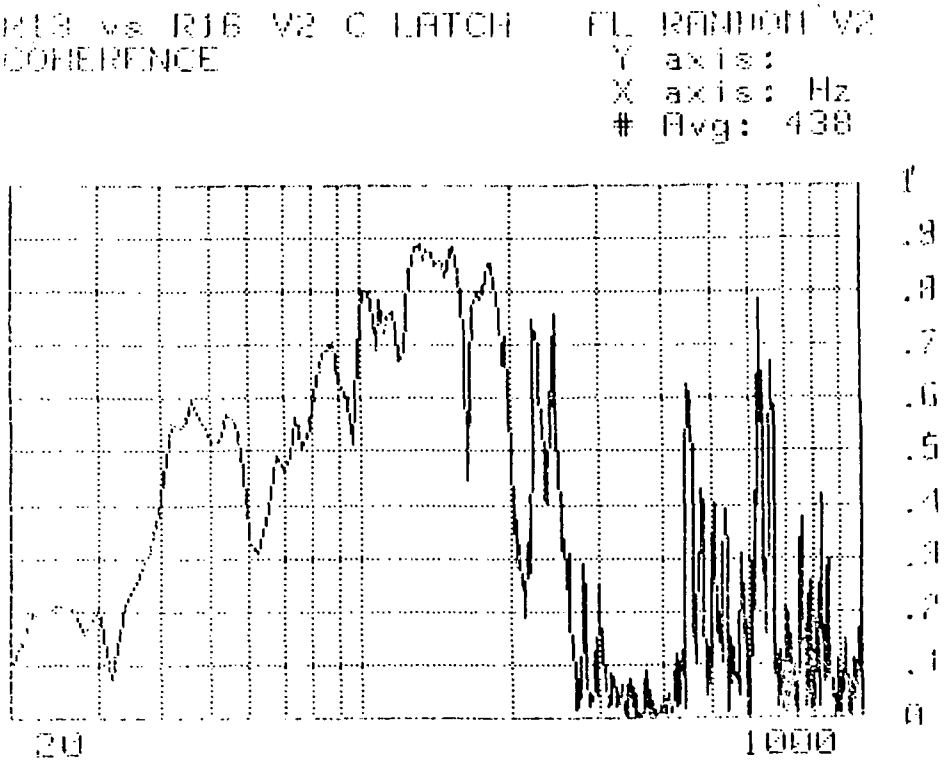

Figure 66. V2 "C" latch coherence.

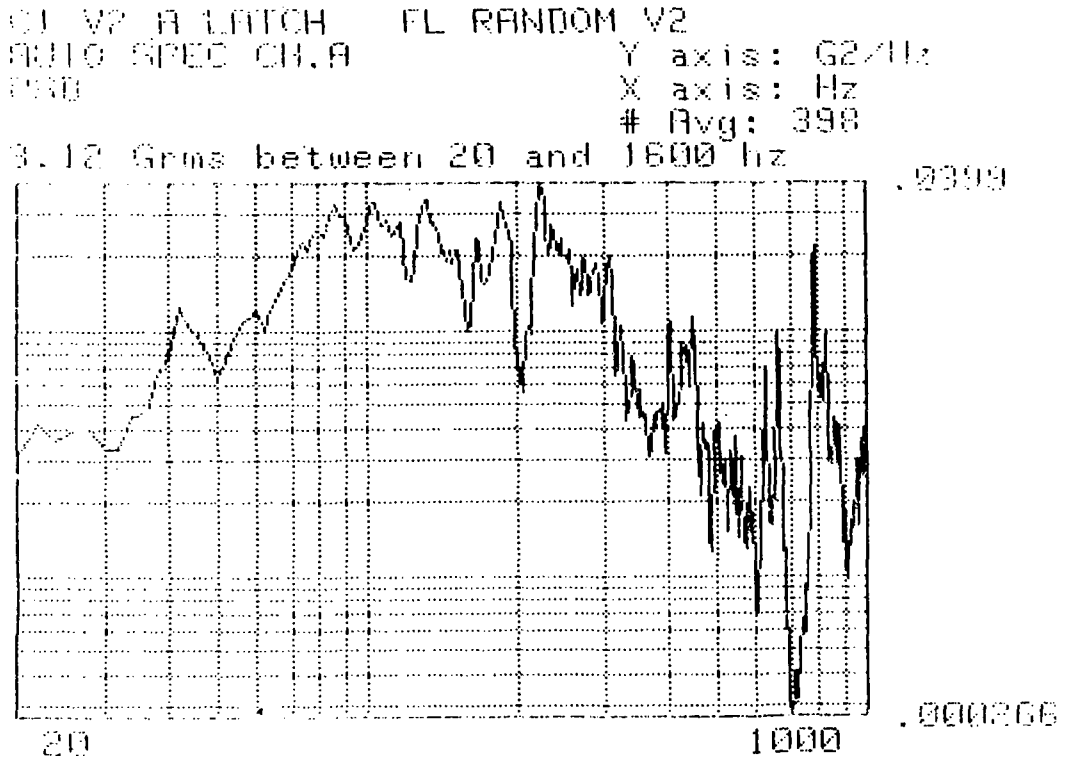

Figure 67. V2 "A" latch random input auto spectral density.

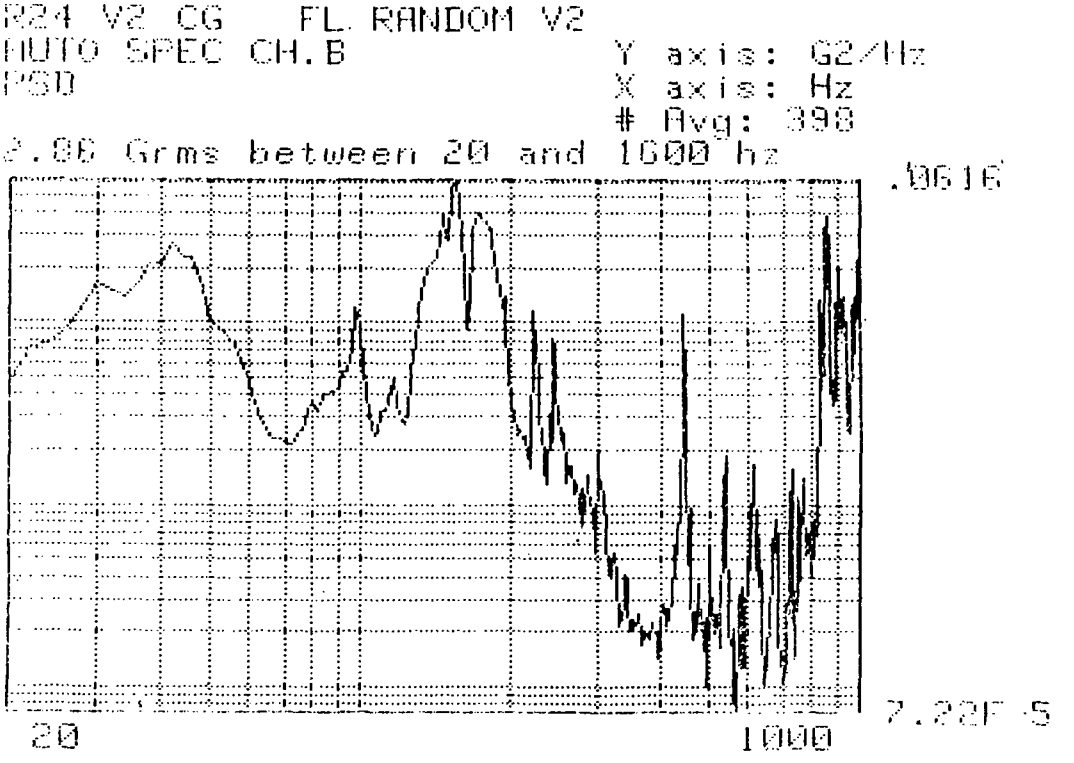

Figure 68. V2 c.g. response auto spectral density.

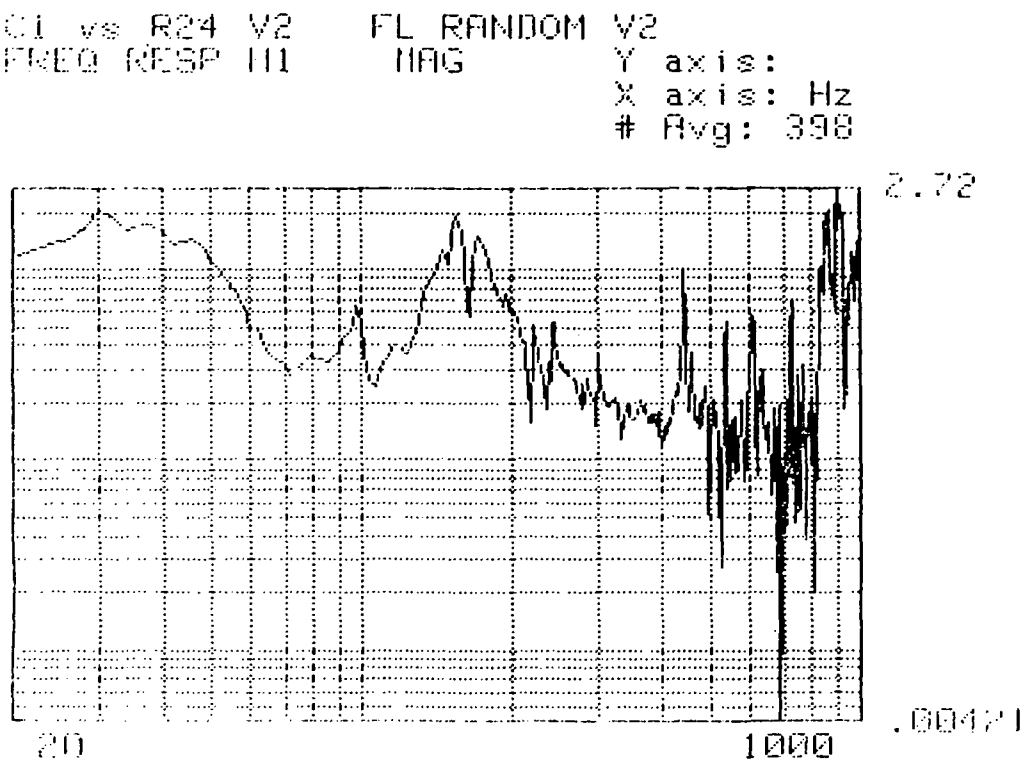

Figure 69. V2 input versus c.g. transfer function.

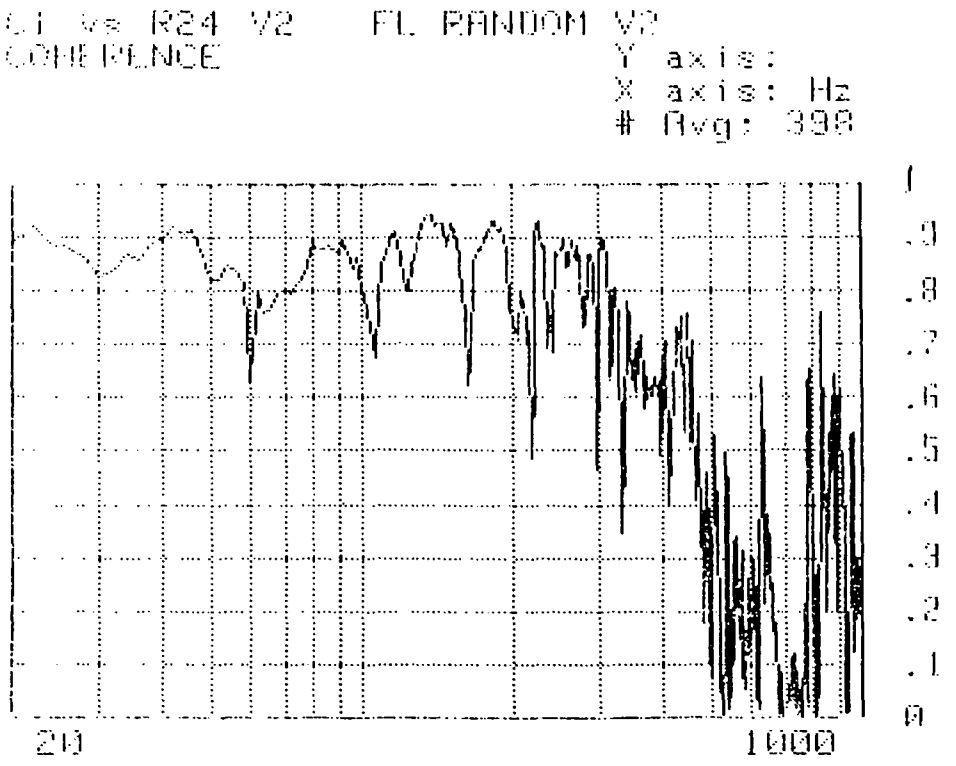

Figure 70. V2 input versus c.g. coherence.

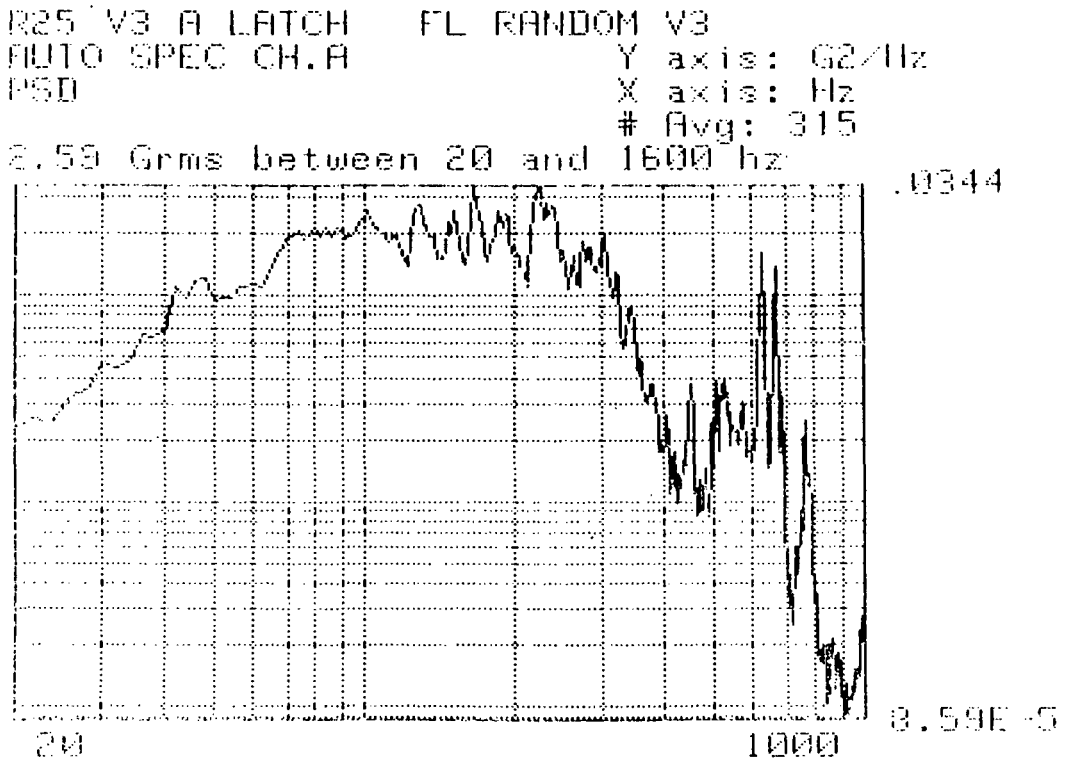

Figure 71. V3 "A" latch random auto spectral density.

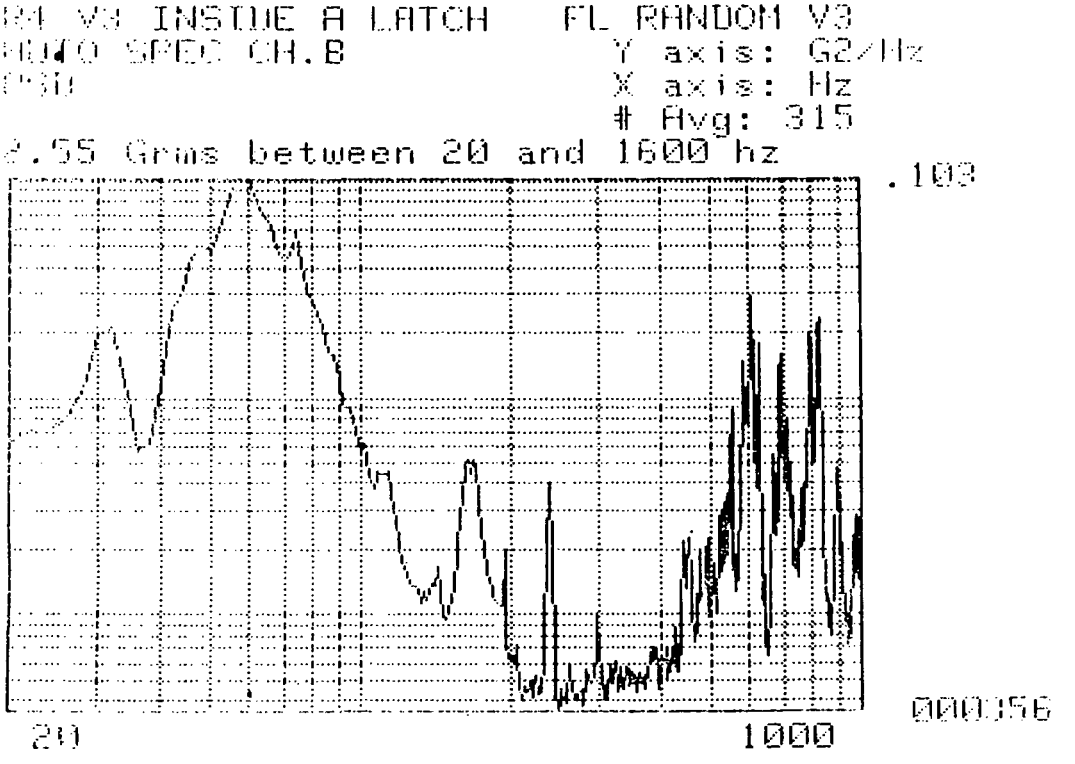

Figure 72. V3 "A" latch inside random auto spectral density.

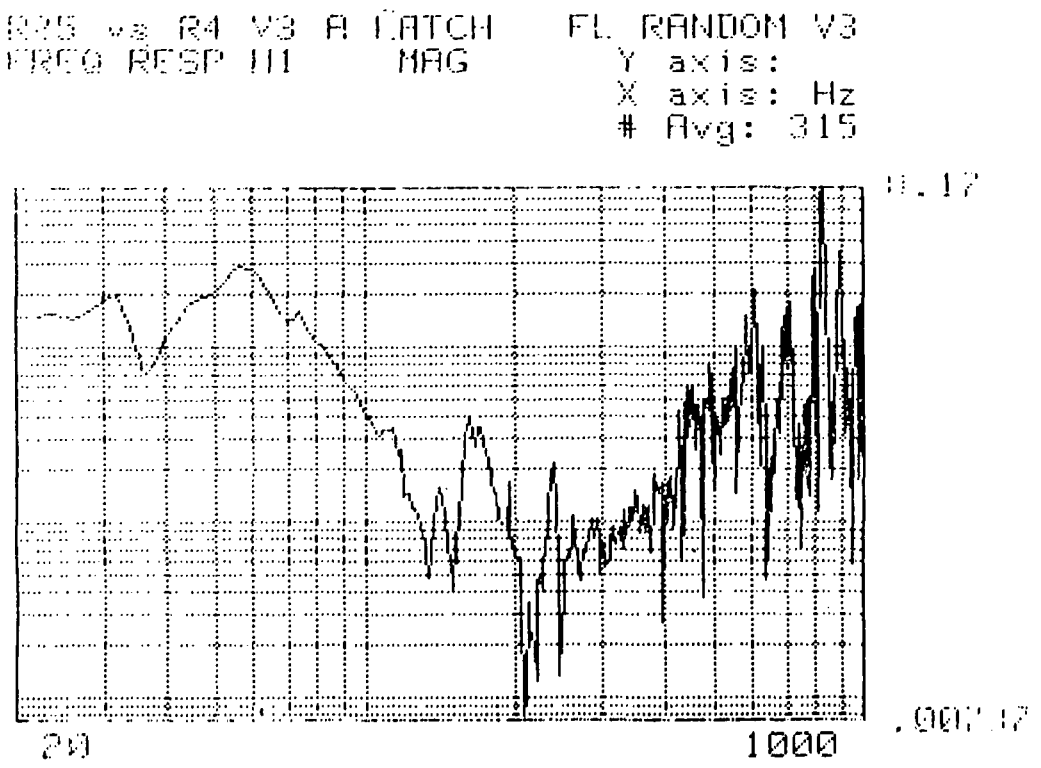

Figure 73. V3 "A" latch transfer function.

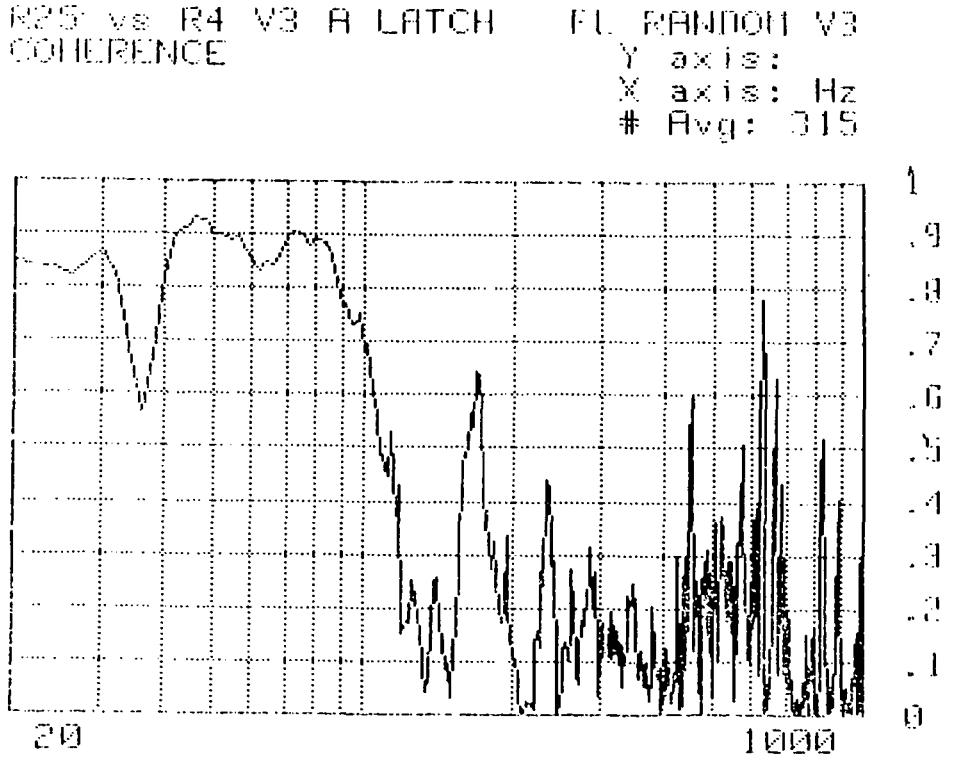

Figure 74. V3 "A" latch coherence.

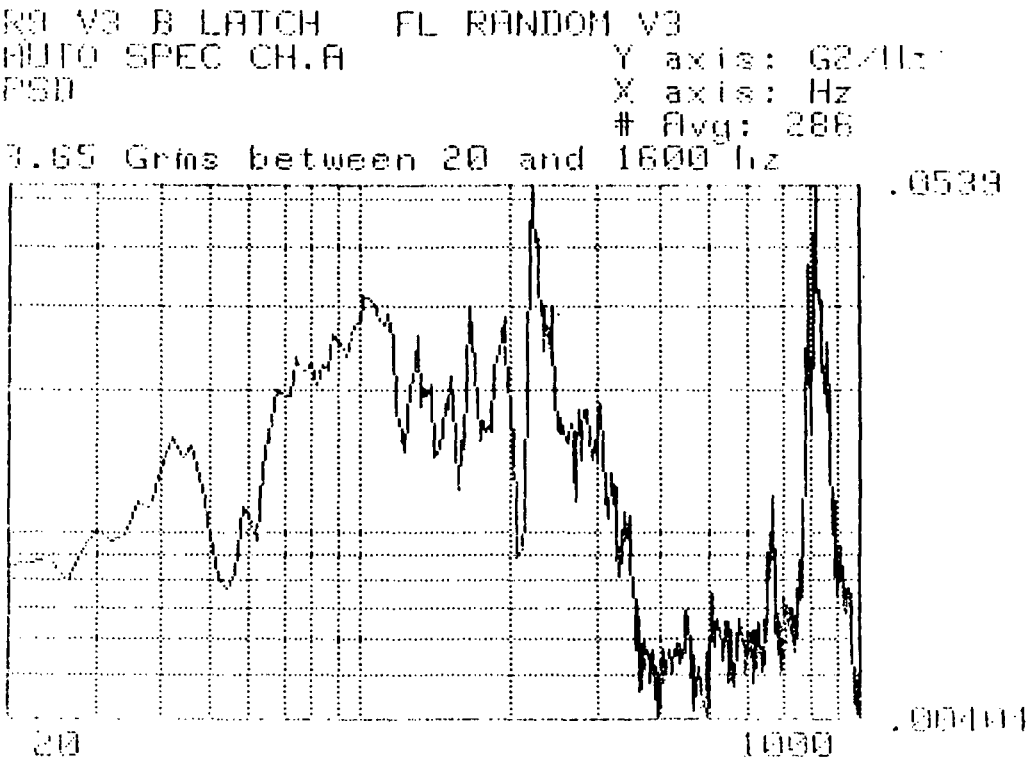

Figure 75. V3 "B" latch random auto spectral density.

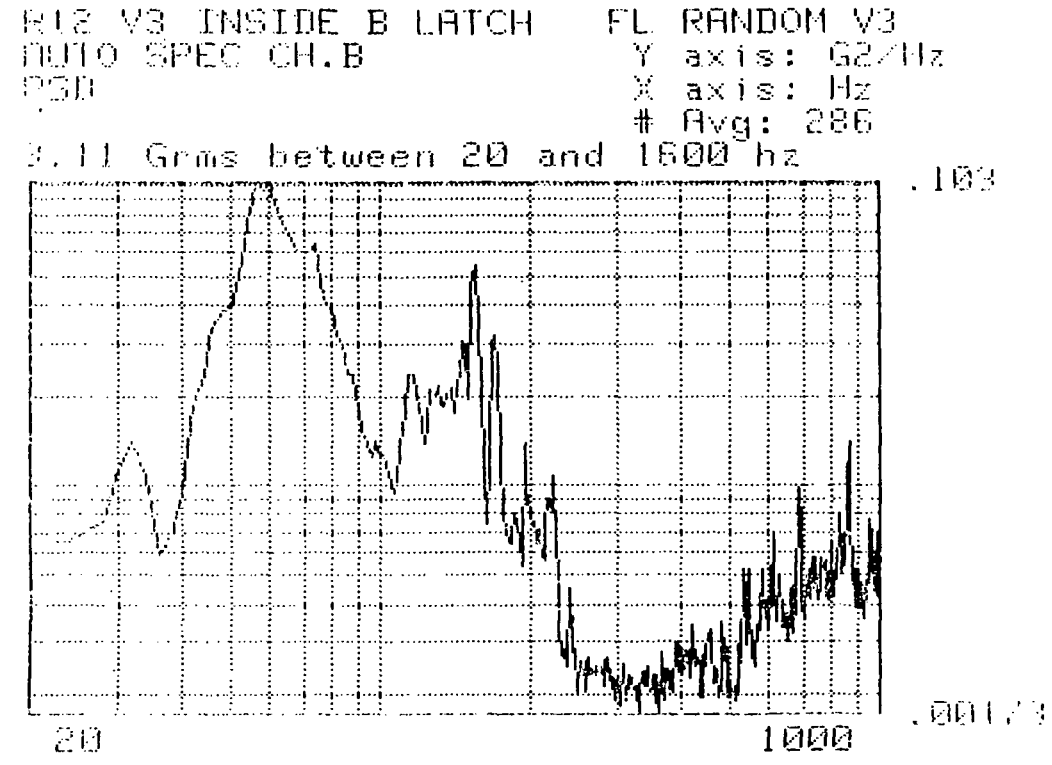

Figure 76. V3 "B" latch inside random auto spectral density.

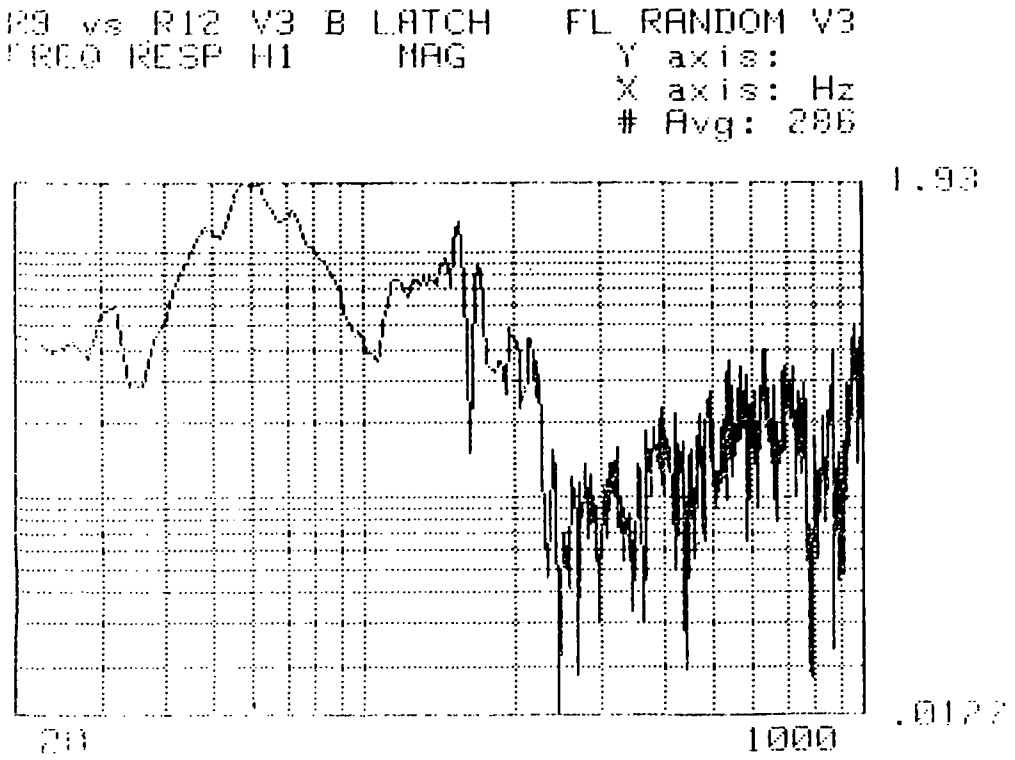

Figure 77. V3 "B" latch transfer function.

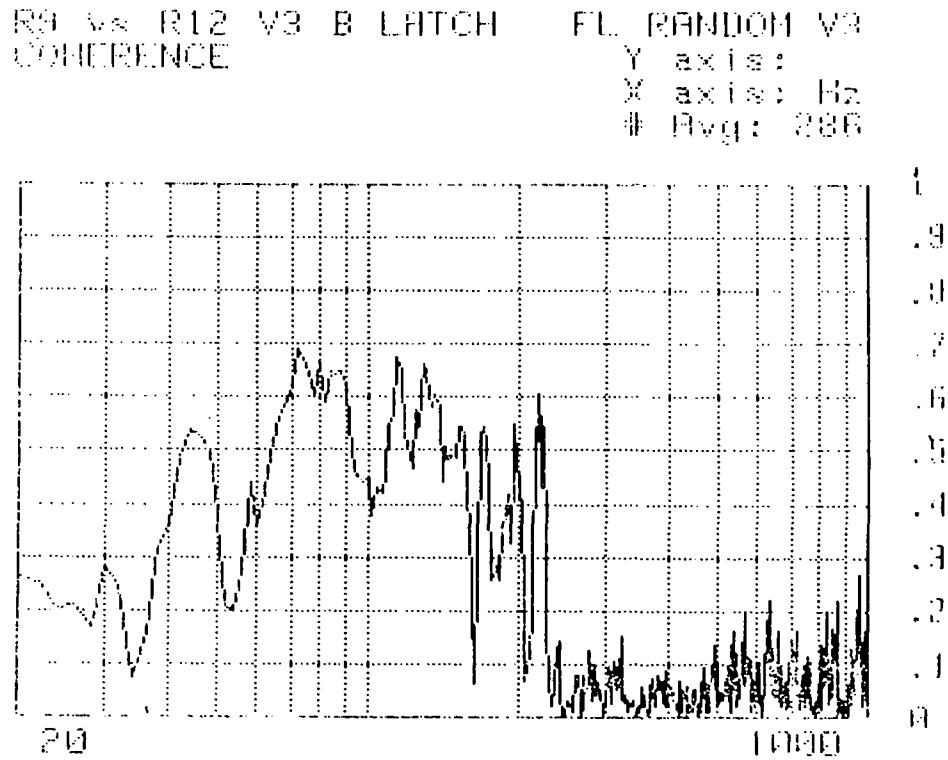

Figure 78. V3 "B" latch coherence.

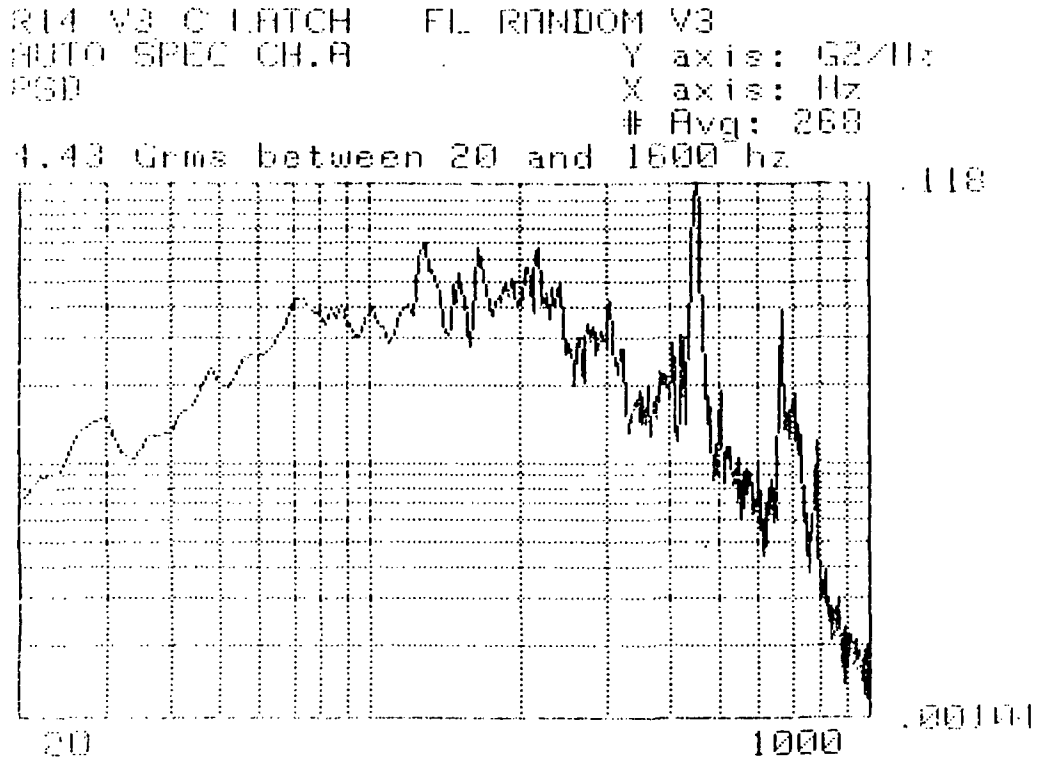

Figure 79. V3 "C" latch random auto spectral density.

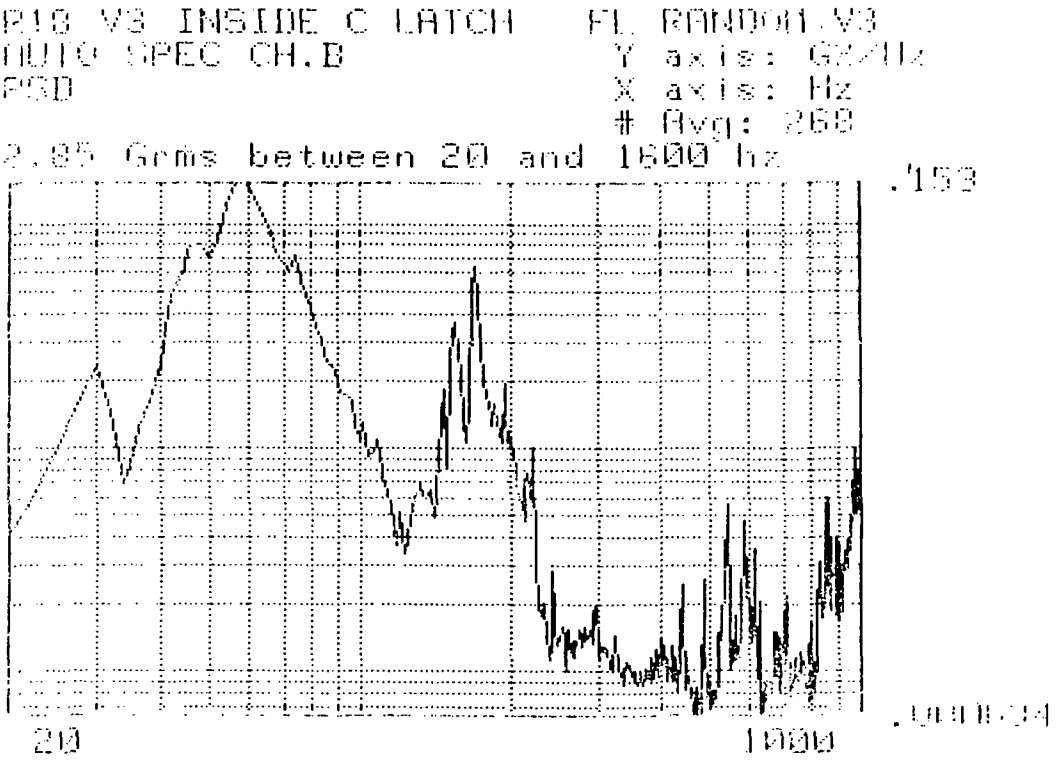

Figure 80. V3 "C" latch inside random auto spectral density.

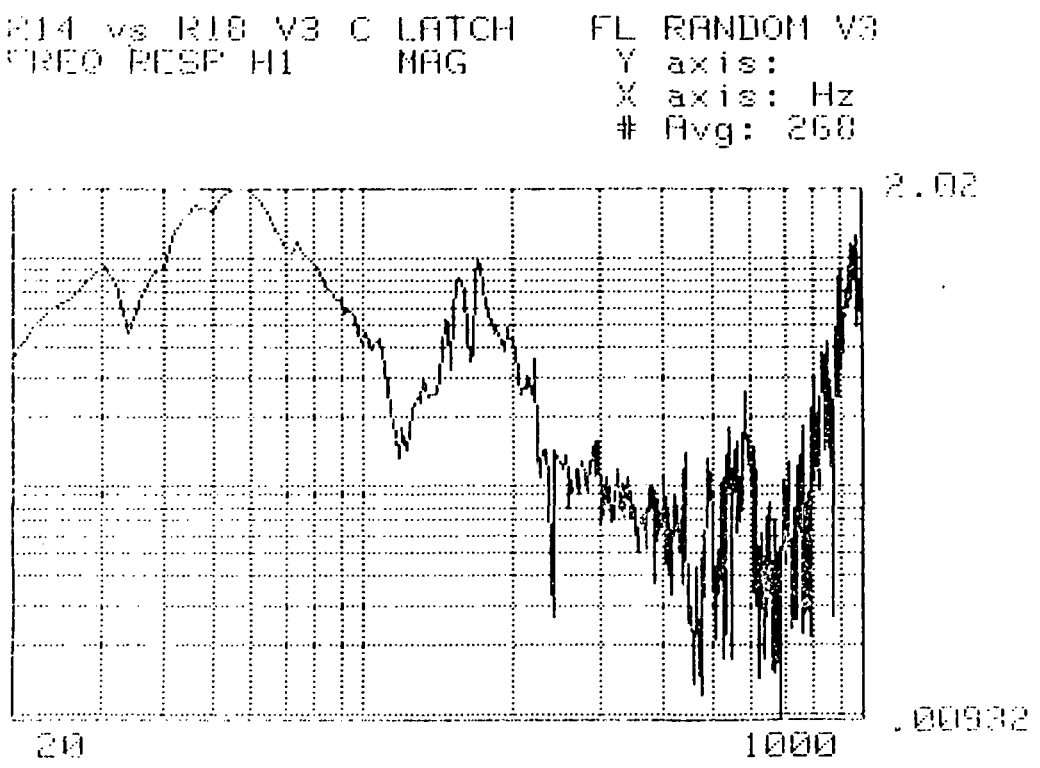

Figure 81. V3 "C" latch transfer function.

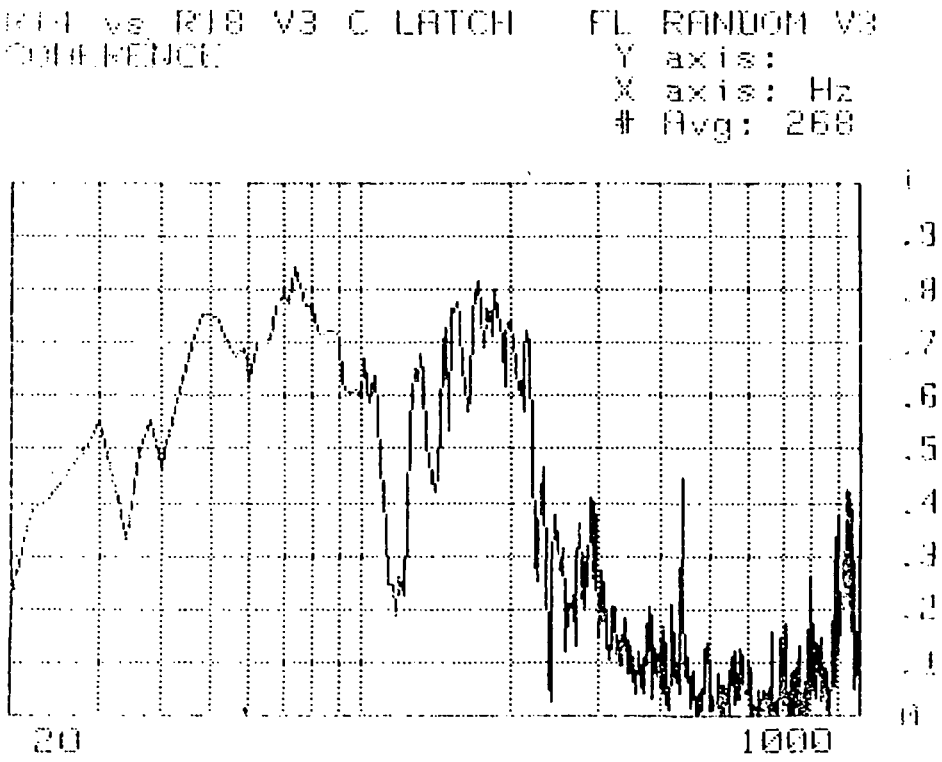

Figure 82. V3 "C" latch coherence.

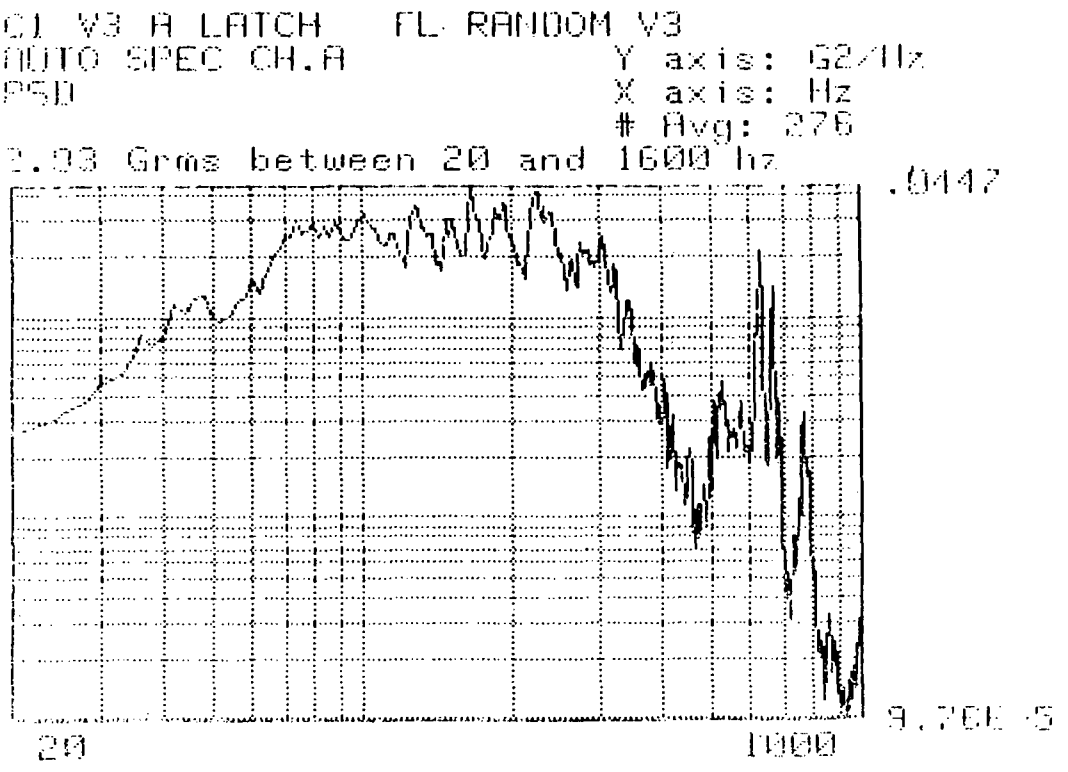

Figure 83. V3 "A" latch random input auto spectral density.

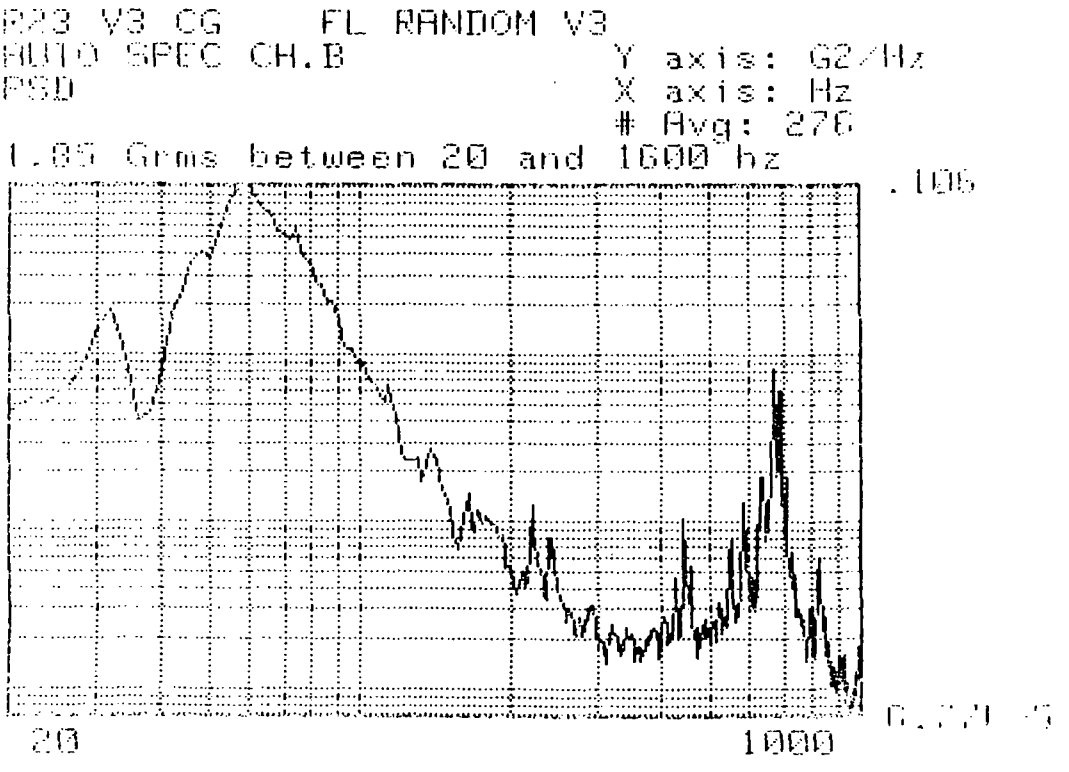

Figure 84. V3 c.g. response auto spectral density.

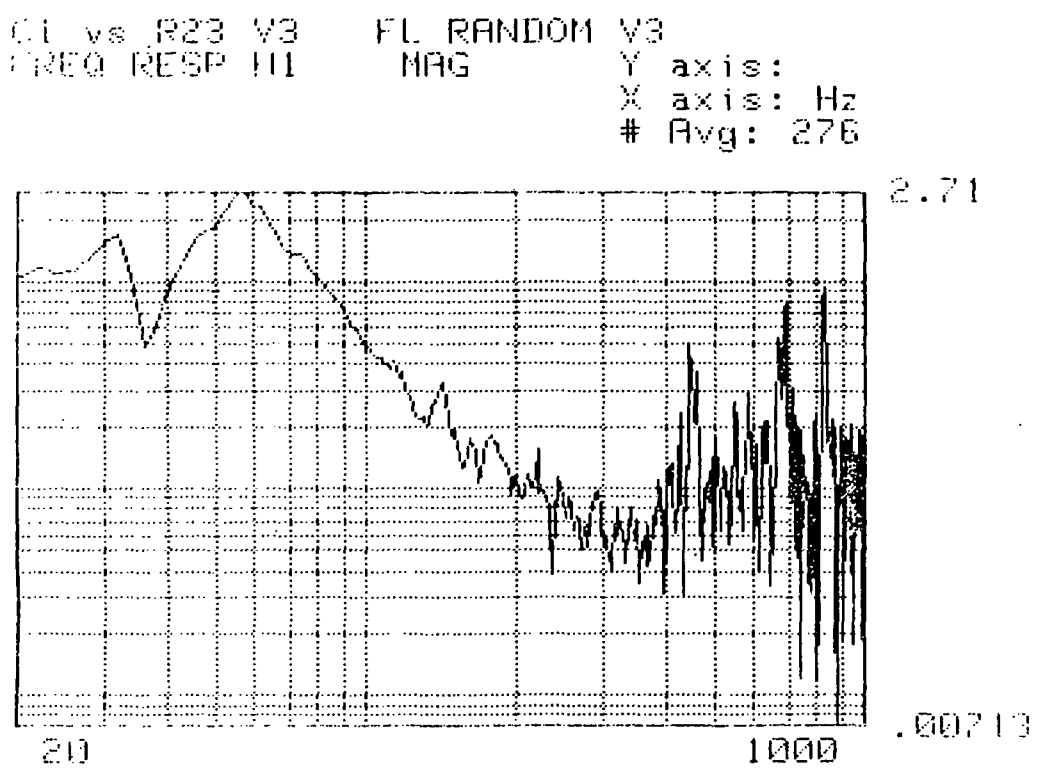

Figure 85. V3 input versus c.g. transfer function.

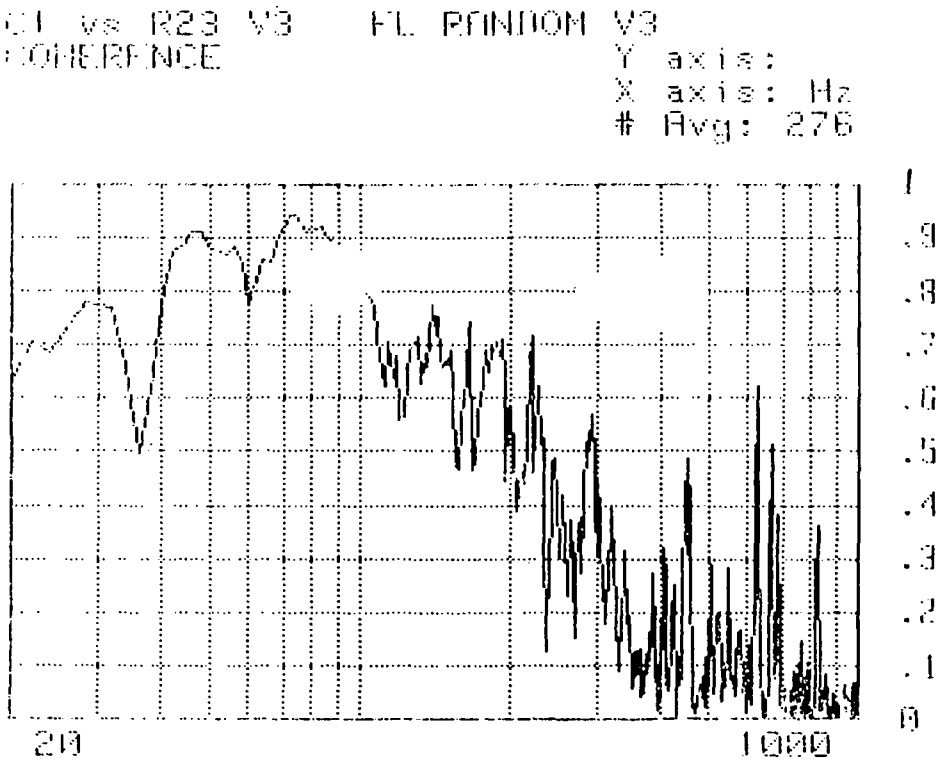

Figure 86. V3 input versus c.g. coherence.

Page intentionally left blank

Page intentionally left blank

APPENDIX C

ANALYSIS EQUATIONS

Correlation is a measure of similarity between two vibration waveforms. It is used to detect hidden periodic signals in noise and to determine other information such as energy transfer, etc.

An autocorrelation analysis multiplies the ordinates at time, t, and t + τ (a time shift), then time averages. Autocorrelation is defined mathematically as follows:

$$R_{XX}(\tau) = \lim_{T\to\infty} \frac{1}{T} \int_{-T/2}^{T/2} X(t)\, X(t+\tau)\, dt \quad .$$

An autocorrelation of a random signal using a small τ will tend to highlight the resonances of the system. Cross correlation is a correlation between two different waveforms. It is defined mathematically as follows:

$$R_{XY}(\tau) = \lim_{T\to\infty} \frac{1}{T} \int_{-T/2}^{T/2} X(t)\, Y(t+\tau)\, dt \quad .$$

Once time domain analysis is completed, frequency domain analysis can begin. The auto spectral density (a power spectral density of the autocorrelation) is defined as follows:

$$G_{XX}(f) = 2 \int_{-\infty}^{\infty} R_{XX}(\tau)\, e^{-i2\pi f\tau}\, d\tau \quad .$$

The cross spectral density is defined as follows:

$$G_{XY}(f) = 2 \int_{-\infty}^{\infty} R_{XY}(\tau)\, e^{-i2\pi f\tau}\, d\tau \quad .$$

The cross spectral density determines frequencies of greatest transfer.

Coherence, in the frequency domain, is analogous to the correlation coefficient in the time domain. Coherence values of $\gamma_{XY}^2 < 1$ indicate that the response is not attributable to the input. Coherence describes the percentage of energy transfer at any particular frequency. It is defined as follows:

$$\gamma_{XY}^2 = \frac{|G_{XY}(f)|^2}{G_{XX}(f)\ G_{yy}(f)} \quad .$$

A transfer function describing energy transfer through a system can be calculated as follows:

$$H(f) = \frac{G_{XY}(f)}{G_{XX}(f)} \quad .$$

APPROVAL

RADIAL SI LATCHES VIBRATION TEST DATA REVIEW

By Phillip M. Harrison and James Lee Smith

The information in this report has been reviewed for technical content. Review of any information concerning Department of Defense or nuclear energy activities or programs has been made by the MSFC Security Classification Officer. This report, in its entirety, has been determined to be unclassified.

G. F. McDONOUGH
Director, Systems Dynamics Laboratory

☆U.S. GOVERNMENT PRINTING OFFICE 1984—746-070/10012